UNIVERSITEIT VAN PRETORIA
UNIVERSITY OF PRETORIA
YUNIBESITHI YA PRETORIA

Modelling the interactions of engineered nanoparticles with natural organic matter using *in silico* techniques

Nangamso Nathaniel Nyangiwe

Student No. 15379958

Submitted in fulfilment of the requirements for the degree

Doctor of Philosophy

in the

Faculty of Engineering, Built Environment and Information Technology, University of Pretoria

Supervisor: Dr Cecil Naphtaly Moro Ouma

March 2020

Modelling the interactions of engineered nanoparticles with natural organic matter using *in silico* techniques.

Nangamso N. Nyangiwe

Executive Summary

With increasing number of nanoproducts being commercialized globally; and consequent release of engineered nanoparticles (ENPs) into different environmental compartments with unknown impacts has raised concerns. Several experimental studies have attempted to elucidate the fate of ENPs in the aquatic systems especially following their interactions with natural organic matter (NOM). This consequently makes valuation of the fate and behavior of ENPs essential especially when it comes to the design of goods that are harmless and function as intended without causing unwanted special effects to biological lifeforms in the aquatic systems. Most of these studies used experiments which require considerable, effort and expensive equipment. Hence therefore there is an urgent need for the development of computational models to envisage the fate and behavior of ENPs in the aquatic systems and use these results to guide experimental investigations. Thus, in this thesis, we employ *in silico* techniques aimed at generating descriptors that can offer insights on fate and behavior of ENPs. We look for descriptors that will enhance our understanding of ENP-NOM interactions at fundamental level. Using density functional theory (DFT) calculations augmented with classical lattice dynamics (CLD), we have investigated several properties of the ENP-NOM systems. This was done using three case studies where different NOM's were adsorbed on different nanoparticle shapes and surfaces.

In the first case, descriptors associated with low molecular weight NOMs were investigated on silver nanoparticles in different shapes (spherical, cylindrical etc.) both gas phase and solvent phase. Findings of adsorption energies showed that molecular weight plays a crucial role because an increasing trend was observed relative to the molecular weight the NOM. Results revealed higher adsorption energies for ascorbic acid. NOM adsorption on tetrahedron-shaped Ag ENP (111) surface was also characterised with high adsorption energies. For Ag, the (111) face is characterised by high metal density (14 Ag/nm2) and low

surface tension (Azcárate et al. 2013) and the close-packed (111) plane has the lowest energy crystal plane with maximum packing, and therefore, is most stable (Marzbanrad et al. 2015). For this reason, the (111) facet is widely studied (Hatchett and White 1996) because silver reactivity favours high atom density facets, (Ajayan and Marks 1988) and similarly, it was chosen as facet of investigation in this study.

Global reactivity descriptors that can offer insights and enhance our understanding as well as account at a fundamental level the fate and behavior of ENPs in the aquatic systems such the dipole moment (μ), molecular surface area (MSA), absolute electronegativity (χ), and absolute hardness (η) were also performed using frontier molecular orbital theory.

In the second case, the interactions of ENPs with high molecular weight NOMs (fulvic acid and humic acid) was considered in both gas and solvent phases. Both fulvic acid and humic acid are ambiguously found in the aquatic systems and hence their choice for this study. Similar to the first case, dispersion corrected density functional theory (DFT-D) techniques was used to generate descriptors. Results from this case study showed that the calculated adsorption energies for humic acid (HA), formic acid(FA) and cryptochrome (Cry) on Ag (111) surface were -1.21 (-0.80) eV, -1.66 (-0.81) eV, and -6.24 (-6.54) eV respectively in the gas (solvent) phase and the equilibrium distances between the surface and HA, FA and Cry molecules were 1.87 (2.18) Å, 2.31(2.31) Å and 1.91 (1.70) Å respectively in the gas (solvent) phase. In both gas and solvent phase Cry showed stronger adsorption which meant it had a stronger interaction with Ag (111) surface compared HA and FA. The results for adsorption energy, solvation energy, *iso*surface of charge deformation difference, total density of state and partial density of states indicated that indeed these chosen adsorbates do interact with the surface and were favorable on Ag (111) surface.

The third case considered was the co-adsorption of Low Molecular Weight (LMW) NOMs mixtures on the surfaces of nAg (111), where $n = 1, 2, 3, 4$ implies 1 to 4 molecules are considered in a given co-adsorption case considered. This is because the NOMs exist as mixtures in aquatic systems. The approach and methodology for this investigation followed that which was applied in both the first and second cases. To the best of our knowledge, this is the first study where adsorption of an NOM mixture of formic acid, acetic acid and

ascorbic on a nanoparticle surface had been done using DFT-D. This study provides understanding to clarify how a mixture of NOMs may have diverse set of implications on the fate of ENPs in aquatic systems using first-principles calculations; and may be a useful reference in designing experiments on the influence of different NOMs on the ENMs fate in aquatic systems. The results for this case study showed that the calculated adsorption energies suggest that the interaction of four molecules of formic acid (4FA), two molecules of acetic acid (2AA1) and two molecules of ascorbic acid (2AA2) with Ag (111) surface is the strongest with the most negative values (-6.54 and -3.84 eV) in both gas phase and Conductor-like screening model (COSMO) respectively which indicates that it is the most stable system. More importantly, the study found that water as a solvent does not play a crucial in enhancing the adsorption. This analysis serves as the first step toward gaining a more accurate understanding of specific interactions at the interface in gas phase and in aqueous media.

Acknowledgements

"I have fought the good fight, I have finished the race, I have kept the faith." 2 Timothy 4:7

Firstly, I would like to thank God for giving me strength, ideas and good health to finish this PhD, indeed His GRACE is sufficient for me.

Secondly, I want to thank my supervisor Dr Cecil N.M.Ouma, without his support this thesis would never come to life. It has been a privileged to be his Ph.D. student. I greatly appreciate his continuous support, patience and useful critiques of this research work. Thank you Dr Cecil N.M. Ouma for introducing me to the world of computational modelling.

I thank the following organizations for their financial and computational support; the Professional Development Programme (PDP) fund offered by Department of Science and Technology (DST), National Research Foundation (NRF), Council for Scientific and Industrial Research (CSIR) and the Centre for High Performance Computing (CHPC).

I also thank my former Research Group Leader at CSIR Dr Melusi Thwala for supporting my trip to United Kingdom, after I returned from the United Kingdom I saw a rapid progress in my project. Thank you to all postgraduates I have interacted with at the CSIR and at the University of Pretoria.

I thank my junior and senior secondary schools mathematics and physical science teachers Mr Nohaji, Mr Mkhutyukelwa and the late Mr Mduzulwana, they taught me to believe in myself at an early age and they never seemed to think there was a ceiling to my potential.

Last but not least the scriptures below kept me going when nothing was making sense.

"Call on me in prayer and I will answer you. I will show you great and mysterious things you did not know before." Jeremiah 33:3

"Do not fear, for I am with you; do not be afraid, for I am your God. I will strengthen you; I will surely help you; I will uphold you with My right hand of righteousness." Isaiah 41:10

"For I know the plans I have for you, declares the LORD, plans to prosper and not to harm you, plans to give you hope and a future." Jeremiah 29:11

"I can do all things through Christ who strengthens me." Philippians 4:13

Declaration

I declare that the thesis, which I hereby submit for the degree programme at the University of Pretoria, is my own work and has not previously been submitted by me for a degree at another university. Where secondary material is used, it has been carefully acknowledged and referenced in accordance with University requirements, I am aware of the University's policy and implications regarding plagiarism.
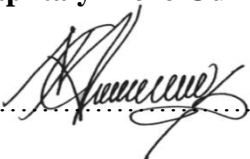
Candidate

Name: **Nangamso Nathaniel Nyangiwe**

Signature: ……………………………………………………………

Date: ………………………………………………………………
22 July 2020

Supervisor

Name: …**Dr Cecil Naphtaly Moro Ouma**…

Signature: …………………………………………………………

22 July 2020

Date: ………………………………………………………………

Dedication

This thesis is dedicated to **Nyangiwe's family**, my wife **Nandipha**, our kids **Siwabonile, Sibonokuhle,** all the deserving students around the world who never got a chance to pursue higher education due to various reasons and all the people who made sacrifices so that I could have the opportunity to pursue the highest education possible. This Ph.D is for you.

List of acronyms

AA1	Acetic acid
AA2	Ascorbic acid
BO	Born Oppenheimer
CNMs	Carbon nanomaterials
COSMO	Conductor-like screening model
Cry	Cryptochrome
DFT	Density Functional Theory
DFT-D	Dispersion corrected density functional theory
ENPs	Engineered nanoparticles
FA1	Formic acid
FA2	Fulvic acid
FMO	Frontier Molecular Orbital
GGA	General Gradient Approximation
HF	Hartree Fock
HOMO	Highest Occupied Molecular Orbital
KS	Kohn Sham
LDA	Local Density Approximation
LMW	Low molecular weight
LUMO	Lowest Unoccupied Molecular Orbital
MP	Monkhorst Pack
MP2	Møller Plesset 2
NEB	Nudged Elastic Band
NOM	Natural Organic Matter
PAW	Projector Augmented Wave
PBE	Perdew Burke Ernzerhof
PDOS	Partial Density of States
PW91	Perdew Wang 1991
QDs	Quantum Dots
SRHA	Alginate and Suwannee River humic acid
TDOS	Total Density of States
TF	Thomas Fermi
TiO2	Titanium dioxide
XC	Exchange Correlation

List of Figures

List of Tables

Table of Contents

Chapter 1: Background

1.1 Introduction

The usage of nano-based products is increasing each day and that leads to the possibility of engineered particles imminent into interaction with human beings and the surroundings (Nel et al. 2009, Mitrano et al. 2019). Ag ENPs are commonly used in several household daily applications such as paints, and in textiles (Donia and Carbone 2019). Even though engineered nanoparticles have many positive applications in our day to day activities, it has been shown on numerous times that engineered nanoparticles may become separated from their product matrices (Benn and Westerhoff 2008, Kaegi et al. 2010, Wu et al. 2019) which contributes to their spreading in the environment. It is enviable that engineered nanoparticles final destination is the environment and when they get into the natural aquatic environments encounter various factors such temperature, pH, concentration, ionic strength, natural organic matter etc. All the above mentioned factors are likely to impact engineered nanoparticles strength in the environment. There is a need for an in depth fundamental understand of the factors that control the removal and release behaviors of ENPs such as silver and gold and it is essential to envisage their conveyance and fate in both natural and aquatic surroundings.

In aquatic systems, ENPs undertake dissimilar likely organic processes and might harmfully influence aquatic environments (Tsyusko et al. 2012, Zhao et al. 2011, Zhao et al. 2013). A lot of studies have investigated environmental transformation methods of ENPs and discussed the importance of natural organic matter in these methods (Tangaa et al. 2016, Espinasse et al. 2018, Wu et al. 2019). The environmental methods of ENPs that are heavily influenced by NOM include but not limited to adsorption, dissolution, stabilization and surface transformation (Levard et al. 2012, Odzak et al. 2014, Francioso et al. 2019, Khan et al. 2019). Furthermore, the modification of the stated methods by NOM in turn is expected to influence the toxicity of ENPs in aquatic systems. Even though a lot has been done to understand the mechanism of the interactions between ENPs and NOM's, a lot more still needs to be done to have a clear understanding (Gajewicz et al. 2012). Therefore, computational (*in silico*) studies have been proposed as useful tools to gain further insight on the interaction of engineered nanoparticles with natural organic matter that are not possible to

probe experimentally (Barnard 2009). Computational modelling of the properties of ENPs allows prediction of biological effects (Barnard 2009, Sangani et al. 2019).

1.2 Problem statement

The release of ENPs into aquatic environment poses new environmental problems that warrants an investigation. It is inevitable that the fate and behavior of Ag ENPs in aquatic systems will be influenced by various environmental methods which include but not limited to adsorption, aggregation, disaggregation, dissolution and surface transformation etc and their interaction with natural organic matter (NOMs). From the above mentioned environmental processes, the scope of this thesis is only limited to adsorption process. Several efforts have been made to understand interactions between Ag ENPs and NOM (Shakiba et al. 2018). Knowledge about the understanding of interactions of NOM and ENPs is still lacking (Alizadeh, Ghoshal, and Comeau 2019, Chen et al. 2019).

1.3 Aims and objective(s)

The main objective was, to generate descriptors that can offer insights and enhance our understanding as well as account at a fundamental level interaction of engineered nanoparticles. In order to meet this objective, the following sub objectives were used;

- To study the interaction of Ag nanoparticles with low molecular weight natural organic matter (formic acid, acetic acid and ascorbic acid) using first principles calculations (**Publication 1 in Appendix B**).
- To model the interaction of high molecular weight NOM's (HA , FA and Cry) on Ag (111) surface (**Publication 2 in Appendix B**).
- To investigate the adsorption and co-adsorption of single and multiple NOM's on Ag (111) surface (**Publication 3 in Appendix B**).

1.4 Rationale/Significance/relevance

Due to their antimicrobial properties Ag ENPs, there is a growing usage of ENPs which then inevitable leads to their discharge into aquatic systems and much attention has focused on the their potential influence on the environment (Su-juan Yu, Yin, and Liu 2013, Cornelis 2015). The need for computational models is not to replace experimental studies but to complement them. The information gained from *in silico* studies may be a useful reference in designing experiments on the influence of different NOMs on the ENPs fate in aquatic systems.

Ag ENPs exhibits different shapes such as cubooctahedral, multiple-twinned decahedral, quasi-spherical shape with pre-dominant (100) facets along a small percentage of (111) facets and rod-like shapes e.g., pentagonal rods which have side surfaces and ends, respectively, bounded by (100) facets and (111) facets (Wiley et al. 2005). Previously Pal et al (Pal, Tak, and Song 2007), and colleagues investigated the effects of Ag ENPs and showed shape-dependent interactions with *Escherichia coli* primarily due to marked differences in reactivity of different crystal facets. In particular, the (111) facet was found to have induced the most significant antibacterial activity linked to high atoms density (Pal, Tak, and Song 2007). Similarly Morones et al (Morones et al. 2005) demonstrated increased Ag ENPs toxicity to several bacterial strains linked to higher reactivity presented by the (111) facets. In addition adsorption of NOM's onto different surfaces and different shapes of NPs is likely to play a significant role in elucidating the NPs' transport and fate in the environment (Hartmann et al. 2014).

1.5 Thesis outline

Chapter 2 details literature review of ENPs and their interaction with NOM's in the environment. Chapter 3 gives a detailed theoretical background and description of density functional theory. Chapter 4 outlines the methodology adopted in this study. Chapter 5 gives results and discussion. Lastly chapter 6 highlights overall general conclusions, the future research and perspectives, limitations of the computational techniques, recommendations, references and appendix B (published papers). Appendix A is only available in electronic version.

Chapter 2: Engineered nanoparticles (ENPs)

2.1 *In vivo* **and** *in vitro* **studies on engineered nanoparticles**

Engineered nanoparticles gradually used in a number of medical applications disease diagnoses, and drug delivery (Ollikainen et al. 2017). Silver engineered nanoparticles are being used in various *in vitro* studies to determine their anti-microbial activities like antibacterial, antifungal, antiviral (Lakshmanan et al. 2018, Behravan et al. 2019). Over the years a lot of research has been done to study engineered nanoparticles using *in vitro* (word performed outside of a living organism) and *in vivo* (work is done with or within an entire, living organism). *In vitro* investigations adopts some explanations with respect to *in vivo* techniques but can expose suggestions about the potential effects or risk their use (Abad-Álvaro et al. 2019). A great number of studies have used *in vitro* incorporation representations (Puchana-Rosero et al. 2016, Z. Zhang et al. 2019) to observe changes of silver engineered nanoparticles after development in imitation environments mimicking the altered intestinal positions. Aggregation of engineered nanoparticles during *in vitro* incorporation in manifestation of nutrition by small-angle X-Ray scattering has been also explained (Puchana-Rosero et al. 2016). A number of studies have established that silver engineered nanoparticles go through processes of agglomeration (Puchana-Rosero et al. 2016), Ramos, Ramos, and Gómez-Gómez 2017). It has been found that in biological environments, a number of engineered nanoparticles are not colloidally stable and have a tendency to agglomerate or even precipitate (Feliu et al. 2016). The most used approach to avoid agglomeration of engineered nanoparticles and to grow the biocompatibility of engineered nanoparticles in biological environments is the encapsulation of the engineered nanoparticles with a covering that contains organic coatings materials such as lipids, proteins, or synthetic polymers (Valdiglesias et al. 2015, Ali et al. 2016, Mohammed et al. 2017). A recent *in vivo* study by (Abad-Álvaro et al. 2019) planned to govern the influence of silver release in the animal and eradication by the faeces, as a result transformations between the two nanocomposites in the segments considered in the *in vitro* tests could be likened to *in vivo* absorption and elimination values.

A clear understanding of the risks of exposure to engineered nanoparticles is very crucial for eluding potential contrary effects and for the development of safety guidelines and appropriate regulation of engineered nanoparticles applicability in user goods (Lojk et al. 2020). A study by (Lojk et al. 2020) reported that toxicity of engineered nanoparticles cannot simple be attributed to engineered nanoparticles characteristics rather to engineered nanoparticles nature of complication and cells, the assessment needs *in vitro* and *in vivo* analysis for each unique engineered nanoparticle type. The toxicity of engineered nanoparticles vary with their size and surface properties, and those relations hold true from corner to corner a spectrum of *in vitro* to *in vivo* nanobio interfaces (Zhu et al. 2013). The impact of engineered nanoparticles on toxicity in terms of their size, surface area and other physicochemical properties are well recognized from *in vitro* and *in vivo* studies (Gatoo et al. 2014), (Petschenka and Agrawal 2016). Even though *in vitro* and *in vivo* findings can provide us with very useful information but are still limited to help prediction of certain physicochemical properties on the cellular behaviour of engineered nanoparticles especially on the methods of biotransformation and removal of engineered nanoparticles (Zhu et al. 2013).

With the marked increase in the number of nanoparticle-enabled products and their sale in global markets, there is need to understand the impacts that engineered nanoparticles (ENPs) released as waste after product on different organisms in the environment. *In vivo and in vitro* experiments have thus far been at the fore front in trying to understand the interactions between engineered nanoparticles' interaction and natural organic matter (NOM) in aquatic systems.

However, although these experiments have received some measure of success in explaining the interaction of ENPs with NOM, the experimental fate studies are not only laborious, time-consuming but also resource-intensive. In addition, at times these experiments are coupled with uncertainties as to why a particular phenomenon is observed at particular experimental conditions. There is therefore a need for the development of computational (*in silico*) models to predict the fate and behaviour of ENPs in the aquatic systems. *In silico* approaches such as density functional theory (DFT) and molecular dynamic (MD) which have been used in this thesis have been successful in aiding experiments in surface science and catalysis, hence the motivation to employ them to investigate the fate and behaviour of ENPs in the aquatic systems.

2.2 Silver engineered nanoparticles in aquatic environments

2.2.1 Introduction

The wide applications of nanotechnologies and developing market demand for nano-enabled products, have steered to a substantial growth in the production of engineered nanoparticles (ENPs) and their use in consumer products (Sargent Jr, 2013, Contado 2015). Engineered silver nanoparticles (Ag ENPs) are among the most produced and widely used in consumer products and industrial applications (Vance et al. 2015, Hansen et al. 2016). As stated above nowadays, ENPs finds numerous applications in textiles, food packaging, cosmetics, medical devices, and household appliances (Duncan & Pillai 2014, Peters et al. 2018). Many previous studies have confirmed that silver has excellent antimicrobial activities (Cho et al. 2005, Maneerung et al. 2008) mainly due to silver ion (Ag^+) release (Lok et al. 2006, Yang et al. 2012). However, with the increase ENPs applications, and in turn, their release into the environment, to date there is vast information on the subject but does not account the fundamental basis on the mechanisms underpinning the interactions of ENPs and NOM, as that is among the key processes that influence the stability of ENPs in the aquatic systems (Z. Wang et al. 2016). Therefore, in light of these limitations of the current studies forms the underpinning objectives of this study.

Natural Organic Matter is ubiquitous in aquatic systems (Beckett and Le 1990) and consists of low molecular weight (LMW) NOM (e.g. formic acid, acetic acid and ascorbic acid) and high molecular weight (HMW) NOM such as natural polymers; hence they have a wide range of MWs from < 100 Da to > 300 kDa (Mostofa et al. 2013). The high diversity of NOMs MW in the aquatic systems have been reported to exert distinctive implications on the stability of ENPs such as Ag ENPs (Yin et al. 2015). In relation to hydrophilicity NOM is classified as a combination of organic compounds that occurs commonly in ground and surface waters. According to (Krasner et al. 1989), NOM has a potential to cause serious challenges as it is transformed into disinfection by-products (DBPs) when chlorine is cast-off during water treatment. The NOM present in water comprise of both hydrophobic and hydrophilic constituents where the major portion is mostly hydrophobic acids, which makes up approximately half of the dissolved organic carbon (DOC) (AIKEN 1985). These can be defined as the humic substances containing of humic and fulvic acids (Lavanya et al. 2019).

Even though a lot of improvement has been made in trying to understand the interaction of ENPs with NOM, there are still major knowledge gaps for even the most widely used ENPs involving their postproduction life cycles, including entry into the environment, environmental pathways, eventual environmental fate and potential ecotoxicological effects.

2.2.2 Sources and release of Ag ENPs

Engineered nanoparticles are everyday goods such as cleaners, sunblock creams and widely used in industry field such as solar cells and electronic devices (Ghosh Chaudhuri & Paria 2011, Yu et al. 2013). ENPs are being used in many modern fields such as the ones stated above which have prompted enormous applications because of their distinctive physicochemical and structural properties (Yu et al. 2017, Khan et al. 2018), increasing their potential for environmental release (Supiandi et al. 2019). Ag ENPs have already been detected in natural waters (Pasricha et al. 2012, Gondikas et al.2014). Once released into the environment, Ag ENPs would undergo different pathways during transport. They may remain as individual particles in suspension and be delivered long distances (Sujuan Yu et al. 2017), or tend to aggregate at high ionic strength (Khaled Abdella Ahmed et al. 2018). After contact with oxygen and other oxidants, partial oxidation and Ag^+ dissolution is also expected. Most probably, Ag ENPs would react with sulfide, chloride or other natural substances, altering the original properties of the nanoparticles (Wei et al. 2015).

The behaviour of the Ag ENPs basically relies on the properties of the engineered nanoparticle themselves and the surrounding environment, including capping agents, electrolyte composition, solution ionic strength, pH and NOM (Su-juan Yu, Yin, and Liu 2013).When engineered nanoparticles are released into the environment, NOM is expected to attach on the surface of ENPs and change the physiochemical properties of ENPs and the interfacial forces or energies between interacting ENPs by altering the aggregation behaviour (Louie et al. 2015). Experimental studies have shown the pH, ionic strength, electrolyte valence and NOM content of an aquatic system to control the surface charge and aggregation state of ENPs. In these studies NOM has been found to influence ENPs stability and surface chemistry for carbon-based nanomaterials (Saleh et al. 2008, Baun et al. 2009, Saleh et al. 2010) and metals (Johnson et al. 2009, Liu et al. 2010).

Figure 2.2.2.1 below shows a schematic representation of ENPs after being released from different sources to the environment.
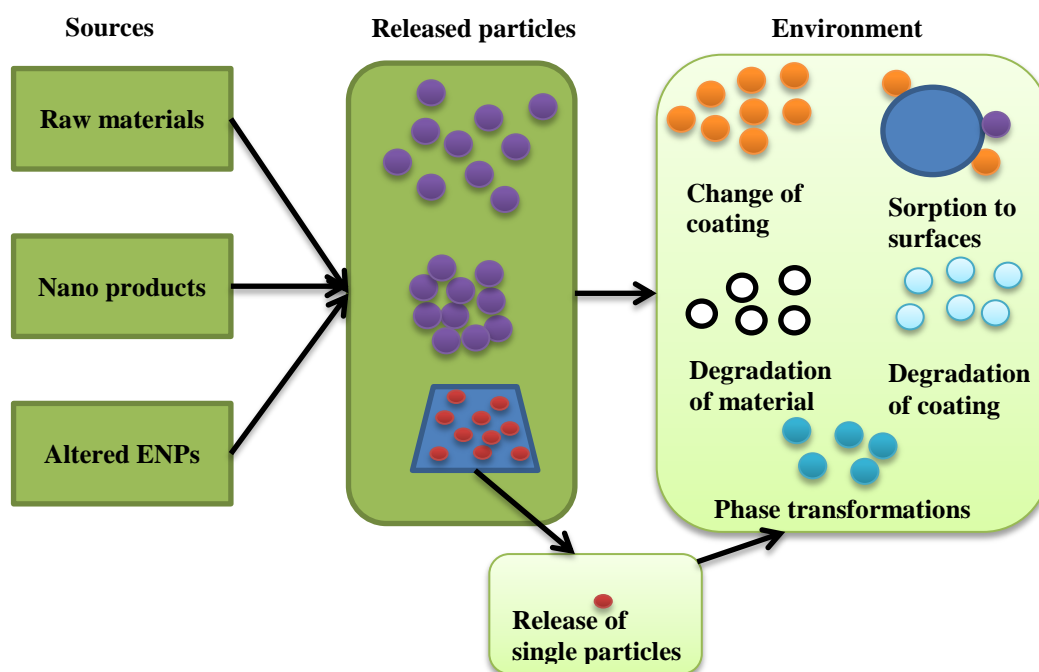
Figure 2.2.2.1: A brief summary of ENPs after are being released from various sources in various forms that are altered by environmental alteration reactions (Westerhoff and Nowack 2012).

Till now numerous scholars have tried to envisage or measure the environmental concentration of silver in aquatic systems. A summary of some of the previous predicted or measured environmental concentrations of Ag ENPs in aquatic systems are presented in Table 2.2.2.1.

Table 2.2.2.1: Shows various modelled and measured environmental concentration of Ag ENPs in aquatic systems.

Modelled	Measured	Reference
0.03–0.08	Not available	Mueller & Nowack 2008
Not available	0.013-0.10	Tiede et al. 2012
0.05–0.20	Not available	Gottschalk et al. 2013
0.00051– 0.00094	Not available	Wagner et al. 2014
0.0001–0.044	Not available	Gottschalk et al. 2015
Not available	0.10	Donovan et al. 2016
0.0004–0.0028	Not available	Sun et al. 2016
0.0003– 0.0025	Not available	Peters et al. 2018

2.3 Environmental transformation of engineered nanoparticles in aquatic environment.

2.3.1 Introduction

Transformations in the environment are very broad and can be divided into chemical, physical and biological processes. Chemical transformations consist of oxidation–reduction reactions and dissolution (Brezonik 2018). Physical transformations include aggregation or disaggregation and adsorption of naturally occurring macromolecules. Biological interactions of NMs can result in additional physicochemical transformations (Louie, Ma, and Lowry 2014). Physical changes such as aggregation/agglomeration, sedimentation and deposition and chemical transformations such as dissolution, ligand exchange, biotic and abiotic redox reactions are estimated to affect the fate and persistence of engineered nanoparticles in the environment (Lowry et al. 2010, Zhang et al. 2018).

It is understandable that ENPs in an environmental matrix do not form a static system, a number of transformation processes will take place. Based on existing literature (Lowry et al. 2012, Nowack et al. 2012) the key transformation processes for ENPs, determining their fate and behavior in the environment have been identified. When ENPs are released to the aquatic medium they can undergo physical, chemical and biological transformations which affect their fate and behavior in the environment (Lowry et al. 2012, Sani-Kast et al. 2017). These transformations processes include dissolution, surface transformation, aggregation/de-agglomeration (Kunhikrishnan et al. 2015, Wang et al. 2016). Below is the brief description of the environmental processes that influence the fate and behavior of engineered nanoparticles in aquatic environment.

2.3.2 Dissolution

Dissolution is one of the main transformation processes of Ag ENPs in aquatic environments, which occurs through oxidation of metallic Ag and other metallic ENPs and release of Ag^+ ions. Dissolution of Ag ENPs is determined by the intrinsic physicochemical properties of Ag ENPs, such as shape, size, and surface coating, and water chemistry conditions, including concentration, electrolyte types, ionic strength, pH, temperature, NOM, and dissolved complexing ligands (Lowry et al. 2012, Levard et al. 2012, Shevlin, O'Brien, and Cummins 2018).The dissolution explained in this part does not involve oxidation or reduction but it

does involve the release of metal ion. Dissolution is one of the leading major potential passageways that engineered nanoparticles can follow in the environment and may translate to full depletion of the solid phase and precipitation of new chemical structures (Wagner et al. 2014, Gruiz 2019). It is a crucial process for the discharge of not only the components of a particles but also other kinds that may have adsorbed on the particles surface (Erbs et al. 2010, Mattsson et al. 2018). There are a number of particle and solution specific properties that control dissolution such as the solubility constant and specific surface area (Stumm and Morgan 2012, Gao and Lowry 2018). For instance dissolution is dependent on the specific surface area, dissolution rates are frequently concentrated by aggregation, attachment, and surface coverage by adsorbed organic compounds such as NOM (Wagner et al. 2014, Wang, Pan, and Gadd 2019).

A number of studies when it comes to dissolution of engineered nanoparticles have concentrated on silver. For metallic silver, oxidation by dissolved oxygen is the slowing down step, and dissolution amounts were established to decrease as the dissolved oxygen concentration decreased by the addition of natural organic matter or a reduction in temperature (J. Liu and Hurt 2010, Markiewicz et al. 2018). When Ag^+ ions are released from Ag ENPs they could undergo precipitation and complexation reactions with ligands such as sulfide, chloride, cysteine, and phosphate ions, thereby mitigating the toxic effects (Xiu et al. 2011, Levard et al. 2013, Zhou et al. 2016).

2.3.3 Surface transformation, aggregation/de-agglomeration

Even though it is clear that transformations will depend on the nature of the ENPs and the environmental conditions, the involvedness and changeability of both these factors make understanding and prediction extremely challenging (Lead et al. 2018). Engineered nanoparticles such as ZnO, whereby their toxicity has been fundamentally credited to the ions (Franklin et al. 2007), and solubility has a major influence on fate and toxicity. Numerous studies have revealed the role of NOM such as humic and fulvic acids in stabilizing ENPs against aggregation (Domingos et al. 2009, Angel et al. 2013, Yang et al. 2017), through both charge and steric repulsion. A study by (Wagner et al. 2014) found that the stability and movement of particles in aqueous environments are controlled by the particle number concentration, the charge, and the structure of the particle surface. Another study by (Thio, Zhou, and Keller 2011) discovered that the most significant key environmental factors

controlling their stability are pH value, ionic strength, and NOM, the pH value and ionic strength are known for affecting the natural organic matter, steric particle-particle interactions and surface charge.

2.3.4 Adsorption

Adsorption is one of the environmental processes for determination of the behavior and fate of ENPs after being released into aquatic environments and it has been the focus of this study. It is almost impossible to find pristine ENPs in natural waters because ubiquitous NOM molecules are able to easily coat onto ENPs (Wang et al. 2016). Adsorption of macromolecules such as NOM or organic and inorganic ligands on ENPs surfaces can considerably affect their surface chemistry and behavior in biological and environmental systems (Lowry,et al. 2012).

As clearly stated above interactions of ENP with NOMs will take place soon after the ENPs are released to the environment. The interactions that take place are explained as an adsorption of other materials onto ENPs (Hartmann et al. 2014). This remains for instance the case of the used NOM's in this theses for the binding of low molecular weight NOM such as formic acid, acetic acid, ascorbic acid and high molecular weight NOM natural organic matter such as humic acid, fulvic acid and protein cryptochrome to ENPs (Hartmann et al. 2014). Surely the interaction with NOM in the environment will alter the surface properties, fate and behavior of the ENP and influence its interactions with other particles and surfaces like agglomeration and the surrounding media such as dissolution, and in turn be determining for its environmental such as sedimentation (Hartmann et al. 2014). Table 2.3.4.1 below summaries the interactions of ENPs with NOM.

Table 2.3.4.1: Processes accounting the interaction of NOM and ENPs

NOM	ENPs	Type of interaction	Reference
Humic substances	ZnO NPs, Al2O3 NPs,	Electrostatic interaction	Yu et al. 2017
	Carbon nanomaterials (CNMs), quantum dots (QDs)	Hydrophobic interaction	Yang and Xing, 2009
	Carbon nanomaterials (CNMs)	Hydrogen bonding	Wang et al.,2011a
Humic acid	Nano-TiO_2	Attraction/steric repulsion	Tan et al. 2018
,			
Fulvic acid	Nano-TiO_2	Attraction/steric repulsion	Tan et al. 2018
Citric acid	Nano-TiO_2	Attraction/steric repulsion	Yu et al. 2017
	CNMs	π–π attraction	Yu et al. 2017
Alginate and Suwannee River humic acid (SRHA).	TiO_2	exothermic binding reaction	Yu et al. 2017
SRHA	Silver (Ag)	Steric and charge stability	Cumberland & Lead 2009

Carbon nanomaterials (CNMs), quantum dots (QDs), Alginate and Suwannee River humic acid (SRHA)

Chapter 3: Application of electronic calculation to molecular surface interactions

3.1 Introduction

In silico electronic structure methods that can be used to calculate molecular surface interactions among them the molecular dynamics (MD), semi-empirical calculations, Monte Carlo methods, and density functional theory (DFT), just to mention a few. Each of these methods have varied degrees of strengths and limitations. These techniques have been used to obtain descriptors used in developing quantitative structure activity relationships (QSAR) in the fields of drug design, toxicity of materials among other applications (Puzyn et al. 2011, Afzal and Hachmann 2019 Ahamed, Rajan, and Muraleedharan 2019). The merits of the chosen technique are, it has been able to efficiently and effectively calculate a variety of properties of the nanoparticles, with acceptable levels of accuracy, which have been used as descriptors. In this thesis in order to achieve the objectives stated in Chapter 1 section 1.3, the methodology is discussed.

3.1.1 Density functional theory (DFT)

Density functional theory is one of the most used quantum mechanics techniques to examine the electronic structure of many-body systems (Brivio and Trioni 1999). To achieve the overall objectives of this study which are to calculate properties of materials which can in turn be used as descriptors, DFT has been used in all case studies more details are given under methodology (Chapter 4).

To date, the molecular Schrödinger equations have undergone a good degree of implementation with the discovery and use of a wide variety of *ab initio* and semi empirical quantum-chemical methods (Roothaan et al. 1960, Karelson et al. 1996). Semi-empirical calculations on a general structure as a Hartree-Fork (HF) calculation constitutes of a Hamiltonian and a wave function including the valence electrons (Sotomatsu, Murata, and Fujita 1989). Although DFT is formally exact, in practice, approximations are essential for

implementation purposes. These approximations, however, can lead to inaccuracies in the predicted properties of the system under question. DFT is different from other quantum mechanical approximations because it is a non-interacting theory which does not give rise to a correlated-body wavefunction (Dreizler & Gross 1990, Fulde 2012). Within the Kohn-Sham formalism (Hohenberg and Kohn 1964), DFT is a one-electron theory and it shares several similarities with HF theory.

3.1.2. Schrödinger equation and many-body problem

In order to generate properties of any time-independent quantum system which can in turn be used as descriptors, the first step is to solve Schrödinger equation using Hamiltonian operator (Schrödinger 1926).

$$H\varphi\ (\mathbf{x}1, \mathbf{x}2, \dots, \mathbf{x}N;\ \mathbf{R}1, \dots, \mathbf{R}Nn) =\ E\ \varphi(\mathbf{x}1, \mathbf{x}2, \dots, \mathbf{x}N;\ \mathbf{R}1, \dots, \mathbf{R}Nn) \qquad (3.1)$$

H is the Hamiltonian,

$\Psi(\mathbf{x}_1, \dots, \mathbf{x}_N)$ is the wavefunction satisfying the many-electron time-independent Schrödinger equation

N-electron system,

E is the total energy,

RNn is the recurrent neural network

It has been proven over years that it is practically impossible to solve Schrödinger equation (3.1) for any structure greater than hydrogen atom and hence it cannot be solved without making approximations.

3.1.3 Born-Oppenheimer approximation

As explained in 3.1.2, Schrödinger equation in 3.1 cannot be solved without approximation, the first approximation to make to attempt to solve Schrödinger equation for more than one electron system is Born-Oppenheimer (Born and Oppenheimer 1927). In Born-Oppenheimer approximation the nuclei are preserved as immovable in relation to the electrons. In this approximation, the electronic structures are explained by making use of plane wave functions. Born Oppenheimer approximation helps Schrödinger equation to decrease to

descriptions of divided nuclei and electron systems. It is known that masses of nuclei are very large and the nuclei travel considerable more slowly compared to electrons, according to the Born-Oppenheimer, the system can be well described by the motion of electrons alone and the kinetic energy of nuclei can be ignored in the Hamiltonian.

Hamiltonian can now be expressed as;

$$H = T_e + T_N + V_{eN} + V_{ee} \tag{3.2}$$

Therefore:

$$H = -\frac{\hbar^2}{2m_e}\sum_{\mu=1}^{N_e}\nabla_\mu^2 + -\frac{\hbar^2}{2}\sum_{k=1}^{N_n}\frac{\nabla_k^2}{m_k} + -\sum_{\mu=1}^{N_e}\sum_{k=1}^{N_n}\frac{Z_k e^2}{4\pi\varepsilon_0\,|\vec{r}_\mu - \vec{R}_k\,|} + \sum_{\mu=1}^{N_e}\sum_{v>\mu}^{N_e}\frac{e^2}{4\pi\varepsilon_0\,|\vec{r}_\mu - \vec{r}_v\,|} \tag{3.3}$$

Where:

M_k – represents the ratio of the mass of nucleus K to the mass of an electron

Z_k – represents the atomic number of nucleus K

T_e – represents the operator for the kinetic energy of the electrons

T_N – represents the operator for the kinetic energy of the nuclei

V_{eN} – represents the operator for the Coulomb attraction between electrons and nuclei

V_{ee} –represents the operator for the repulsion between electrons

V_{NN} –represents the operator for the repulsion between nuclei

With all the attempt made so far, it is still impossible to solve equation (3.3), more approximations are needed

3.1.4 Hartree approximation

Hartree (Hartree 1928) proposed the use of the molecular orbital (MO) method in order to approximate the wavefunctions. What makes Hartree approximation different it is the fact that it assumes that each electron moves independently within its own orbital and comprehends only an average field produced by entirely the supplementary electrons.

3.1.5 The Hartree-Fock method

Even though Hartree tried to solve complication of many-body Schrodinger equation, it fell short in meeting all the requirements the Pauli Exclusion Principle which is the importance of the spin-statistics connection (Pauli 1940) and plays a significant part in giving insights of many physical and chemical occurrences. In late 1920s, two uncomplicated particle-independent methods were discovered which are known as Hartree (Hartree 1928) and Hartree-Fock methods (Fock 1930). With all the promises, still both methods do not take into account the correlation among electrons, but Hartree-Fock method includes the antisymmetric property of the electronic wave function. Slater discovered that the resulting wavefunction was the determinant of a matrix, the Slater determinant (Slater 1929, Slater 1951). The wave function is expected to be a Slater determinant where φ_i are the spin orbitals and x_i includes both the space and spin coordinates.

$$\Phi(x_1,...,x_N) = \frac{1}{\sqrt{N!}} \begin{vmatrix} \varphi_1(x_1) & \varphi_2(x_1) & \cdots & \varphi_N(x_1) \\ \varphi_1(x_2) & \varphi_2(x_2) & \cdots & \varphi_N(x_2) \\ \vdots & \vdots & \ddots & \vdots \\ \varphi_1(x_N) & \varphi_2(x_N) & \cdots & \varphi_N(x_N) \end{vmatrix} \tag{3.4}$$

By taking out the nuclear kinetic energy and repulsion terms, a simplified Hamiltonian can be derived. The Hamiltonian is then reduced to a set of one-electron equations of the form:

$$\hat{H} = -\sum_{j=1}^{N} \frac{\nabla_j^2}{2} + \sum_{j=1}^{N} V(\mathbf{r}_j) + \frac{1}{2} \sum_{j \neq k}^{N} \frac{1}{|\mathbf{r}_j - \mathbf{r}_k|} \tag{3.5}$$

Solving the full many-body Schrödinger equation is impossible. Instead, apply a variational approach.

$$\frac{\delta}{\delta \varphi_j^*(\mathbf{r})} \left\{ \langle \Phi | \hat{H} | \Phi \rangle - \sum_{l=1}^{N} \varepsilon_l \int d^3 r \, \varphi_l^*(\mathbf{r}) \varphi_l(\mathbf{r}) \right\} = 0 \tag{3.6}$$

Below is the Hartree- Fock equation, also known as the self- consistent field (SCF) equation.

$$\left[-\frac{\nabla^2}{2}+V(\mathbf{r})+\int d^3r'\frac{n(\mathbf{r}')}{|\mathbf{r}-\mathbf{r}'|}\right]\varphi_j(\mathbf{r})-\sum_{k=1}^{N}\int d^3r'\frac{\varphi_k^*(\mathbf{r}')\varphi_k(\mathbf{r})}{|\mathbf{r}-\mathbf{r}'|}\varphi_j(\mathbf{r}')=\varepsilon_j\varphi_j(\mathbf{r}) \qquad (3.7)$$

Hartree potential: local operator

$$V_H(\mathbf{r})=\int d^3r'\frac{n(\mathbf{r}')}{|\mathbf{r}-\mathbf{r}'|} \qquad (3.8)$$

Nonlocal exchange potential, acting on the jth orbital. "Nonlocal" means that the orbital that is acted upon appears under the integral.

$$[\hat{V}_X^{nonloc}\varphi_j](\mathbf{r})=-\sum_{k=1}^{N}\int d^3r'\frac{\varphi_k^*(\mathbf{r}')\varphi_k(\mathbf{r})}{|\mathbf{r}-\mathbf{r}'|}\varphi_j(\mathbf{r}') \qquad (3.9)$$

The total Hartree-Fock ground-state energy is given by

$$E_{HF}=\sum_{i=1}^{N}\int d^3r\varphi_i^*(\mathbf{r})\left[-\frac{\nabla^2}{2}+V(\mathbf{r})\right]\varphi_i(\mathbf{r}+\frac{1}{2}\int d^3r\int d^3r'\frac{n(\mathbf{r})n(\mathbf{r}')}{|\mathbf{r}-\mathbf{r}'|}$$
$$-\frac{1}{2}\sum_{i,j=1}^{N}\int d^3r\int d^3r'\frac{\varphi_i^*(\mathbf{r}')\varphi_j(\mathbf{r}')\varphi_i(\mathbf{r})\varphi_j^*(\mathbf{r})}{|\mathbf{r}-\mathbf{r}'|} \qquad (3.10)$$

Even though the HF approximation is qualitatively correct, the single-determinant system of the wave function does not take the effect of correlations between electrons into account. This equates to the electronic structure not being accurately described.

3.1.6 Exchange-Correlation Functionals

In order to solve the Kohn Sham equations stated above and make the DFT theory to be used in practical calculation, numerous approaches to the exchange-correlation (X_C) functionals have been suggested and established. At present, there is no collective X_C functional for all systems to calculate the properties and all the approaches stated above have their own limitations. Substantial attempts have been made to expand the accuracy of DFT predictions by using better X_C potentials (Heyd et al. 2003, Paier et al. 2006, Perdew et al. 2008, Shang

et al. 2011). Table 3.1.6.1 describes the strengths and limitations of the mostly used X_C potentials.

Table 3.1.6.1: Strengths and limitations of local density approximation (LDA) and generalized gradient approximation (GGA).

Approximation	Strengths	Limitations	Reference
LDA	LDA approximation is precise, though some usual deficiencies, such as the poor elimination of self-interaction contributions.	In LDA, the correlation energy EC per particle is challenging to get independently from the exchange energy.	Sousa, Fernandes, & Ramos, 2007
	Appropriate for structures having slowly changing densities, but surprisingly good results for numerous structures with quite large density slopes have also been observed.	LDA inclines usually to underestimate atomic ground-state energies and ionization energies, while binding energies are normally overestimated.	Sousa, Fernandes, & Ramos, 2007
GGA	GGA method tends to offer better total energies, atomization energies, structural energy differences, and energy barriers.	With all the improvements, the precision of GGA method is still not sufficient for a correct explanation of many chemical aspects of molecules.	Becke, 1992,(Perdewet al., 1992,
	GGA is created on the adjustment of the LDA exchange-correlation hole, therefore its hole is local and it inclines to be an enhancement over the LDA when the LDA is a noble first-order approximation	When it comes to solid state, GGA functionals do not yield meaningfully better results than LDA, nor in the control of ionization potentials.	Perdew et al., 1992,Perdew, 1986

3.1.7 Local density approximation

As described in Table 3.1.6.1, because of its strength LDA is one of the approximations used to solve Schrödinger equation. One of its short falls is that it has a tendency to over-estimate bond strengths in non-metallic materials. Within LDA, the X_C energy for a given density is expressed as:

$$E_{XC}^{LDA}[\rho] = \int \rho(r)\varepsilon_{XC}(\rho)dr \qquad (3.11)$$

$\varepsilon_{XC}(\rho)$ represents the exchange –correlation energy of each electron and gas density

3.1.8 Generalized gradient approximation

In terms of accuracy, GGA outperforms LDA but it also has its limitations as explained in Table 3.1. The GGA approximation does not depend on the density but also on the density gradient $\nabla\rho$.

$$E_{XC}^{GGA} = \int \rho(\mathbf{r})\varepsilon_{XC}(\rho(\mathbf{r}),\nabla\rho(\mathbf{r}))d\mathbf{r} \qquad (3.12)$$

3.1.9 Basis sets

Within Material Studio, DMol3 has basis sets such as Minimal (MIN) which uses minimal basis set, it uses only atomic orbital for each orbital that is occupied in the free atom. Table 3.1.9.1 describes the strengths and limitations of MIN, Double numerical (DN) and Double Numerical Polarization (DNP). The DNP includes p-function on all hydrogen atoms and one of its advantages is that it has the best accuracy, one of its disadvantages is that it has the highest cost, it is important for hydrogen bonding (da Silva Ribeiro et al. 2014). Within DNP, the atomic energies are calculated, and then stored in the basis file. The calculated energies are exact atomic energies at the DFT level on a spherically symmetric grid (da Silva Ribeiro et al. 2014).

Table 3.1.9.1: Strengths and limitations of MIN, DN and DNP.

Basis set	Strengths	Limitations	Reference
Minimal (MIN)	Fast computation	Produces low accuracy	Delley, 1990, BIOVIA, 2016
Double numerical (DN)	Enhanced precision over MIN	Works well for the small clusters only	Delley & Steigmeier, 1995
Double Numerical Polarization (DNP)	It has the best accuracy	Highest cost	da Silva Ribeiro et al. 2014

Pseudopotentials are used reduce computational effort by replacing some basis functions with a simplified analytic or numerical form. The background elements over these functions need to be computed only once and are excluded from the self-consistent field procedure. Figure 3.1.9.1 depicts typical shapes for the all-electron orbitals and pseudo orbitals. Matrix elements of this potential can be computed efficiently.
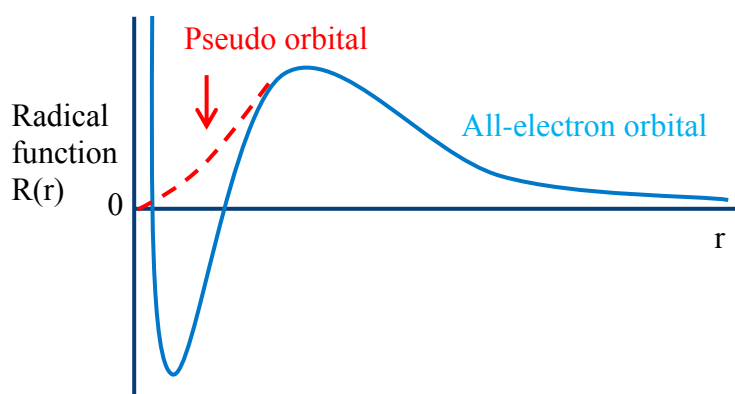
Figure 3.1.9.1: Typical shapes for the all-electron orbitals and pseudo orbitals.

3.2 Corrected density functional theory (DFT+D) and the associated flavours of DFT+D.

DFT+D also known as (DFT-D) has been developed by S. Grimme's unlike a standard DFT, the method uses density-independent dispersion corrections, as its name suggests, this method has quite significant impact in correcting a standard DFT (Grimme 2006, Grimme et al. 2010). In this study, only DFT-D has been used, below is the list of other DFT-D associated flavours that have not been used in this thesis. DFT-D2 (Grimme 2006), DFT-D2 shows a long-range behaviour $C_{6,ij=}$ R_{ij}^6 where $C_{6,ij}$ is the dispersion coefficient and R_{ij} is the distance between the atoms (Van Troeye, Torrent, and Gonze 2016). This method has been found to give way better agreement with the experiments than DFT for utmost non-covalently bound systems, DFT-D2 method only make use of one coefficient for each chemical pair and thus may not be able to catch fundamental trends of these interactions.

According to (Gobre and Tkatchenko 2013) dispersion coefficient can alter by a feature of two in the instance of armchair carbon nanotubes depending of their size. Another associated flavour of DFT-D is DFT-D3 (Goerigk and Grimme 2010), in this flavour the problem is

undertaken with the use of environment dependent dispersion coefficients. All the stated scenarios above, what is important is to take the corrections into account in the computation of atomic derivative-related quantities like forces, stresses, interatomic force constants, dynamical matrices, or elastic tensor (Van Troeye, Torrent, and Gonze 2016).

3.3 The theory of conductor-like screening model (COSMO)

What sets COSMO methods apart from other dielectric methods is the fact that COSMO removes the outlying charge error, which is instigated by small parts of the electron density of the solute lying outside the cavity (Klamt and Schüürmann 1993). The exterior charges are the calculated straight from the electrostatic potential of the charge distribution within the cavity (Andzelm, Kölmel, and Klamt 1995). The COSMO methodology is relevant in this study because it defines the solvent response ground by means of obvious separation charges distributed on the hollow surface that are resolute by commanding that the total electrostatic likely abandons out on the surface. The electrostatic quantity of the solvation energy is a quadratic purpose of the solute charge sprinkling and it can be comprised in the solute Hamiltonian (Andzelm, Kölmel, and Klamt 1995).

3.4 Frontier molecular orbital analysis

Using the highest occupied molecular orbital (HOMO) and the lowest unoccupied molecular orbital (LUMO) within Frontier Molecular Orbital (FMO) theory (Fukui 1992) the HOMO-LUMO interactions of the adsorbates were investigated. The focus on the Frontier orbitals (HOMO and LUMO) was due to their effect on the reaction mechanisms of molecules; which largely accounts for many chemical and optical properties of the molecule. For example, HOMO and LUMO levels can thus be used predict chemical activity of a molecule under different exposure media (Zarrouk et al. 2012). This means different molecules will have different values for the HOMO and LUMO. According to FMO theory, chemical reactivity is as a result of electron transitions due to HOMO-LUMO interaction (Musa et al. 2010).

The energies of the HOMO, E_{HOMO}, and LUMO, E_{LUMO} are related to the ionization potential (IP) and the electron affinity (EA) in that: IP = - E_{HOMO} and EA = - E_{LUMO}; respectively. IP is the minimum energy required to remove an electron from the ground state of the molecule, and EA is the energy released when an electron is added to a molecule. For EA > 0 signifies the addition of an electron releases energy which results to stabilization of the molecule.

The parameters consist of IP, EA, the HOMO-LUMO gap, E_{LUMO}-E_{HOMO} or IP-EA, (ΔE), dipole moment (μ), Molecular Surface Area (MSA), and absolute electronegativity (χ). Notably, the μ and χ are a measure of polarity of a polar covalent bond, and the chemical property that describes the ability of a molecule to attract electrons towards itself in a covalent bond, respectively (Geerlings and De Proft 2002) η is the absolute hardness, and ΔN denotes the number of electrons transferred. The number of transferred electrons were calculated using the expression below results are shown in Table A25 (Appendix A).

$$\Delta N = \frac{\chi_{Ag} - \chi_{ads}}{2(\eta_{Ag} + \eta_{ads})} \qquad (3.13)$$

where χ_{Ag} and χ_{ads} denotes the absolute electronegativity of silver and the adsorbate molecule, respectively; η_{Ag} and η_{ads} are the absolute hardness of silver and the adsorbate molecule, respectively. The frontier orbital energies E_{HOMO} and E_{LUMO} are shown in Table 5.1.3.6, according to the Koopman's theorem (Sastri and Perumareddi 1997) these quantities are related to electron affinity (EA) and ionization potential (IP) as follows:

$$\chi = \frac{IP + EA}{2} \qquad (3.14)$$

$$\eta = \frac{IP - EA}{2} \qquad (3.15)$$

IP and EA are related in turn to E_{HOMO} and E_{LUMO} as $IP = -E_{HOMO}$, and EA $= -E_{LUMO}$

$$\Delta E = E_{HOMO} - E_{LUMO} \qquad (3.16)$$

The equations stated above were used derive the results for the descriptors presented in Chapter 5

Table 3.4.1 shows studies where DFT and DFT-D have been successfully applied in describing molecular surface interactions, DFT has been adopted as a method of choice to calculate the properties of Ag (111) surface and Ag ENPs interacting with natural organic matter, where some of the calculated properties will be then used as descriptors.

Table 3.4.1: DFT application to molecular surface interactions.

Method	Key findings	Descriptors derived	Reference
DFT-D	The results of global reactivity descriptors showed that a change from the gas phase to water the chemical hardness decreased and decreased while the electrophilicity increased.	HOMO, LUMO, Eg, absolute hardness, chemical potential and electrophilicity	Chermahini, Teimouri, and Farrokhpour 2015
	This study found that the solvation energy and adsorption energy values suggest that the BN sheet is more suitable as an adsorption surface for amino acids and also the electronic changes have been monitored through the HOMO–LUMO gap and work function.	HOMO–LUMO gap and work function	Singla et al. 2016
DFT	They observed that thermodynamically, H2O adsorbs dissociatively on ZrO_2 (111), but in the presence of Ni both dissociated and molecular H_2O can coexist. On the other hand, molecular water is likely to be present on YSZ (111) and Ni/YSZ (111), depending on the experimental conditions.	Adsorption energy, Electron localization, Total density of states (DOS), projected DOS	(Cadi-Essadek, Roldan, and de Leeuw 2016)
	They found that corrosion inhibitor molecules preferably adsorb on the grain boundary with the larger distortion degree and more adsorption sites.	Work function, Adsorption energies, HOMO, LUMO, Fukui indices	(Wang et al. 2018)

Chapter 4: Computational details (Methodology)

4.0 Introduction

This chapter presents the calculation details for the calculations carried in this study. It also explains how adsorbates, pristine Ag nanoparticles and Ag (111) surface were optimized and the total energies were obtained. Even though computational details are very similar for each case study, each case study had its unique computational details and unique set of parameters, this chapter gives a brief overview of computational details for each case study.

4.1 Computational details for case study one

All calculations were performed with the DMol3 module (Biovia 2016) as implemented in Materials Studio BIOVIA (Biovia 2016). Since the adsorbate can be adsorbed at different locations on the ENPs surfaces, the adsorption locator (AL) module within Materials Studio BIOVIA (Biovia 2016) was used to obtain the best adsorption site on the surface hereafter referred to as a configuration. The AL utilizes Monte Carlo within a lattice dynamics approach to obtain the best configuration, which, in turn, was used as an input for the DFT calculations. The theoretical face centered cubic (fcc) lattice constant was obtained following unit cell optimization estimated to be 4.02 Å; and in good agreement with results of (Haas, Tran, and Blaha 2009) at 4.01 Å.

4.1.1 The unit cell

The unit cell of bulk silver was optimized with a 12 x 12 x 12 Monkhorst-Pack (Monkhorst and Pack 1976) mesh of k-points and kinetic energy cut-off of 4.5 Å the unit cell was then relaxed using the conjugate gradient method until the total forces acting on each atom was less than 0.02 eV/ Å. The bulk Ag optimized structure shown in Figure 4.1.1.1 was used to build Ag surfaces explained in the following section. The bulk silver in Figure 4.1.1.1 was then used to build surfaces and nanoparticles of different shapes.
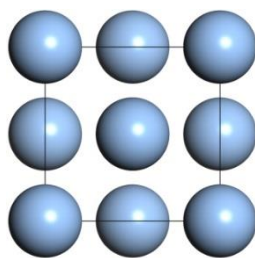
Figure 4.1.1.1: Schematic representation of Bulk Ag.

4.1.2 Surface construction

After optimizing the unit cell, surfaces were constructed using a 3×3 supercell consisting of five layers, where the top two layers of the surface were allowed to relax without and with the adsorbed molecules. The remaining three substrate layers were frozen and a vacuum distance of 15 Å was used. Spherical, cylindrical and tetrahedron engineered nanoparticles were constructed with the (111) surface as the bonding surface. The most stable planer surface of Ag (111) surface was identified by obtaining the equilibrium properties of bulk Ag. In Figure 4.2 we constructed low index surfaces such as (100), (110) and (111) surfaces but we only considered (111) surface and all structures were geometrically optimized by solving the Kohn−Sham equation self-consistently under spin-unrestricted conditions (Ordejón, Artacho, and Soler 1996, Kohn and Sham 1965). Different planar surfaces of Ag ENPs (100), (110) and (111) are shown in Figure 4.1.2.1 and the adsorption energies were calculated using the expression equation 4.1
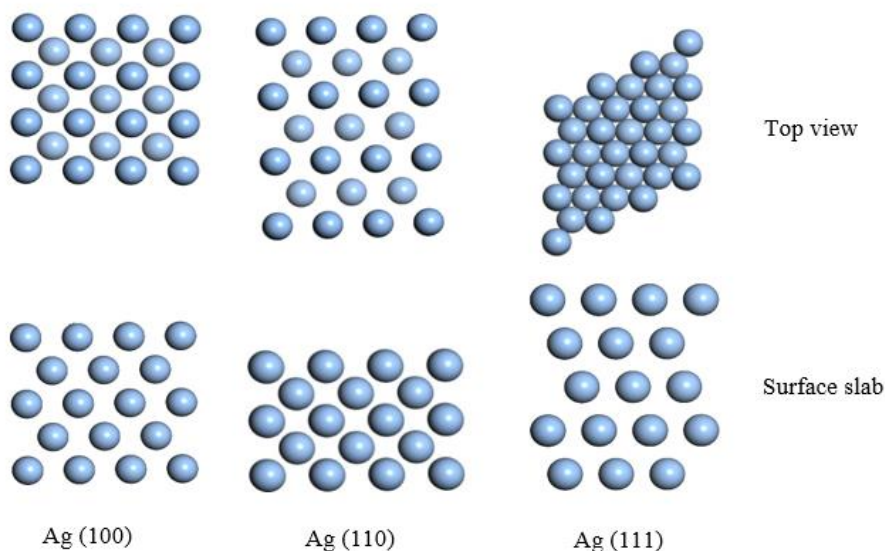
Figure 4.1.2.1: Showing relaxed surfaces of both top and side views of low-index surface.

27

$$E_{ads} = E_{adsorbate} + E_{surface} - E_{adsorbate/surface} \qquad (4.1)$$

The exchange-correlation energy was approximated using the PW91 generalized gradient approximation (GGA) (Perdew and Wang 1992). A double-numeric quality basis set with polarization functions was chosen (Lu et al. 2016). Core electrons were treated with DFT semi core-pseudo potentials (DSPPs) (B Delley 2002). Spin polarization was also applied, and real space cut-off radius was maintained at 4.5 Å. Convergence accuracy of energy was set as $1.0e^{-5}$ Ha, while the energy gradient and atom displacement were set as 0.002 Ha/Å and 0.005 Å, respectively. To accelerate convergence speed of charge density of self-consistent field calculation time and enhance efficiency, direct inversion of iterative subspace (DIIS) was used. Using the bulk optimized structure and the relaxed Ag ENPs (111) surface (stable surface) yield different geometrical pristine shapes investigated in this study shown in Figure 4.1.2.2.

(a)	(b)	(c)
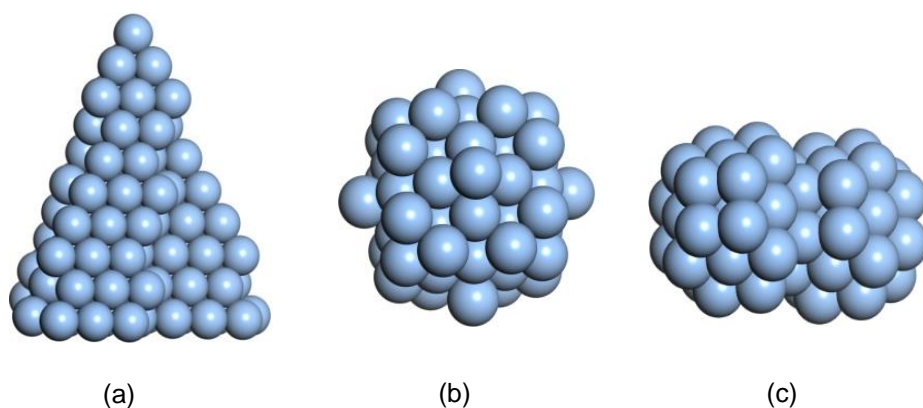
Figure 4.1.2.2: Pristine (a) tetrahedron (b) sphere (c) cylinder.

4.1.3 Optimization of Ag (111) surface with adsorbates

As explained in section 4.1.2, Ag (111) surface was constructed using a 3x3 unit cell to adsorb low molecular weight NOM's (formic acid, acetic acid and ascorbic acid) using the adsorption locator module, and configurations with minimum energy for the adsorbates on the Ag (111) surface are shown in Figure 4.1.3.1. The obtained minimum energy configurations from the adsorption locator calculations were then used as inputs for DFT calculation where the atomic positions of the adsorbates and surface atoms were relaxed at constant volume. Using the adsorption locator as already mentioned allowed different adsorbate-sorbate configurations to be generated via Monte Carlo technique as embedded

within the module, to relax with respect to all degrees of freedom (including rotations of the adsorbate on the surface) without additional constraints. The minimum energy configurations of the sorbate adsorbate systems were obtained using the adsorption locator, which one of the modules with Material Studio. This was done for instance, in the case of placing ascorbic acid on Ag (111) surface. A series of configurations were obtained as listed in Table 4.1.3.1 The best configuration was the one with the most negative adsorption energy, so from Table 4.1.3.1 only the first adsorption energy (-69.567 mV) were used as DFT input to get the total energies for DFT using DMol^3 code. Similar approach was followed in dealing with other adsorbates and the different configurations derived are summarized in Tables (A.1-A.24, B.1-B.3 and C.1-C.15) in the electronic version A, B and C, respectively that accompany this thesis.

Top view

Surface slab

(a)   (b)   (c)
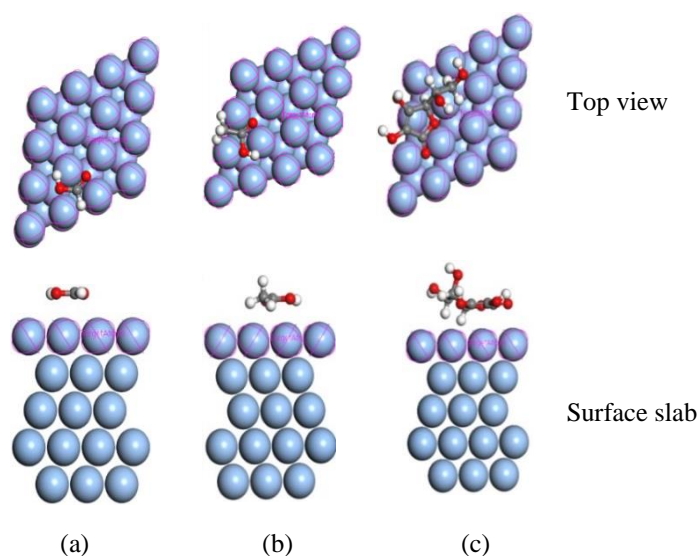
Figure 4.1.3.1: Shows (a) formic acid (b) acetic acid and (c) ascorbic acid adsorbed on Ag (111) surface slab with the top and side view (color code;oxygen: red, grey: carbon and white: hydrogen).

Table 4.1.3.1: Different configurations of Ag (111) surface when the ascorbic acid (AA2) was attached.

Structures	TE	Ads	RAE	DE	AA2 : dEad/dNi
Ag (1 1 1) - AA2 - 1	-30.92835639	-69.56749644	-52.72580615	-16.8416903	-69.56749644
Ag (1 1 1) - AA2 - 2	-29.71113474	-68.3502748	-50.98543449	-17.36484031	-68.3502748
Ag (1 1 1) - AA2 - 3	-28.90593146	-67.54507152	-53.12121462	-14.4238569	-67.54507152
Ag (1 1 1) - AA2 - 4	-28.22842513	-66.86756518	-52.63108961	-14.23647557	-66.86756518
Ag (1 1 1) - AA2 - 5	-27.71112826	-66.35026832	-50.22504463	-16.12522369	-66.35026832
Ag (1 1 1) - AA2 - 6	-27.12512961	-65.76426967	-52.28601924	-13.47825042	-65.76426967
Ag (1 1 1) - AA2 - 7	-26.8409285	-65.48006856	-47.21185318	-18.26821538	-65.48006856
Ag (1 1 1) - AA2 - 8	-25.72204061	-64.36118066	-48.51110938	-15.85007128	-64.36118066
Ag (1 1 1) - AA2 - 9	-25.15092031	-63.79006037	-48.31141508	-15.47864528	-63.79006037
Ag (1 1 1) - AA2 - 10	-22.76485026	-61.40399032	-43.31471353	-18.08927679	-61.40399032
Ag (1 1 1) - AA2 - 11	-22.56469285	-61.20383291	-43.16749363	-18.03633927	-61.20383291

NB: Total energy (TE), Adsorption energy (Ads), Rigid adsorption energy (RAE), Deformation energy (DE), Ascorbic acid (AA2).

4.2 Computational details for case study two

In this case study**,** calculations were performed using the DFT-D (Ortmann, Bechstedt, and Schmidt 2006, Tkatchenko and Scheffler 2009) approach as implemented in the DMol3 (Bernard Delley 2000) within the Materials Studio BIOVIA (Biovia 2016). DFT-D was used to accurately account for the van der Waals (vdW) interactions between the NOM and Ag (111) surface (Ortmann, Bechstedt, and Schmidt 2006). The generalized gradient approximation (GGA) method as proposed by Perdew and (Wang PW91) was used to approximate the exchange–correlation functional (Perdew, Burke, and Ernzerhof 1996) as it provides better overall description of the electronic system (Liang, Li, and Zhang 2009) and the double-numerical quality basis set with polarization functions (DNP) were employed (Lu et al. 2016). DFT semi-core pseudopotential (DSPP) was set to account for relativistic effects to balance calculation accuracy and computational efficiency (M. Zhang et al. 2017).

4.2.1 Surface construction

Ag (111) surface was modelled by a slab consisting of four layers repeated in a 4x4 surface unit cell with a separation of 15 Å between clean slabs to ensure no interactions between the sorbate and its periodic image. The adsorbates used in this case study were high molecular weight NOM's such as humic acid (HA), fulvic acid (FA) and cryptochrome (Cry). As explained in section 4.1.3, the obtained minimum energy configurations from the adsorption locator calculations were then used as inputs for DFT calculation where the atomic positions of the adsorbates and surface atoms were relaxed at constant volume. Using the adsorption locator as already mentioned allowed different adsorbate-sorbate configurations to be generated via Monte Carlo technique as embedded within the module, to relax with respect to all degrees of freedom (including rotations of the adsorbate on the surface) without additional constraints. The minimum energy configurations of the sorbate-adsorbate systems were obtained using the adsorption locator, which one of the modules with Material Studio. This was done for instance, in the case of placing ascorbic acid on Ag (111) surface. Uppermost two layers of the Ag atoms were relaxed along with the adsorbates, and the remaining substrate layers were constrained. The optimized geometrical structure of model Ag (111) surfaces used to adsorb the NOMs are shown in Figure 4.2.1.1. An adsorption equation mentioned in section 4.1.2 was used to calculate adsorption energies.
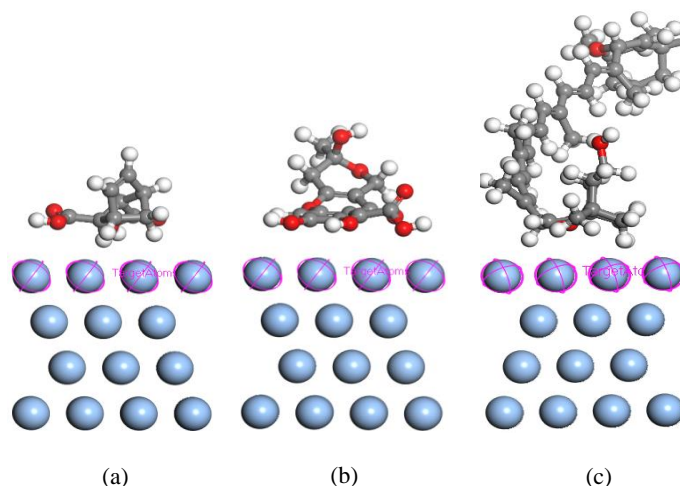
Figure 4.2.1.1: Optimized geometrical structures and relaxed configurations of (a) HA, (b) FA and (c) Cry molecules adsorbed on Ag (111) surface.

Gamma point *k*-point sampling was used and a real-space cut-off radius was maintained at 4.5 Å to improve the computational performance (Lu et al. 2016). The electronic energy convergence criteria, gradient, and atom displacement, were set as 0.00001 Ha (Ha is hartree), 0.002 Ha/Å, and 0.005 Å, respectively. To accelerate convergence speed of charge density of self-consistent field calculation time, and also enhance efficiency, direct inversion of iterative subspace (DIIS) was used.

4.2.2 Conductor-like screening model (COSMO)

To model the solvation effects in water, where electrostatic interactions of solutes with solvent are taken into account, solvation calculations on Ag (111) surface, HA, FA, and Cry complexes were performed using the conductor-like screening model (COSMO) as implemented in DMol3 (BIOVIA 2016). The continuum solvation model, COSMO, was selected since it is both simple and computationally efficient in comparison with explicit solvent phase simulations (Klamt and Schüürmann 1993). It also aids in the prediction of physicochemical properties of chemical species in solution media (Tomasi and Persico 1994, Cramer and Truhlar 1999) with the goal of generating results valuable to experimentalists (Vincent and Hillier 2014). In this study, water with permittivity (ε) = 78.4 was chosen as solvent primarily to mimic the interactions of ENPs with different NOMs defined by wide variations of MWs present in the aquatic systems.

4.3 Computational details for case study three

This case study adopted the method explained in section 4.2 as it is.

4.3.1 Surface construction

The Ag (111) surface was modelled using a seven-layer slab with a (4×4) unit cell and only the top three layers were allowed to relax while the four bottom layers were fixed in the optimized bulk position as shown in figure 4.3.1.1. A 20 Å vacuum space between the periodic slabs was utilized to eliminate spurious interactions. In this case study the NOM's used were formic acid (FA), acetic acid (AA1) and ascorbic acid (AA2). All other parameter were fixed like the ones shown in 4.2.1.
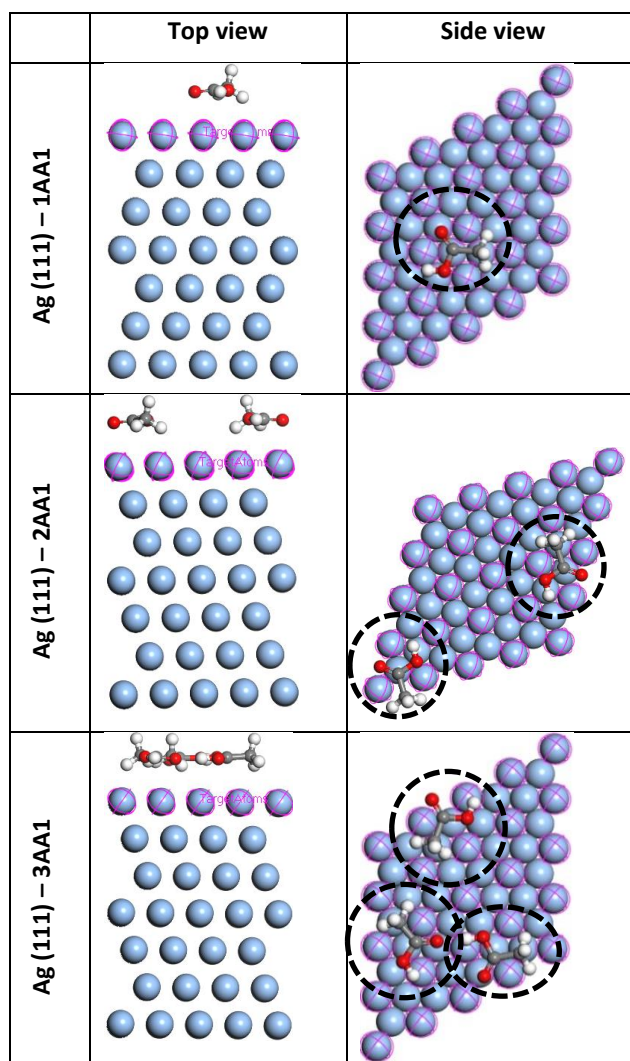
Figure 4.3.1.1: Side and top view snapshot of Ag (111)-1AA1, Ag (111)-2AA1 and Ag (111)-3AA1.

As explained in section 4.1.3, the obtained minimum energy configurations from the adsorption locator calculations were then used as inputs for DFT calculation where the atomic positions of the adsorbates and surface atoms were relaxed at constant volume. COSMO model as explained in section 4.2.2 was used to mimic water.

4.4 Adsorption energy

Adsorption process can be either be physical or chemical based on dominant forces. Physisorption arises from relatively weak (< 0.4 eV) interactions such as Van der Waals force whereas chemisorption involves stronger (> 0.4 eV) chemical interactions due to chemical bonding with transfer of electrons between the adsorbent and adsorbate (Hill 1977, Chantaramolee et al. 2015). Understanding the nature of the interactions between ENPs and NOMs is of crucial importance in understanding the fate and behavior of ENPs in the environment. The adsorption energies were calculated using both the DFT and dispersion corrected density functional theory (DFT-D). The adsorption of low and high molecular weight natural organic matter on Ag (111) surface in both gaseous and aqueous phases has been investigated using the equation below.

$$Eads = E_{(surf+adsorbate)} - E_{surf} - E_{adsorbate} + \text{BSSE} \tag{4.1}$$

where $E_{surface+adsorbate}$ is the total energy of the relaxed surface and adsorbate, $E_{surface}$ is the total energy of the relaxed surface, whereas $E_{adsorbate}$ is the total relaxed energy of the adsorbate. A more negative value that can be found suggests stronger adsorption energy (Chantaramolee et al. 2015). Notably, equation 4.1 removes the deformation energy and the basis set superposition error (BSSE) correction as numerical basis sets reduce these effects (Saikia and Deka 2013). The calculated adsorption energies using equation 4.1 are discussed in Chapter 5.

4.5 Solvation energy

By definition solvation energy is the process of transferring a solute from a fixed position in an ideal gas phase into a fixed position in the solvent (Ratkova, Palmer, and Fedorov 2015), (Ben-Naim 2006). In this work, the solvation energy was calculated to understand the stability of the interaction of the Ag (111) surface with adsorbates. The solvation energy was

obtained using the expression in equation 4.2. Solvation was not done on Ag ENPs, it was done on the last two cases on surface.

$$\Delta E_{solvation} = E_{water} - E_{gas} \qquad\qquad (4.2)$$

where $\Delta E_{solvation}$ is the solvation energy of the system, and E_{water} and E_{gas} are the total energies of the systems in the water phase and the gas phase, respectively (Salehzadeh, Bayat, and Gholiee 2013). Negative values of $\Delta E_{solvation}$ indicates that the molecule is stable in its solvent phase.

Following the determination of the adsorption and solvation energies other descriptors including the HOMO, LUMO, energy gap (Eg), chemical potential (μ), ionization potential (I), electron affinity (A), electronegativity (χ), hardness (η) and electrophilicity (ω) have been calculated.

Chapter 5: Results and discussion

5.1 Case study 1: *In silico* studies of LMW NOM's adsorption on different shapes of Ag ENPs

5.1.1 Introduction

Herein, DFT, CLD, and quantum mechanical calculations based on FMO theory were applied to elucidate the interactions of ENPs and NOMs. Results were derived for the adsorption energies of formic acid (CH_2O_2), acetic acid ($C_2H_4O_2$), and ascorbic acid ($C_6H_8O_6$) on silver (Ag) ENPs (111) surface and its shapes, namely: spherical, cylindrical, and different tetrahedron positions (faces, vertices and edges) using the DFT and CLD as described in Chapter 3. Results showed that the adsorption energies increased as molecular weight of the adsorbate increased with $C_6H_8O_6$ showing the highest adsorption energies for surface, spherical- and cylindrical-shaped Ag ENPs. For different positions of tetrahedron Ag ENP (111) surface, results indicated faces had the highest adsorption energies; hence, likely to be the most preferred adsorption sites. Therefore, results of both *in silico* techniques indicate that Ag ENPs are likely to be easily adsorbed by NOMs with larger molecular mass. In addition, calculations using FMO theory showed a direct relationship with each of the four parameters, viz.: the dipole moment (μ), molecular surface area (MSA), absolute electronegativity (χ), and absolute hardness (η) to the molar mass of the adsorbate.

Due to the influence of shape on the interactions of ENPs with organic matter, in this study adsorption of different NOM's on different shapes of Ag ENPs with (111) bound surfaces were investigated using *in silico* techniques. This is because shape plays a crucial role in controlling surface reactivity, for example, in terms of energy between the ENPs and other surfaces (Barnard and Zapol 2004). Secondly, determine plausible descriptor(s) likely to account for ENPs fate in the environment. For instance, experimental findings have shown that MW of the sorbing organic matter controls the ENPs stability (Louie, Tilton, and Lowry 2013). Moreover, the interactions between Ag ENPs and their coatings, in this case NOM coating have a direct bearing to their fate, stability, and eventual toxicity to biological lifeforms in the aquatic systems (Sharma et al. 2014). Clearly, this implies the formation of a natural coating on uncoated ENPs (herein regarded as pristine ENPs); can aid to account for

likely scenarios of ENPs consequent fate and stability, for example, after losing their original coating once in the aquatic systems. In particular, the adsorption energies as well as structural characteristics of stable adsorbed NOM complexes to Ag NPs (111) facets of three shapes, viz.: spherical, cylindrical Ag ENPs (111) surface, and tetrahedron Ag ENPs (111) surfaces were evaluated.

5.1.2. Computational details

All calculations were performed with the DMol3 module (Biovia 2016) as implemented in Materials Studio BIOVIA (Biovia 2016). Since the adsorbate can be adsorbed at different locations on the ENPs surfaces, the adsorption locator (AL) module within Materials Studio BIOVIA (Biovia 2016) was used to obtain the best adsorption site on the surface hereafter referred to as a configuration. The AL utilizes Monte Carlo within a lattice dynamics approach to obtain the best configuration, which, in turn, was used as an input for the DFT calculations. The theoretical face centered cubic (fcc) lattice constant was obtained following unit cell optimization estimated to be 4.02 Å and in good agreement with results of,(Haas, Tran, and Blaha 2009) at 4.01 Å. The unit cell of bulk silver was optimized with a 12x12 x12 Monkhorst-Pack (Monkhorst and Pack 1976) mesh of k-points and kinetic energy cut-off of 4.5 Å the unit cell was then relaxed using the conjugate gradient method until the total forces acting on each atom was less than 0.02 eV/ang. Silver has a face centred cubic (fcc) crystal structure with a Ag-Ag distance of 2.88 Å (Davey, 1925, Suh et al., 1988), bounded by low-index e.g. (100), (110) and (111) of high atom densities (Molleman and Hiemstra 2015).

For Ag, the (111) face is characterised by high metal density (14 Ag/nm^2) and low surface tension (Azcárate et al. 2013) and the close-packed (111) plane has the lowest energy crystal plane with maximum packing, and therefore, is most stable (Marzbanrad et al. 2015). For this reason, the (111) facet is widely studied (Hatchett and White 1996) because silver reactivity favours high atom density facets, (Ajayan and Marks 1988) and similarly, it was chosen as facet of investigation in this study. The exchange-correlation energy was approximated using the PW91 generalized gradient approximation (Perdew and Wang 1992). A double-numeric quality basis set with polarization functions was chosen (Lu et al. 2016). Core electrons were treated with DFT semi core-pseudo potentials (B Delley 2002).

Spin polarization was also applied, and real space cut-off radius was maintained at 4.5 Å. Convergence accuracy of energy was set as $1.0e^{-5}$ Ha, while the energy gradient and atom displacement were set as 0.002 Ha/Å and 0.005 Å, respectively. To accelerate convergence speed of charge density of self-consistent field calculation time and enhance efficiency, direct inversion of iterative subspace (DIIS) was used. After optimizing the unit cell, surfaces were constructed using a 3×3 supercell consisting of five layers, where the top two layers of the surface were allowed to relax without and with the adsorbed molecules. The remaining three substrate layers were frozen and a vacuum distance of 15 Å was used. Spherical, cylindrical and tetrahedron engineered nanoparticles were constructed with the (111) surface as the bonding surface. The adsorption energy calculations were done using equation 4.1 in Chapter 4.

5.1.3 Results and discussion

Bond lengths of the elements for the adsorbates used in this study as shown in Table 5.1.3.1, after results are discussed starting by NOM's on Ag ENP (111) surface, spherical Ag ENPs, cylindrical Ag ENPs (111) and different positions of tetrahedron Ag ENP (111) surface.

Table 5.1.3.1: Measured bond lengths for formic acid , acetic acid and ascorbic acid on Ag (111) surface where C-O is the distance between carbon and oxygen, H-O is the distance between hydrogen and oxygen, C-H is the distance between carbon and hydrogen, H-H is the distance between hydrogen and Hydrogen, C-C is the distance between carbon and carbon.

Adsorbate	d_{C-O} (Å)	d_{H-O} (Å)	d_{C-H} (Å)	d_{H-H} (Å)	d_{C-C} (Å)
Formic acid	1.0	0.62	0.62	-	-
Acetic acid	1.37	1.08	1.09	-	1.52
Ascorbic acid	1.0	0.62	0.85	0.62	1.0

Using the adsorption locator module the minimum energy configurations for the adsorbates on the Ag ENP (111) surface as shown in Figure 5.1.3.1, adsorption energies were calculated.
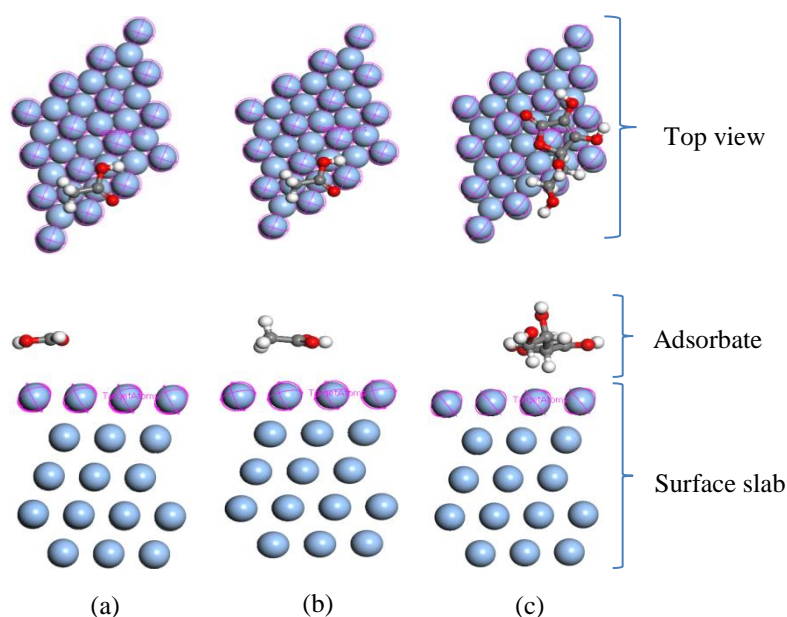
Figure 5.1.3.1: Shows (a) formic acid (b) acetic acid and (b) ascorbic acid adsorbed on Ag (111) surface slab with the top and side view (color code; oxygen: red, grey: carbon, white: hydrogen).

Notably, in Table 5.1.3.2 both *in silico* techniques show similar results, and therefore, are consistent. The adsorption energy results in Table 5.1.3.2 were calculated using equation 4.1 in Chapter 4. The adsorption energies increased as the MW of the adsorbates increased; ascorbic acid shows the highest adsorption energies for Ag ENP (111) surface (-0.55 eV), spherical (-0.63 eV) and cylindrical Ag ENP (111) (-0.85 eV). A similar trend was observed for CLD as well in terms of estimated adsorption energies i.e. Ag (111) ENP surface (-2.90 eV), spherical shape (-2.02 eV), and cylindrical Ag ENP (111) (-2.27 eV). The results indicate ascorbic acid can be easily adsorbed compared to formic acid or acetic acid.

Table 5.1.3.2: Calculated adsorption energies in (eV) for Ag (111) surface, spherical Ag nanoparticle, and cylindrical Ag nanoparticle on formic acid, acetic acid and ascorbic acid as adsorbates.

Adsorbates	DMol3			AL		
	E_ads (eV)			E_ads (eV)		
	FA	AA$_1$	AA$_2$	FA	AA$_1$	AA$_2$
Ag(111) surface	-0.07	-0.28	-0.55	-0.67	-0.95	-2.90
Ag (spherical)	-0.31	-0.31	-0.63	-0.55	-0.73	-2.02
Ag(111) cylindrical	-0.22	-0.25	-0.85	-0.48	-0.68	-2.27

FA: formic acid, AA$_1$: acetic acid, AA$_2$: ascorbic acid.

From the computed adsorption energies, it was possible to deduce the nature of adsorption mechanisms i.e. whether chemical or physical. Physical adsorption (physisorption) arises from relatively weak (< 0.4 eV) interactions such as van der Waals force whereas chemical adsorption (chemisorption) involves stronger (>0.4 eV) chemical interactions due to chemical bonding with transfer of electrons between the adsorbent and adsorbate (Chantaramolee et al. 2015, Hill 1977). In the present study, chemisorption was observed in the case of ascorbic acid on the surfaces, edges as well as vertices. Physisorption was, however, only observed in the case of acetic acid and formic acid adsorption with the exception of two vertices as shown in Table 5.1.3.3.

Table 5.1.3.3: Calculated adsorption energies of formic acid, acetic acid and ascorbic acid at the vertices of tetrahedron Ag (111) surface.

Adsorbate	Vertices	DMol3	AL
		E_ads (eV)	E_b (eV)
FA	1	-0.21	-0.53
	2	-0.44	-0.84
	3	-0.19	-0.63
AA_1	1	-0.27	-0.77
	2	-0.49	-1.13
	3	-0.26	-0.89
AA_2	1	-0.78	-2.34
	2	-0.95	-2.81
	3	-0.95	-2.81

The calculated adsorption energies were all negative indicating that the adsorption process is exothermic and spontaneous (X. Zhang et al. 2013). Negative adsorption energies suggest that the adsorption process involves an associative mechanism, and no significant change occurs in the internal structures of the adsorbent during the adsorption process. The calculated adsorption energies suggests that these adsorbates do bind with the Ag ENPs, and in turn, exert some of the properties which in turn influences the fate Ag ENPs in the environment. This is consistent with the findings of Loosli et al. (2015) where NOM's were found to coat on ENPs. Moreover, adsorbates that are more negatively charged enhances ENPs stability either through electrosteric stabilization and/or steric hindrance mechanisms (Chen et al. 2007, Gilbert et al. 2007). Adsorption of adsorbates to the surfaces ENPs is known to influence their surface properties and aggregation behavior. The adsorption energy is usually affected not only by the electronic interactions in and between the adsorbate and the surface, but also via energetic cost of changing the atomic geometry (Borck and Schröder 2005).

A similar methodology as presented for Ag ENP (111) surface was followed to determine adsorption energies for spherically shaped Ag ENP. Using AL, results of minimum energy

configuration for sphere with different adsorbates are shown in Figure 5.1.3.2 (a), (b) and (c) for formic acid, acetic acid and ascorbic acid respectively.

| (a) | (b) | (c) |
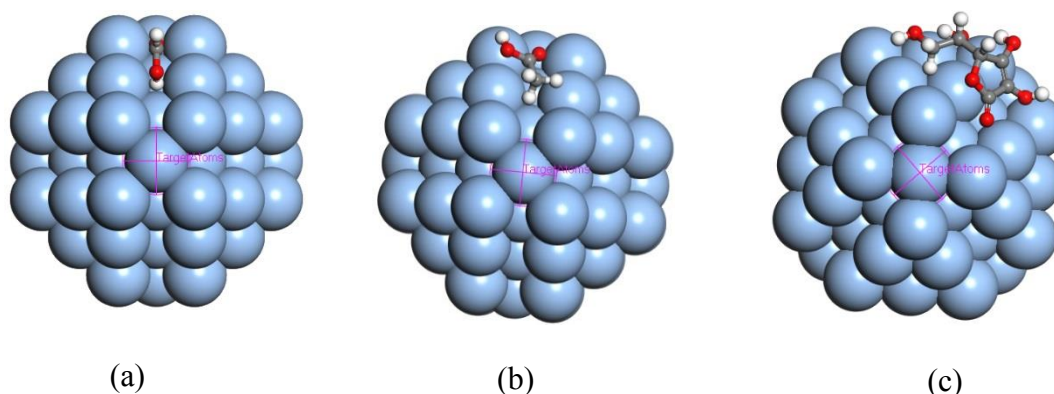
Figure 5.1.3.2: Schematic representation of adsorption of (a) formic acid, (b) acetic acid and (c) ascorbic acid on spherical silver engineered nanoparticles.

However, unlike in the case of Ag ENP (111) surface where all surface atoms were chosen as possible target atoms for the adsorbate, for the sphere, target atoms were selected individually after carrying out adsorption locator calculations. It should be noted that the adsorption energies obtained were similar irrespective of the target atom. This is because all surface atoms of a sphere are symmetrically equivalent, and as a result, have a uniform charge distribution over the entire sphere. Both techniques density functional theory and classical lattice dynamics showed similar trend in the adsorption energies for the surface (111). The high adsorption energies of ascorbic acid results again show that it can easily bind to the spherical nanoparticles as compared to formic acid and acetic acid (Table 5.1.3.2).

For the cylindrically shaped Ag ENP bound by (111) surface on both edges, AL was used to identify possible adsorption sites. Table 5.2 summarises the DFT and CLD adsorption energies. As can be seen (Table 5.2), the higher the molar mass, the greater the adsorption energies and higher the minimum energy configurations for the cylindrical surface with different adsorbates are shown in Figure 5.3.

| (a) | (b) | (c) |
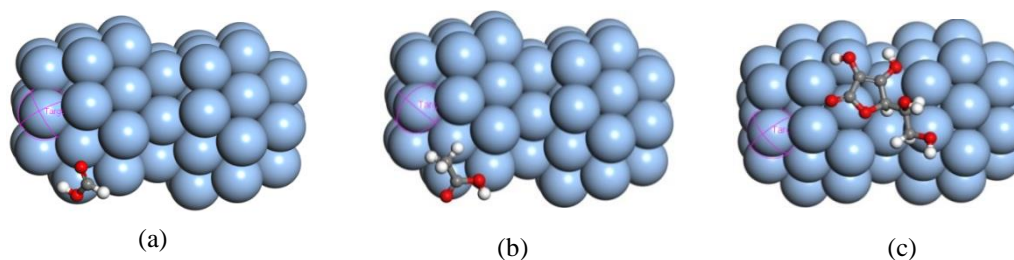
Figure 5.1.3.3: Schematic representation of adsorption of (a) formic acid, (b) acetic acid and (c) ascorbic acid on cylindrical Ag ENP (111) surface.

For tetrahedron, the calculated adsorption energies using both DFT and CLD were similarly done as the case for sphere and the cylinder and the results are summarized in Table 5.1.3.2. Adsorption energies of formic acid, acetic acid and ascorbic acid at the vertices, faces and edges of different positions of tetrahedron Ag ENPs (111) surface were calculated. Figures 5.1.3.4-5.1.3.6 show how formic acid, acetic acid and ascorbic acid were attached on vertices, faces, and edges on tetrahedron Ag ENPs (111).
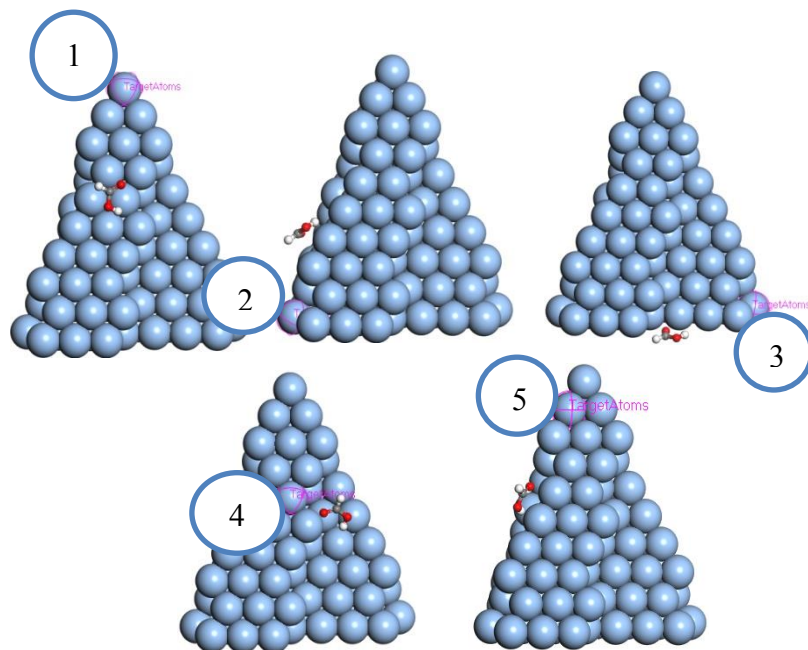
Figure 5.1.3.4: Adsorption of formic acid at different vertices of tetrahedron Ag ENP (111) surface (position 1-3), adsorption of formic acid at the face of tetrahedron Ag ENP (111) (position 4), and adsorption of formic acid at the edge of tetrahedron Ag ENP (111) (position 5).
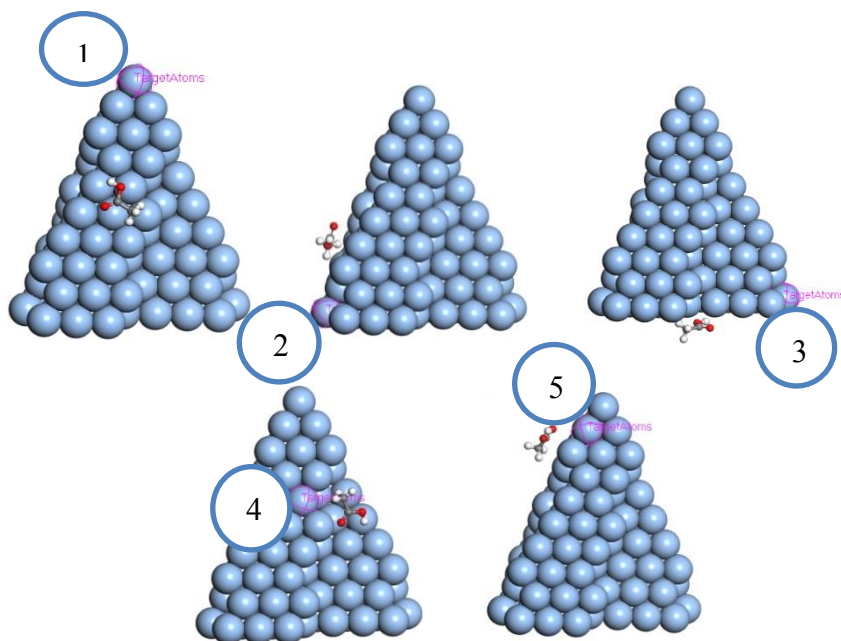
Figure 5.1.3.5: Adsorption of acetic acid at different vertices of tetrahedron Ag ENP (111) surface (position 1-3), adsorption of acetic acid at the face of tetrahedron Ag ENP (111) (position 4) and adsorption of acetic acid at the edge of tetrahedron Ag ENP (111) (position 5).
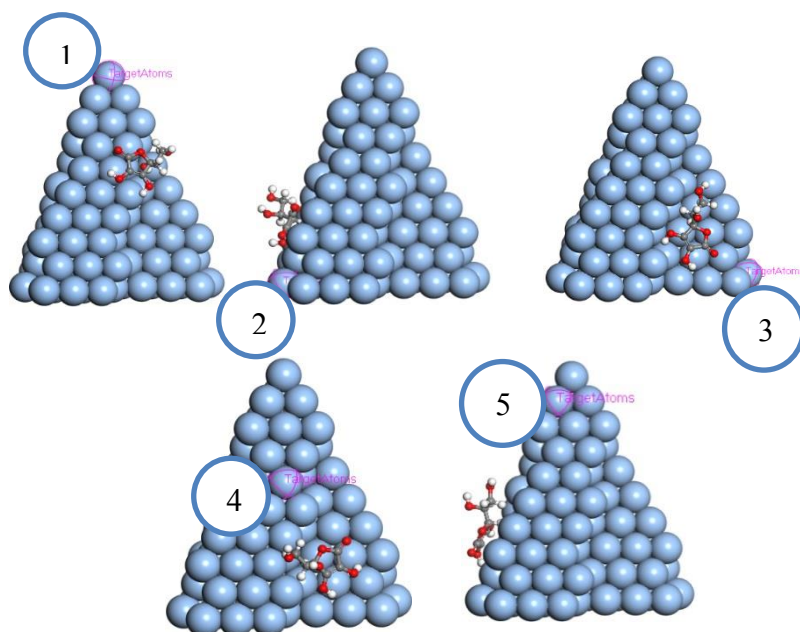
Figure 5.1.3.6: Adsorption of ascorbic acid at different vertices of tetrahedron Ag ENP (111) surface (position 1-3), adsorption of ascorbic acid at the face of tetrahedron Ag ENP (111) (position 4) and adsorption of ascorbic acid at the edge of tetrahedron Ag ENP (111) (position 5).

Results derived using both *in silico* techniques indicated that faces had the highest adsorption energies; hence are likely to be the most preferred adsorption sites. Therefore, ascorbic acid can be easily adsorbed on the face of tetrahedron Ag (111) surface than at the vertices and edges. However, for the physisorption of lower MW NOMs, adsorptions may occur at any face as all energies were found to be similar as shown in Tables 5.1.3.3 and 5.1.3.4.

Table 5.1.3.4: Calculated adsorption energies of formic acid, acetic acid and ascorbic acid at the faces and edges of tetrahedron Ag (111) surface.

	DMol3			AL		
	E_ads (eV)			E_ads (eV)		
Adsorbates	FA	AA_1	AA_2	FA	AA_1	AA_2
Face (1)	-0.46	-0.48	-1.15	-0.75	-0.97	-2.83
Edge (1)	-0.46	-0.23	-0.83	-0.75	-0.75	-2.81

Using the values of IP and EA obtained from modified neglect of differential overlap (MNDO) calculations, values of χ and η calculated for formic acid, acetic acid and ascorbic acid are shown in Table 5.1.3.5. The method and equations used to derive the results in Table 5.1.3.5 is shown in chapter 4.

Table 5.1.3.5: Quantum chemical parameters of adsorbates calculated using VAMP in Material Studio BIOVIA (PM6 semi-empirical calculation).

	IP (eV)	EA (eV)	TE (eV)	ΔE (eV)	DM	MSA(Å^2)	χ	η
FA	8.63	2.62	-713.67	6.01	3.23	51.80	5.63	3.00
AA_1	8.45	2.5	-827.88	5.95	3.24	62.68	5.47	2.97
AA_2	8.81	1.54	-2367.54	7.27	5.47	121.13	5.17	3.63

Molecular Surface Area (MSA), DM: dipole moments in Debye units

Bulk metals are softer than neutral metal atoms, and therefore IP = EA for bulk metals (Dewar and Thiel 1977). From Table 5.1.3.5, there is direct relationship between the dipole moment (μ), molecular surface area (MSA), absolute electronegativity χ, absolute hardness η, and the molar mass of the adsorbate. As was earlier mentioned, when EA > 0 (Chapter 3) the addition of the electron leads to release of energy. In particular, these properties were found to increase with increasing molar mass. Among the adsorbates investigated herein, only ascorbic acid met this criterion. The high μ value for ascorbic acid indicates it is a good adsorbate as previous studies have shown that μ influences the adsorption between a chemical compound and a metal surface (Li et al. 2009).

According to Wang et al (Wang et al. 2007) larger values of the energy difference (ΔE) implies low reactivity to a chemical species; thus, lower values of ΔE are indicative of good adsorption efficiency. However, in this study results of μ and ΔE may suggest they are not in agreement. For instance, the acetic acid had a lower ΔE which, in turn suggest it to be a better adsorbate than ascorbic acid and formic acid. This implies that the acetic acid can easily donate electrons to appropriate acceptor molecules with low energy molecular orbitals. Nonetheless, such phenomenon is highly feasible as results of (Domenicano and Hargittai 1992) showed that the adsorption of an adsorbate on metal surfaces can occur on the basis of donor–acceptor interactions between the π-electrons of the heterocyclic compound and the vacant d-orbital of the metal surface atoms. In Figure 5.1.3.7, a 3D plot of HOMO and LUMO orbital density distributions of adsorbates are presented.
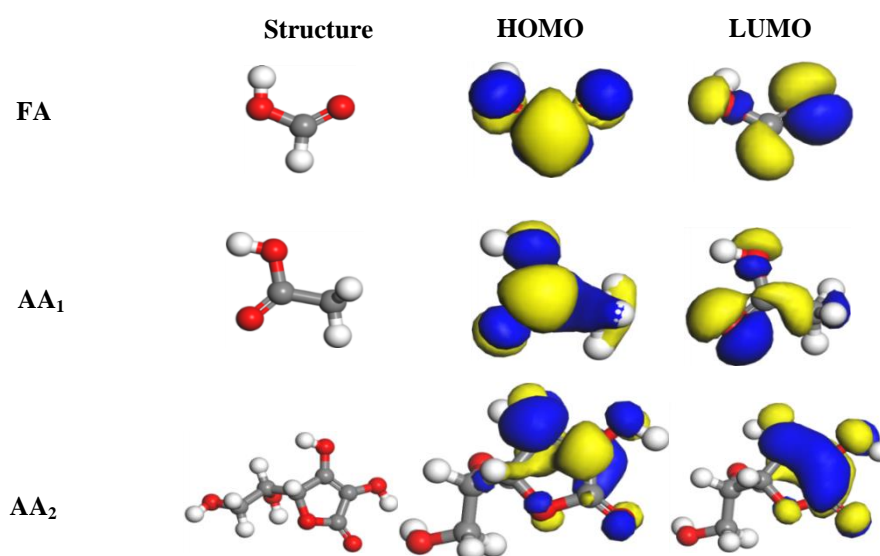
Figure 5.1.3.7: Orbital density distributions of FA, AA$_1$, and AA$_2$.

Use of different colours signifies various phases of the orbital where blue and yellow colours, respectively, reflects positive and negative phases of the orbitals. The energy gap of the adsorption structure was calculated for the energy levels of HOMO and LUMO defined as ΔE equation 3.4 in Chapter 3 equation 3.13

The energy gap width determines how much energy an electron needs to jump into the LUMO from the HOMO. The wider the gap, the more energy is required, and the more difficult it is for the electrons to transfer between the valence band (VB) and the conduction band (CB). Table 5.1.3.6 lists results of energy gaps.

Table 5.1.3.6: Energy gaps of the adsorbates alone and adsorbates with different shapes.

System	EHOMO (eV)	ELUMO (eV	ΔE (eV)
Adsorbate	-	-	-
AA2	-8.81	-1.54	-7.27
AA1	-8.45	-2.5	-5.95
FA	-8.63	-2.63	-6.01
Sphere	-27.79	-25.72	-2.08
Sphere-AA2	-27.19	-25.31	-1.88
Sphere-AA1	-27.58	-25.64	-1.93
Sphere-FA	-27.49	-25.48	-2.01
Cylinder	-28.62	-27.45	-1.17
Cylinder-AA2	-28.27	-26.57	-1.7
Cylinder-AA1	-29.04	-27	-2.04
Cylinder-FA	-29.05	-27.11	-1.95
Tetrahedron	-28.88	-27.3	-1.58
Tetrahedron-AA2	-28.65	-27.12	-1.54
Tetrahedron-AA1	-29.04	-27.37	-1.67
Tetrahedron-FA	-28.98	-27.26	-1.7

The adsorption of ascorbic acid on different shapes reduces the energy gap width, and improves the electron transfer to the surface, however, the other adsorbates showed no improvement of electron transfer on the surface.

Previous studies by Puzyn et al (Puzyn et al. 2011) calculated descriptors such as total energy, HOMO, LUMO, gap etc using the quantum-chemical PM6 method (Gramatica 2007) and they found that particle size does not influence toxicity in the studied size range, the selected descriptors predominantly reflect reactivity-related electronic properties.

5.1.4 Concluding remarks

In this part of the work DFT and CLD calculations have been performed to determine the adsorption energies of formic acid, acetic acid and ascorbic acid on Ag ENPs (111) surface, spherical Ag ENP, cylindrical Ag ENP (111) surface, and tetrahedron Ag ENP (111) surface. The adsorption energies results found to be dependent on the type of adsorbate – represented by the adsorbate MW and the shape of the ENPs. Moreover, the nature of the adsorption i.e. physisorption or chemisorption likely to occur following release of ENPs into the environment will be dependent on the NOM characteristics, and in turn, would imply the degree to which the ENPs are stabilized or not. The results indicate that the stability of same ENPs will not be uniform; and will be influence by the constituent characteristics of NOM present. It is worthy to note that because ascorbic acid due to its large MW induced the highest degree of polarization compared to formic acid and acetic acid, and the results are consistent with earlier findings of Becke and Edgecombe et al (Becke and Edgecombe 1990). It is however unclear which functional group plays a crucial role in the molecular adsorption of formic acid, acetic acid and ascorbic acid. From the FMO results, is has been observed that there is direct relationship between the dipole moment (μ), molecular surface area (MSA), absolute electronegativity χ, absolute hardness η, and the molar mass of the adsorbate. In particular, these properties were found to increase with increasing molar mass. As was earlier mentioned, when EA > 0 the addition of the electron leads to release of energy. Among the adsorbates investigated herein, only ascorbic acid met this criterion. The high μ value for ascorbic acid indicates it is a good adsorbate as previous studies have shown that μ influences the adsorption between a chemical compound and a metal surface (Li et al. 2009).

5.2 Case study 2: Adsorption of natural organic matter on Ag (111) surface using DFT-D.

5.2.1 Introduction

Understanding the nature of the interactions between (NOM) and (ENPs) is of crucial importance in understanding the fate and behavior of ENPs in the environment. In the present study, (DFT-D) has been used to elucidate the molecule-surface interactions of (HMW) NOM ambiguously present in the aquatic systems, namely: humic acid (HA), fulvic acid (FA) and Cryptochrome (Cry) on Ag (111) surface. Investigations were done in the gas phase and to mimic real biological environment, water has been used as a solvent within (COSMO) framework. The results for adsorption energy, solvation energy, *iso*surface of charge deformation difference, total density of state and partial density of states indicated that indeed the studied adsorbates do interact with the surface and are favorable on Ag (111) surface. In terms of charge transfer, one of many calculated descriptors in this study, electrophilicity (ω) agree that charge transfer will take place from the adsorbates to Ag (111) surface. This is evident from Table 5.6 because the electrophilicity values of adsorbates are less than the electrophilicity of the Ag (111). In this case study, within the (DFT-D) formalism, the Ag (111) surface, as prototype ENP surface, was used to investigate surface-NOM interaction with three representative (HMW) NOMs namely; HA, FA and Cry) widely found in the aquatic systems (MacCarthy & Rice 1985, Stevenson 1994 ,Sutton & Sposito 2005).

5.2.2 Computational details

All calculations were performed using the DFT-D (Ortmann et al. 2006, Tkatchenko & Scheffler 2009) approach as implemented in the DMol3 (Bernard Delley 2000) within the Materials Studio BIOVIA (Biovia 2016). DFT-D was used to accurately account for the van der Waals (vdW) interactions between the NOM and Ag (111) surface (Ortmann, Bechstedt, and Schmidt 2006). The generalized gradient approximation (GGA) method as proposed by Perdew and (Wang PW91) was used to approximate the exchange–correlation functional (Perdew, Burke, and Ernzerhof 1996) as it provides better overall description of the electronic system (Liang, Li, and Zhang 2009) and the double-numerical quality basis set with polarization functions (DNP) were employed (Lu et al. 2016).

DFT semi-core pseudopotential (DSPP) was set to account for relativistic effects to balance calculation accuracy and computational efficiency (Zhang et al. 2017). Ag (111) surface was modelled by a slab consisting of four layers repeated in a 4x4 surface unit cell with a separation of 15 Å between clean slabs to ensure no interactions between the sorbate and its periodic image. Uppermost two layers of the Ag atoms were relaxed along with the adsorbates, and the remaining substrate layers were constrained.

The optimized geometrical structure of model Ag (111) surfaces used to adsorb the NOMs are shown in Figure 5.2.2.1. Gamma point *k*-point sampling was used and a real-space cut-off radius was maintained at 4.5 Å to improve the computational performance (Lu et al. 2016). The electronic energy convergence criteria, gradient, and atom displacement, were set as 0.00001 Ha (Ha is hartree), 0.002 Ha/Å, and 0.005 Å, respectively. To accelerate convergence speed of charge density of self-consistent field calculation time, and also enhance efficiency, direct inversion of iterative subspace (DIIS) was used.

Carlo technique as included within the module, to relax with respect to all degrees of freedom (including rotations of the adsorbate on the surface) without additional constraints. It uses molecular dynamic (MD) simulations with force fields. In this study, universal force fields were used. To model the solvation effects in water, where electrostatic interactions of solutes with solvent are taken into account, solvation calculations on Ag (111) surface, HA, FA, and Cry complexes were performed using the conductor-like screening model (COSMO) as implemented in DMol3 (BIOVIA 2016). The continuum solvation model, COSMO, was selected since it is both simple and computationally efficient in comparison with explicit solvent phase simulations (Klamt and Schüürmann 1993). It also aids in the prediction of physicochemical properties of chemical species in solution media (Tomasi & Persico 1994, Cramer & Truhlar 1999) with the goal of generating results valuable to experimentalists (Vincent and Hillier 2014). In this study, water with permittivity (ε) = 78.4 was chosen as solvent primarily to mimic the interactions of ENPs with different NOMs defined by wide variations of MWs present in the aquatic systems. Figure 5.2.2.1 shows optimized geometries of Ag (111) surface with the respective adsorbates.
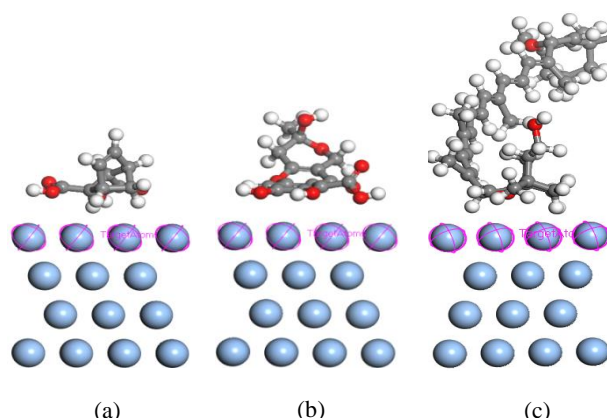
Figure 5.2.2.1: Optimized geometrical structures and relaxed configurations of (a) HA, (b) FA and (c) Cry molecules adsorbed on Ag (111) surface.

From Figure 5.2.2.1 (a) and (c), it is evident that HA and Cry adsorption occurred through its hydrogen atom facing the Ag (111) surface while for the FA (Figure 5.2.2.1(b)) adsorption occurred through one oxygen in the carbonyl group, and hydrogen atom. The calculated adsorption energies listed in Table 5.2.3.1,were obtained using equation 4.1 in Chapter 4.

5.2.3 Results and discussion

Interest in adsorption of Cry, FA and HA on Ag (111) surface stems from the fact that NOMs substantially modify the physical and chemical properties of the surface by accepting (donating) electrons (Mannix et al. 2015). The results in Table 5.2.3.1 show that the adsorption of Cry, FA and HA is energetically favorable since only negative adsorption energy values were obtained.

Table 5.2.3.1: Adsorption energies (eV) and the equilibrium distance between NOM's and Ag (111) surface.

System	E_{ads} (eV)	d_{H-Ag} (Å)
Gas phase		
Ag (111)-HA	-1.21	1.87
Ag (111)-FA	-1.66	2.31
Ag (111)-Cry	-6.24	1.91
COSMO (Water)		
Ag (111)-HA	-0.80	2.18
Ag (111)-FA	-0.81	2.31
Ag (111)-Cry	-6.53	1.70

According to (L. Liu et al. 2013) the NOM's can interact with Ag (111) surface via several different ways by utilizing H, N atoms and O lone pair electrons. The chemical formula for HA, FA and Cry are ($C_9H_9NO_6$), ($C_{14}H_{12}O_8$) and ($C_{40}H_{56}O_3$), the strong interaction as shown by the highest adsorption of Cry can be attributed to fact that it has many carbon and hydrogen atoms interacting with the Ag (111) surface. As observed by (Singla et al. 2016) the adsorption energy is maximum for larger sized Cry this can be explained on the basis of fundamentals of Van der Waals forces that are directly proportional to the size and mass of the interacting molecules (Singla et al. 2016). From Table 5.2.3.1, FA has the second strongest interaction, that can also be attributed to the fact that it has the highest number of carbon, hydrogen and oxygen atoms interacting with the surface. The higher and the more negative the adsorption energy, the more stable the molecule. Similar conclusion was observed by (Guo et al. 2017) while working on interaction of inhibitor with Fe (110) surface. Chemahini and co-workers (Chermahini, Teimouri, and Farrokhpour 2015) while working on the interaction between lactic acid and single-wall carbon nanotubes arrived to same conclusion. It is evident from the Table 5.2.3.1 that moving from gas phase to water the adsorption energy values of HA and FA decrease, while the adsorption energy value for Cry moving from gas phase to water phase increase. The reason for Cry to behave differently compared to HA and FA could lie to the fact that Cry is the protein while HA and FA are humic substances. In the case of HA and FA water did not enhance adsorption or make the interaction between the NOM and Ag (111) surface. A previous study by (Chermahini, Teimouri, and Farrokhpour 2015) reported decreasing and increasing adsorption energies values moving from gas phase to water while working on the interaction between lactic acid and single-wall carbon nanotubes.

Experimental results have shown that adsorbed NOM molecules with high MW could introduce steric repulsion and prevent the direct contact between ENPs and cells/organisms, thus decreasing the toxicity of ENPs (Wang et al. 2016) thus, an NOM is expected to attach to the surface of ENPs which in turn may change their physiochemical properties and the interfacial forces or energies between interacting ENPs thereby, altering the ENPs' aggregation behavior (Wang et al. 2016). Stronger NOM-surface interaction by means of adsorption energies indicate that in the environment the NOM is likely to stay longer attached to the ENPs, whereas in the case of weak NOM-surface interaction, the NOM is likely to separate from the ENPs because of weak adsorption energy. Once NOM detaches from the ENP's surface, a process of dissolution takes place resulting in the release of silver ions

(Mudunkotuwa et al. 2011) hence the importance of the NOM binding strongly to the ENP surface.

As stated in Chapter 4, the energy needed to move a molecule from its gas to solvent phase is referred to as the solvation energy. The results presented in the text below were calculated using equation 4.2 (Chapter 4), Ag (111)-HA (-0.16), Ag (111)-FA (-0.23) and Ag (111)-Cry (-1.04 eV) respectively. As seen from the solvation energy values, a direct relationship between the calculated $\Delta E_{solvation}$ and the molecular weights of the NOMs was also observed. The solvation energy results followed a similar trend to those of adsorption energy. The molecular weight is the contributing factor.

5.2.4 Analysis of density of states (DOS)

To better understand the interactions between Ag (111) surface and adsorbates the electronic properties were studied using the total density of states (TDOS) especially near the Fermi level. In Figure 5.2.4.1 (a-c), results for TDOS of pristine alone, adsorbates alone and Ag (111) surface with adsorbates calculated using DFT-D/GGA in gas phase and in water as a solvent are summarised. From TDOS plot in Figure 5.2.4.1 (a), the pristine Ag (111) surface show peaks at and above Fermi level, which is typical for metals. The TDOS plots for HA and FA were found to be very similar as both adsorbates are humic substances; where the peaks observed below Fermi level and above Fermi level were at the same energy positions between -9.9 and -0.4 eV below the Fermi level, and 0.4 eV and 4.4 eV above Fermi level (Figure 5.2.4.1 (b)). In the case of Cry, fewer peaks were observed below and above the Fermi level. Following adsorption of adsorbates on Ag (111) surface, the calculated TDOS for the adsorbed systems were observed to be relatively similar to that of pristine Ag (111) surface in the energy range -8 to 5 eV. This indicates that around the Fermi level, the adsorbates had no significant influence on the electronic properties of Ag (111) surface based on TDOS analysis. Previous study showed that the total DOS of Cu (1 1 1) after C_3F_7CN adsorption has some change, which is manifested by the increased DOS near the range from −6 eV to −8 eV (Carr et al. 2012). The adsorption of NOM's on Ag (111) surface can substantially modify the physical and chemical properties of molecules and enhance the stability of the system by accepting the electrons from antibonding states (Mannix et al. 2015).

Projected density of states (PDOS) plots for the surface alone, adsorbates alone and Ag (111) surface with adsorbates calculated using DFT-D/GGA in gas phase and in water as a solvent are shown in Figures B.2-B.3 in Appendix B. Further, to gain insights on NOM-Ag (111) surface electronic because silver is a transition metal where *d* and *f* orbitals are (semi) filled. In Figures B1 (A-B) in electronic version B, the PDOS of HA, FA, Cry, Ag (111) surface pristine, and HA, FA, Cry Ag (111) surface in gas phase and COSMO have been shown. The PDOS values of s- and p-, and-orbitals are all decreased after adsorption both in gas and water phase (Figure B.5, electronic version B). Only the *s* and *p* orbitals were considered

It suggests that NOM's have influence towards the orbitals of Ag (111) formed bond interaction, similar observations were reported by (Ji et al. 2016). In turn, the adsorption process is enhanced. The change shows distinct change in all orbitals indicating a strong bond interaction. In conclusion, the strong orbital hybridization among HA, FA and Cry atoms orbitals stabilizes the adsorption of Ag (111) surface. For comparison both TDOS and PDOS pristine Ag (111) surface, HA on Ag (111) surface and FA on Ag (111) surface are drawn from -10 eV to 5 eV, this was done to show the electronic states around the Fermi level.
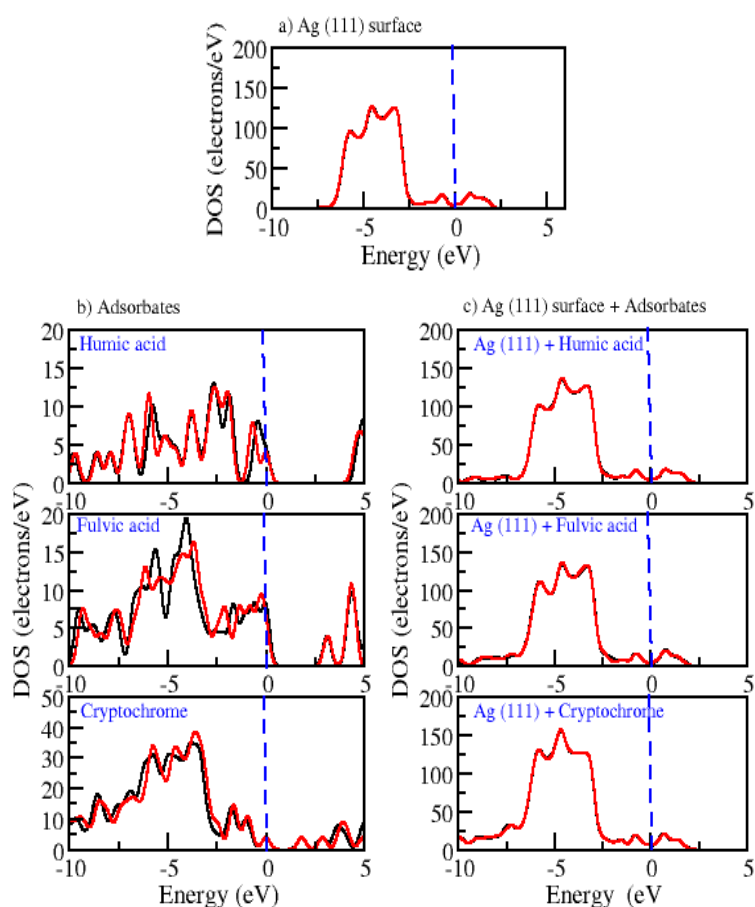
Figure 5.2.4.1: The TDOS calculated using DFT-D/GGA formalism for adsorbed HA, FA and Cry in gas and water as a solvent.

5.2.5 Quantum chemical calculations

It is a known fact that the bonding interaction between molecules and metal surface relies on the frontier orbital energetic position and the Fermi energy of metal (Hammer and Nørskov 2000). The quantum chemical descriptors have been calculated to understand the properties of the studied molecules that could be used as possible inputs in creating either a Quantitative structure–activity relationship (QSAR) or quantitative structure–property relationships (QSPR) are needed for the development of ENP toxicity model. The most commonly investigated descriptors for QSAR include (HOMO), (LUMO), HOMO-LUMO gap (Eg) which were also calculated in this study (Puzyn et al. 2011, Chermahini et al. 2015).

Several studies have confirmed that the reactivity of a molecule depends on the molecular orbital distribution (Zhang et al. 2012). HOMO regularly indicates the electron donating ability of a molecule, while LUMO is associated with its ability to accept electrons (Gece & Bilgiç 2009, Khaled 2008). The molecular structures of these three adsorbates and the frontier molecule orbital density distributions are shown in Figures B.10-B.11 (electronic version). It is seen that the HOMO of HA is mostly distributed on the C-H atoms indicating that it is the C-H bonds which will most likely donate electrons to the surface while the HOMO of FA and Cry is distributed throughout the inner atoms and indications that for these adsorbates all atoms will donate electrons to the surface. The HOMO distributions of HA, FA and Cry molecules have been plotted in Figures B.10-B.11 in electronic version B. It had been previously reported (Armaković et al. 2014) that ω is a descriptor that could indicate the direction of charge transfer. The higher the value of ω, the higher the electrophilic power of the investigated structure (Armaković et al. 2014). From Table 5.2.5.1, the electrophilicity index values of HA, FA and Cry in both gas and water phases are lower than that of Ag (111) surface, indicating that there will be a charge transfer from these molecules to Ag (111) surface. It is worth noting that higher adsorption energy and narrow HOMO-LUMO energy gap suggest a strong binding interaction of the Cry molecule to Ag (111) and this can be attributed to its hydrophilicity. From Table 5.2.5.1, results indicate that all the adsorbates before and after the adsorption on Ag (111) surface exhibit very similar values of HOMO and LUMO.

Before adsorption in the gas phase the HOMO values for HA, FA and Cry were -5.97, -5.48 and -4.25 eV respectively. Still in the gas phase the HOMO values after adsorption for HA, FA and Cry were -5.31, -5.08 and -5.09 respectively. The HOMO values in water for HA, FA and Cry were –6.02, -5.77 and -4.57 eV before adsorption, after adsorption the HA, FA and Cry HOMO values changed to -5.38, -5.24 and -5.40 eV respectively. In the case of LUMO values before adsorption in the gas phase for HA, FA and Cry were -1.28, -2.38, -2.44 eV respectively. After adsorption in the gas phase the LUMO for HA, FA and Cry changed to -4.90, -4.69 and -5.04 eV respectively. The LUMO values in water before adsorption for HA, FA and Cry were -1.47, -2.63 and -2.76 eV respectively, after the adsorption the LUMO values for HA,FA and Cry changed to -4.97, -4.84 and -5.16 eV respectively. The higher value of HOMO and the lower value of LUMO indicate a tendency of the molecule to donate and accept electrons, respectively (A. Liu et al. 2014). A less negative HOMO energy

(E_{HOMO}) gives more charges to unfilled d orbitals of Ag (111) surface, while a LUMO (E_{LUMO}) containing smaller energy could easily receive more electrons.

The HOMO and LUMO values show noticeable changed after the adsorption of NOM's on the Ag (111), these results are consistent to what was reported by (Guo et al. 2017). As shown in Table 5.2.5.1, the Eg values of isolated HA, FA and Cry molecules are 4.69, 3.10 and 1.81 eV respectively in gas phase, after the adsorption on Ag (111) surface, the Eg values changed to 0.41, 0.39 and 0.05 eV respectively confirming the interaction, similar observation was noticed also in the water phase. This suggests that a decreased energy gap gives rise to an intensified charge sharing at interface of HA, FA and Cry and Ag (111) surface, which in turn brings about strengthened interactions (Alibakhshi et al. 2018). The energy gap Eg is often assumed to prompt the chemical reactivity of the NOM molecules toward the substrate surface. Some scholars contemplate that a low Eg value ordinarily corresponds to a high NOM efficiency in the NOM molecule (Gece 2008, Gong et al. 2015).

In another study (Kovačević and Kokalj 2011) argue that, the factors that affect NOM efficiency are multifarious, for example, the molecule absorption location is subtle to the dipole–dipole interaction. Also Hahn (Hahn and Kang 2010) reported that the energy gap of pyridine molecule decreases about 0.9 eV while interacting with Ag(110) surface. One way of clarifying this is that the charging process of the top most metal surface appeared to affect the electronic structure of the adsorbate in such a way that its molecular orbitals were fully stabilized by adsorption (Guo et al. 2017). Previous study by (Carr et al. 2012), obtained similar result and arrived to a similar conclusion that the energy of the HOMO is found to be higher (Table 5.2.5.1), while that of the LUMO is lower under the influence of high dielectric environment, resulting in lowering of the HOMO-LUMO gap. This is consistent with what was observed elsewhere (Carr et al. 2012). It is evident from Table 5.2.5.1 that the adsorption of NOM's reduces the energy gap, this has been reported by (Guo et al. 2017) before.

Table 5.2.5.1: Calculated global reactivity descriptors in COSMO at DFT-D/GGA level of theory.

System	MW (g/mol)	DFT-D Gas phase (eV)					DFT-D COSMO (eV)				
		I	A	χ	η	Ω	I	A	χ	η	ω
HA	226.16	5.97	1.28	3.63	2.34	2.81	6.02	1.47	3.74	2.28	3.08
FA	308.24	5.48	2.38	3.93	1.55	2.98	5.77	2.63	4.20	1.57	5.63
Cry	584.88	4.25	2.44	3.34	0.91	6.16	4.57	2.76	3.66	0.91	7.40
Ag (111)	-	5.38	4.85	5.12	0.27	49.35	5.39	4.86	5.13	0.27	49.50
Ag (111) –HA	-	5.31	4.90	5.10	0.21	63.39	5.38	4.97	5.17	0.21	64.70
Ag (111) –FA	-	5.08	4.69	4.88	0.20	60.43	5.24	4.84	5.04	0.20	62.22
Ag (111) –Cry	-	5.09	5.04	5.06	0.02	523.57	5.40	5.16	5.28	0.12	115.13

Table 5.2.5.2: Calculated global reactivity descriptors in the gas phase at DFT-D/GGA level of theory.

System	MW*	DFT-D Gas phase (eV)				DFT-D COSMO (eV)			
		E_{HOMO}	E_{LUMO}	Eg	μ	E_{HOMO}	E_{LUMO}	Eg	M
HA	226.16	-5.97	-1.28	4.69	-3.63	-6.02	-1.47	4.55	-3.74
FA	308.24	-5.48	-2.38	3.10	-3.93	-5.77	-2.63	3.14	-4.20
Cry	584.88	-4.25	-2.44	1.81	-3.34	-4.57	-2.76	1.82	-3.66
Ag (111)	-	-5.38	-4.85	0.53	-5.12	-5.39	-4.86	0.53	-5.13
Ag (111) –HA	-	-5.31	-4.90	0.41	-5.10	-5.38	-4.97	0.41	-5.17
Ag (111) –FA	-	-5.08	-4.69	0.39	-4.88	-5.24	-4.84	0.41	-5.04
Ag (111) –Cry	-	-5.09	-5.04	0.05	-5.06	-5.40	-5.16	0.24	-5.28

*MW expressed in g/mol

Among all systems, it can be seen that the Cry had the highest electrophilicity index which means Cry has highest reactivity among all systems. This observation implies a direct relation with adsorption energy as well as molecular weight. The results of other calculated global reactivity descriptors presented in Tables 5.2.5.1 and 5.2.5.2 show that while going from the gas phase to water the HOMO, LUMO, μ, I, χ and ω increase while Eg, A and η values in some cases vary or remain unchanged. While working on Carbon Nanotubes (Chermahini, Teimouri, and Farrokhpour 2015) also made a similar observation that, electrophilicity increases going from the gas phase to the solvent phase. Previous studies (Rad 2016b , Rad & Abedini 2016, Rad 2016a, Zhou et al. 2009) have also shown that lower Eg means higher electrical conductivity and in contrast higher Eg corresponds to the lower electrical conductivity. It can be concluded that for all systems, Cry has higher electrical conductivity than HA and FA.

The η of Ag (111) decreases upon the adsorption of HA, FA and Cry decreases, from Table 5.2.5.1, the decrease in hardness of Ag (111) surface upon adsorption is in order of HA > FA

> Cry, these results were consistent as they increased going from gas phase to solvent. If the μ value is negative, it means that the compound is stable and can exist in this configuration (Lopez et al. 2018). The calculated chemical potential and electronegativity values in Tables 5.2.5.1 and 5.2.5.2 for the HA, FA and Cry show that after the adsorption on Ag (111) surface, the chemical potential for HA, FA and Cry increased from -3.63, -3.93 and -3.34 respectively before adsorption to -510, -4.88 and -5.06 respectively after adsorption. The increase was consistent in both gas phase and water as the solvent and a trend was observed where μ values increased moving from gas phase to solvent.

5.2.6 Structure and charge analysis

The effect of HA, FA and Cry adsorption on Ag (111) surface has been investigated by plotting the charge deformation difference (provided in electronic version B). In Table B.1 and Figure B.4 in electronic version B, structural properties and charge deformation difference of adsorbates are shown. The interatomic bonds of the HA, FA, and Cry molecules were calculated and compared before and after relaxation as summarized in Table B.1. From the results small differences were noted for bond distances before and after relaxation. To the authors' knowledge, no previous theoretical and experimental studies on reported bond lengths of HA, FA and Cry hence no comparison were made on this.

To better understand the distribution patterns of charges around the adsorbates, the charge density difference at the interface between the adsorbate and the surface were plotted in three-dimensional (3D) (see Figure B.4). For the FA and Cry shown in Figure B.4 (b) and (c), respectively, a strong redistribution of charges between C=O, C-C, C-H and -OH group was observed, and possibly could yield a change in electron structure. The 3D iso-surfaces Figure B.4 (b-d) of Ag (111)-HA, Ag (111)-FA and Ag (111)-Cry at the interface indicate that the charge was localized mostly on the HA, FA, and Cry with smaller amounts on the pristine Ag (111) surface as shown in Figure B.1 (a). In addition, results in Figures B.5-B.7 (a) clearly show that regions with oxygen atom had higher charges, and hence the functional group likely to exert strong influence on the Ag (111) surface. The electron density difference show the strong interaction between HA, FA and Cry Ag (1 1 1) surface. The isosurface charge density difference for (a) Ag (111) pristine, (b) Ag (111)-HA, (c) Ag (111)-FA and (d) Ag (111)-Cry were the same irrespective of formalism used to perform the calculations (Figures B.8-B.11).

5.2.7 Summary findings of HMW NOM's on Ag (111) surface

Dispersion correction density functional theory (DFT-D) has been used to gain insight on the adsorption of high molecular weight natural organic matter with Ag (111). The calculated adsorption energy indicates that the adsorption was spontaneous and exothermic. The calculated solvation energies indicate that the adsorbates are stable while in solution and there was a direct relation between the adsorbate's molecular weight and the calculated solvation and adsorption energies. From the calculated adsorption energies it can be concluded that FA and Cry will strongly bind to the ENP surface and reside longer in the environment in comparison to HA implying that FA and Cry can stabilize the ENP longer than HA would. Total density of states of Ag (111) surface, HA, FA, Cry, HA on Ag (111), FA on Ag (111) and Cry on Ag (111) surface have been plotted. TDOS is drawn from -10 eV to 5 eV, this was done to show the electronic structures near the Fermi level. The global reactivity descriptors such as HOMO LUMO, Eg, μ, I, A, χ, η and ω were calculated. The results of calculated global reactivity descriptors show that while going from the gas phase to water the HOMO, LUMO, chemical potential, ionization potential, electronegativity and electrophilicity values increased, while Eg, A and η values in some cases vary or remain unchanged, that has been shown by DFT-D level of theory.

5.3 Case study 3: Adsorption and co-adsorption of more than one NOM on Ag (111) surface: A DFT-D study

5.3.1 Introduction

To the best of the candidate's knowledge, this is the first study to provide insight to elucidate how a mixture of formic acid (FA), acetic acid (AA_1) and ascorbic acid (AA_2) may have diverse set of implications on the fate of ENPs in aquatic systems using first-principles calculations; and may be a useful reference in designing experiments on the influence of different NOMs on the ENPs fate in aquatic systems.

The purpose of the work is to gain insight on the adsorption and co-adsorption of natural organic matter on Ag (111) surface. This part of the work aimed at answering the following questions; can we adsorb more than one NOM on the Ag (111) surface? It is possible to co-adsorb a mixture of NOM's on Ag (111) surface? The goal of this study is to further understand the Ag (111) surface adsorption and co-adsorption with low molecular weight (LMW). The investigations in this study go beyond those in the current literature considering the implications of adsorption and co-adsorption of LMW NOMs mixtures on the surfaces of nAg (111) to establish the likely implications of a mixture of NOM's on the adsorption. Overall, this theoretical based-study attempts to offer better insights on how NOMs MW singularly and mixtures of NOMs co-existing in the aquatic system may influence the fate of ENPs.

The nature of the interaction of low molecular weight natural organic matter with the Ag (111) surface is of crucial importance in the environment. The low molecular weight organics used in this study are FA, AA_1 and AA_2. In this part of the study, a realistic environment where single, multiple or even a mixture of NOM's can attach on one Ag (111) surface, has been conceptualised as such critical information is relevant in order to understand the behavior of (ENPs) when they get into the environment, to bridge this gap the adsorption and co-adsorption properties of one, or more than one and a mixture of NOM's on Ag (111) surface using dispersion-corrected density functional theory (DFT-D) in the gas phase and water as a solvent have been investigated.

The COSMO was used to mimic water in these environmental effects on the Ag (111) surface. Throughout this thesis the number behind the letter represent the number of molecules e.g. nFA where $n = 1, 2, 3, 4$ implies 1 to 4 molecules are considered in a given co-adsorption case considered.

5.3.2 Computational studies

Computational details in this section were the same as in section 5.2.1, the paragraph below describes points that have been added for the co-adsorption. Convergence accuracy of charge density of self-consistent field was $1.0e^{-6}$ Ha and Brillouin k point was 1x1x1. In addition, direct inversion of iterative subspace (DIIS) was chosen to accelerate convergence speed of charge density of self-consistent field to reduce calculation time and enhance efficiency. A Fermi smearing of 0.005 hartree and a real-space cutoff of 4.4 Å were employed to improve the computational performance. The Ag (111) surface was modelled using a seven-layer slab with a (4x4) unit cell and only the top three layers were allowed to relax while the four bottom layers were fixed in the optimized bulk position. A 20 Å of vacuum space between the periodic slabs was utilized to eliminate spurious interactions. The effect of solvent was modelled by COSMO (Klamt 1995) where water has been used as a solvent. COSMO is a considerable simplification of the continuum solvation model without significant loss of accuracy (Anafcheh and Ghafouri 2013). For solvation studies, water which has the highest dielectric constant (78.4), is used as solvating medium as it mimics the human biological system in recognizing the behavior of NOM's on Ag (111) surface in aquatic systems in the environment. Figures 5.3.2.1-5.3.2.5 show the optimized structures of side and top view snapshot. Throughout this part the number behind the letter represent the number of molecules i.e. nFA, nAA1, nAA2 (n=1,2,3,4).

	Top view	**Side view**
Ag (111) – 1FA		
Ag (111) – 2FA		
Ag (111) – 3FA		
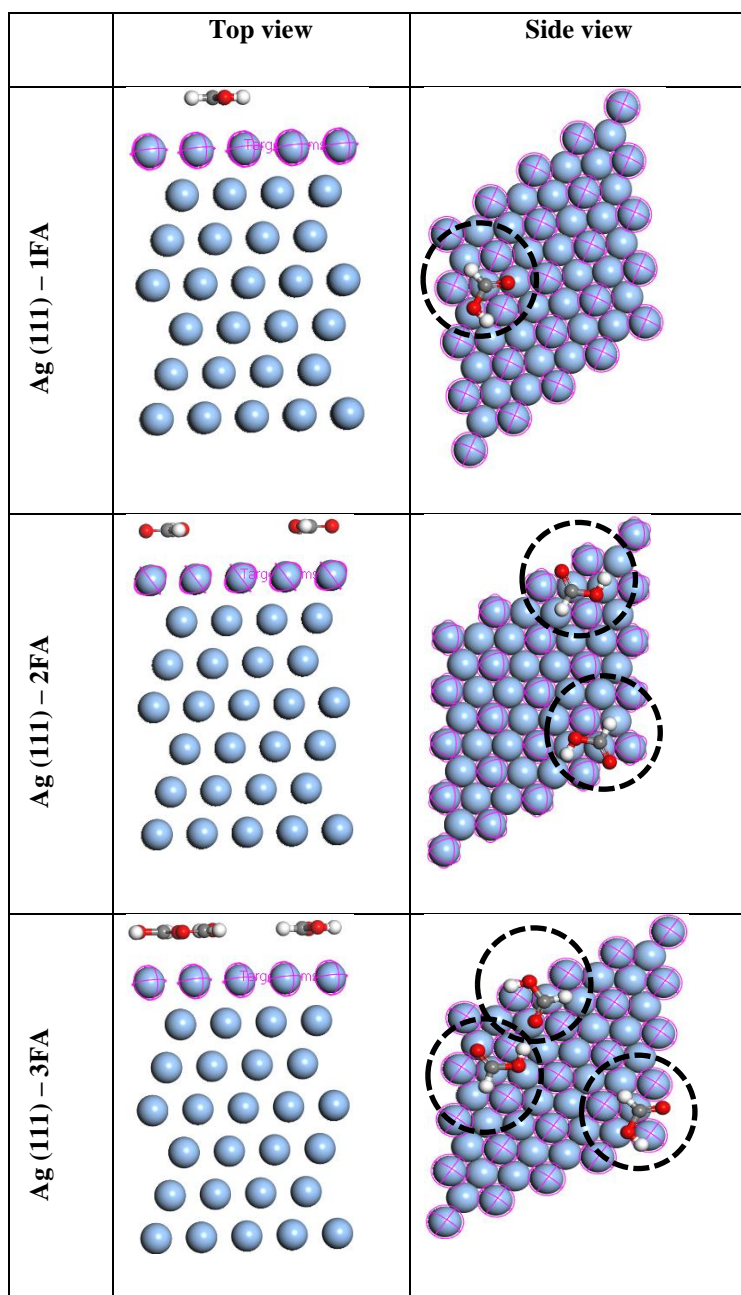
Figure 5.3.2.1: Side and top view snapshot of Ag (111) – 1FA, Ag (111) – 2FA and Ag (111) -.3FA.

	Top view	**Side view**
Ag (111) – 1AA1		
Ag (111) – 2AA1		
Ag (111) – 3AA1		
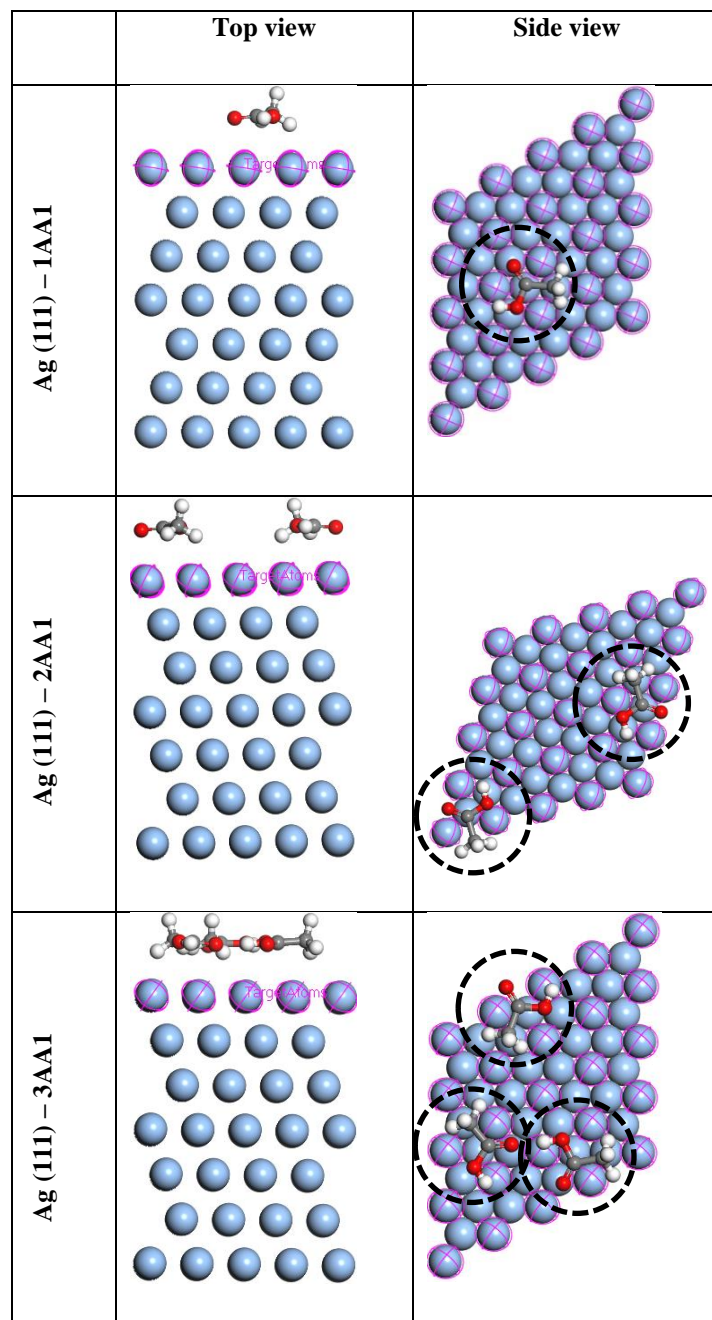
Figure 5.3.2.2: Side and top view snapshot of Ag (111) – 1AA1, Ag (111) – 2AA1 and Ag (111) -.3AA1.

	Top view	Side view
Ag (111) – 1AA2		
Ag (111) – 2AA2		
Ag (111) – 3AA2		
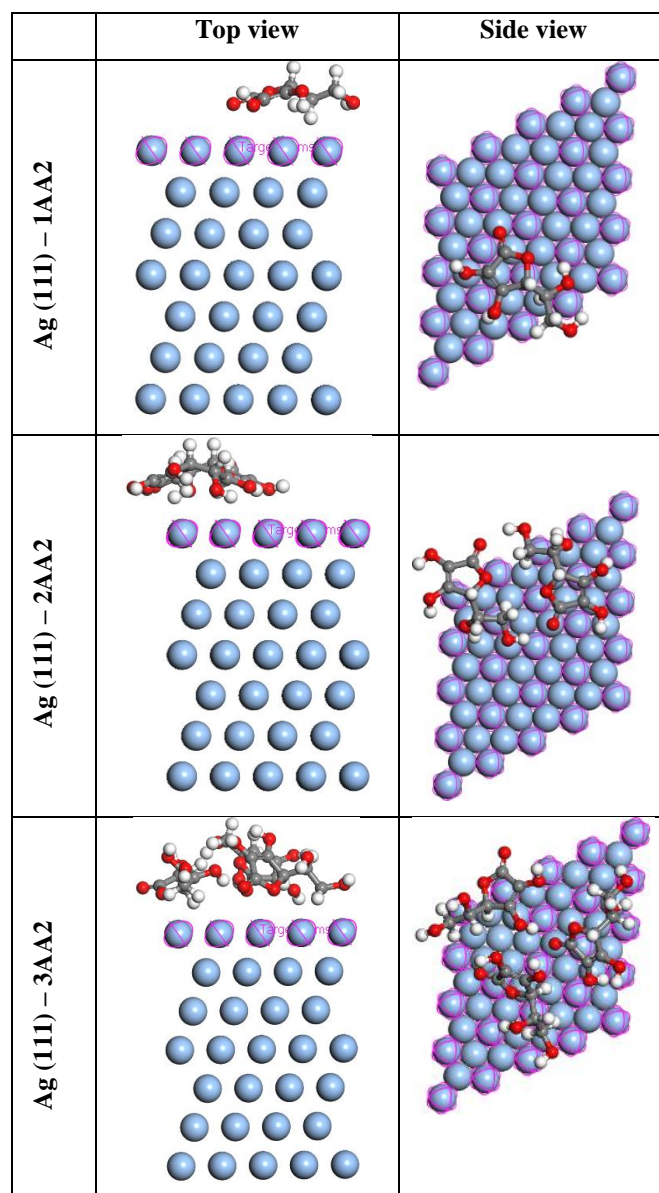
Figure 5.3.2.3: Side and top view snapshot of Ag (111) - 1AA2, Ag (111) – 2AA2 and Ag (111) -3AA2.
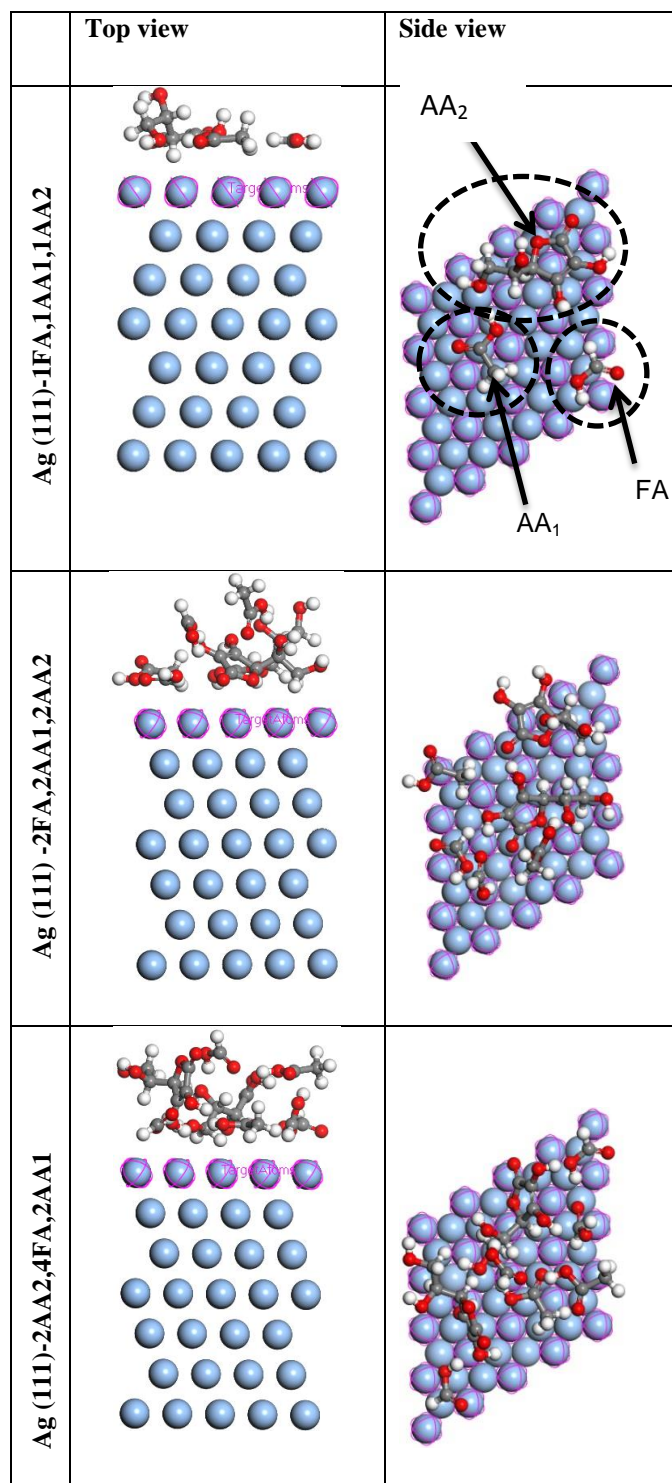
Figure 5.3.2.4: Side and top view snapshot of Ag (111)-1FA, 1AA1, 1AA2, Ag (111) -2FA, 2AA1, 2AA2 and Ag (111) -1AA1, 1AA2.
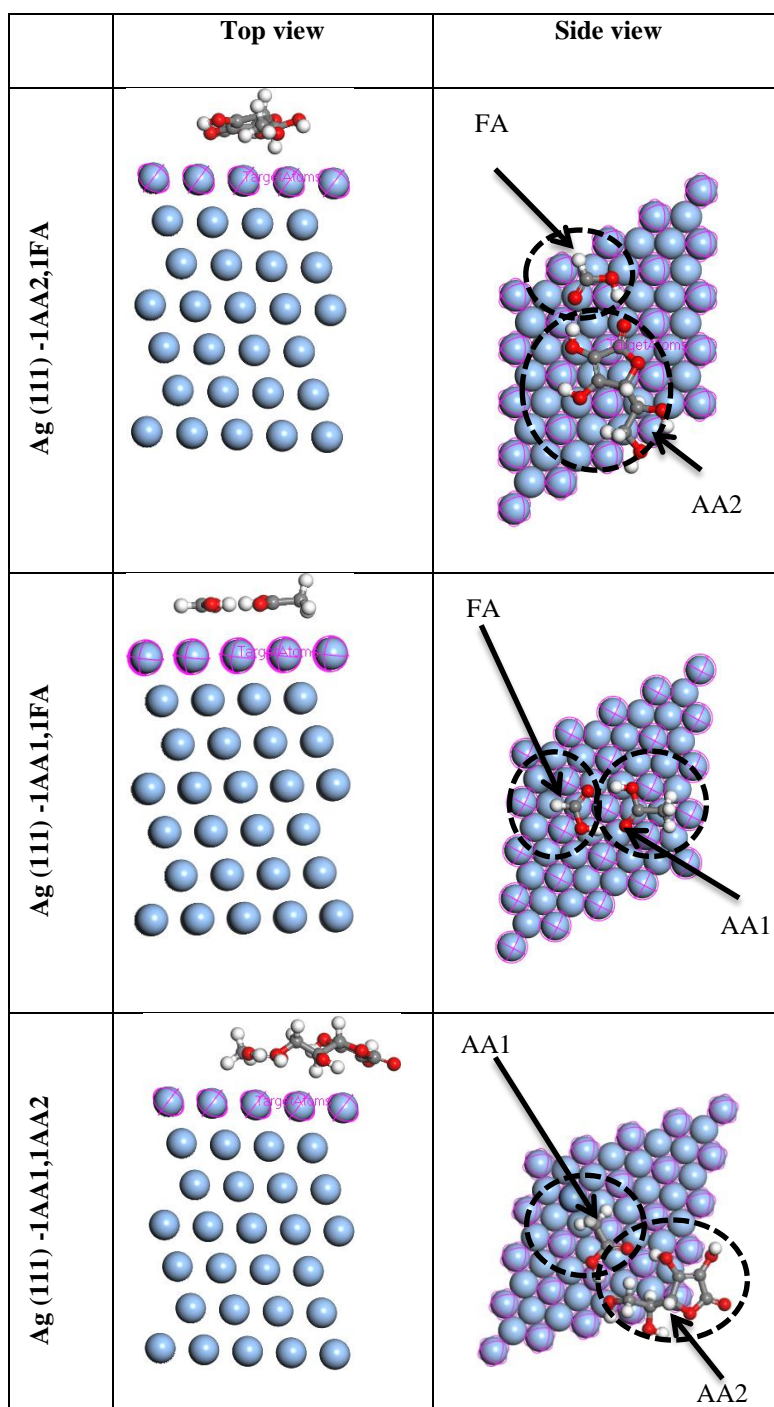
Figure 5.3.2.5: Side and top view snapshot of Ag (111) -1AA2, 1FA, Ag (111) -1AA1,1FA and Ag (111)-2AA2,4FA,2AA1.

5.3.3 Results and discussion

This adsorption and co-adsorption study was motivated by the fact that in a real environment, it is highly possible for single, multiple or even a mixture of different NOM to attach on one Ag (111) surface at the same time, a realistic environmental scenario has been mimicked.

This study has suggested that it is possible to adsorb more than one NOM on the Ag (111) surface using computational modelling. After optimization, the adsorption and co-adsorption configurations of 1AA1, 2AA1 and 3AA2 on Ag (111) surface were obtained, as presented in Figure 5.3.2.1-5.3.2.3. The adsorption and co-adsorption energies are shown in Table 5.3.3.1 were obtained from the expression.

$$E_{ads} = E_{NOM/surface} - nE_{NOM} - E_{surface} \hspace{2cm} (5.10)$$

$E_{NOM/surface}$ is the total energy of the surface and the NOM, where E_{NOM} is the energy of the NOM without the surface, $E_{surface}$ is the energy of the surface without the adsorbate In the expression above, n is the number of adsorbates on the Ag (111) surface.

Table 5.3.3.1: Adsorption and coadsorption of NOM's on Ag (111) surface and equilibrium distance in gas phase and in water as a solvent as well as molecular weights.

| System	MW g/mol	Eads (eV) gas phase	dH-Ag (Å) gas phase	dO-Ag (Å) solvent	Eads (eV) solvent	dH-Ag (Å) solvent	dO-Ag (Å) solvent
Ag (111)-1FA	46.02	-0.19	5.16	-	-0.07	5.16	-
Ag (111)-2FA	92.02	-1.38	5.23	-	-0.49	-	5.22
Ag (111)-3FA	138.06	-1.81	-	5.18	-0.65	5.18	5.18
Ag (111)-1AA1	60.05	-0.32	4.46	-	-0.17	4.46	-
Ag (111)-2AA1	120.1	-1.52	4.43	-	-0.61	4.43	-
Ag (111)-3AA1	180.15	-2.06	4.44	-	-0.90	4.44	-
Ag (111)-1AA2	176.12	-0.53	3.57	-	-0.32	4.30	-
Ag (111)-2AA2	352.24	-3.05	3.77	-	-1.63	3.77	-
Ag (111)-3AA2	528.36	-3.77	3.90	-	-1.72	3.59	-
Ag (111)-1AA1,IFA	106.07	-2.29	4.05	-	-1.32	3.86	-
Ag (111) -1AA2,1FA	222.14	-4.41	3.80	-	-2.49	3.91	-
Ag (111) -1AA1,1AA2	236.17	-2.06	3.63	-	-0.80	3.85	-
Ag (111)- 1FA,1AA1,1AA2	282.19	-1.92	3.61	-	-1.10	3.61	-
Ag (111) -2FA,2AA1,2AA2	564.38	-1.00	4.42	-	-0.55	4.42	-
Ag (111)-4FA,2AA1,2AA2	656.42	-6.54	3.36	-	-3.84	3.75	-

According to Table 5.3.3.1, our computations, both gas phase and COSMO results reveal that the adsorption and co-adsorption of NOM's on Ag (111) surface is favorable. As shown in Table 5.3.3.1, the adsorption and co-adsorption energy becomes stronger as the number of number of molecules increases on the Ag (111) surface. The adsorption energy of 3AA2 on Ag (111) surface is the most negative value -3.77 eV and -1.72 eV respectively in the gas (solvent) phase. From Table 5.3.3.1, an increase in equilibrium distances between the Ag (111) surface and NOM's as the adsorption energy increases 3.90 Å and 3.59 Å in gas and

water phase has been observed. Another trend was observed for the co-adsorption with the exception of 1FA, 1AA1, 1AA2 on Ag (111) surface, the reason for these molecules to have less adsorption energy could be attributed to the fact that molecules with unique properties such as, molecular weight, electronegativity melting point etc. when put on one surface are likely to compete for the active adsorption sites.

When the system consists of adsorbates with different molecular properties, the difference in interaction energies will lead to enhancement of one adsorbate relative to the others. Previous study by (Timón, Senent, and Hochlaf 2015) while working on structural single and multiple molecular adsorption of CO_2 and H_2O in zeolitic imidazolate framework crystals dealt with the issue of competition, even though some of the molecules in their study were not favorable unlike in this study where all the molecules are favorable. Another study that dealt with the issue of competition was conducted by (Nalaparaju, Zhao, and Jiang 2010) on molecular understanding for the adsorption of water and alcohols in hydrophilic and hydrophobic zeolitic metal−organic frameworks. This study found that the adsorption energy increases as you increase the number of molecules.

For the co-adsorption results we observed that a mixture of 2AA2, 4FA and 2AA1 on Ag (111) has the highest adsorption energy -6.54 eV (-3.84 eV) respectively in the gas (solvent) phase making it the most stable compared to other mixtures of different NOM's. The equilibrium distances between the Ag (111) surface and NOM's were 3.36 Å (3.75 Å) respectively in the gas (solvent) phase.

It has been observed that from individual adsorption energies of FA, AA1 and AA2, the adsorbate with the highest adsorption energy will adsorb first on the Ag (111) surface, in our case AA2, as shown above AA2 has the highest adsorption energies compared to FA and AA1.

5.3.4 Quantum chemical calculations

In this section quantum chemical calculations were calculated by using DMol^3 density functional of Materials Studio (BIOVIA 2016). Figure 5.3.4.1 reveals the charge distribution, HOMO and LUMO of FA, AA1 and AA2.
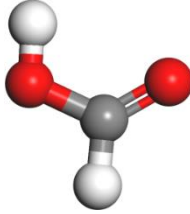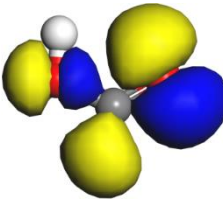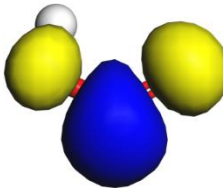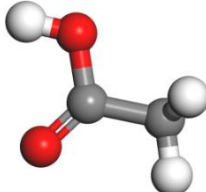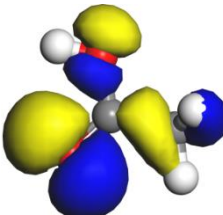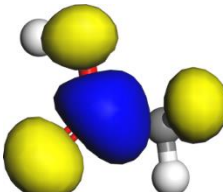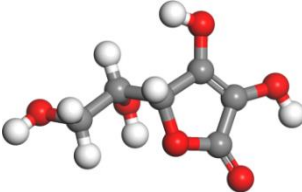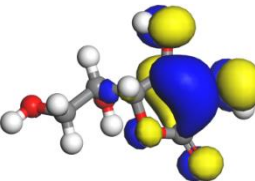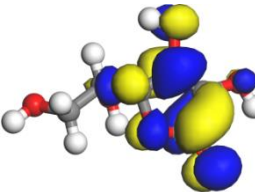
DFT-D COSMO		
Adsorbate	**HOMO**	**LUMO**
FA		
AA$_1$		
AA$_2$		

Figure 5.3.4.1: Optimized structures and the frontier molecular orbital density distributions (HOMO and LUMO).

To better understand the adsorption and co-adsorption process of NOM's on Ag (111) surface, frontier molecular orbitals (HOMO and LUMO) were analysed. The HOMO and LUMO for FA, AA1 and AA2 (Fig 5.3.4.1) show density uniformly distributed on all atoms. It is worth noting that going from gas phase to water as a solvent the HOMO and LUMO distribution slightly change shown in Table 5.3.4.1 and 5.3.4.2 . Tables 5.3.4.1-5.3.4.2 give the global reactivity descriptors calculated using equations in Chapter 4 (equation 4.1).

Table 5.3.4.1: Calculated global reactivity descriptors (eV) in water as a solvent.

System	EHOMO	ELUMO	Eg	μ	IP	EA	χ	η	ω
				DFT-D COSMO					
FA	-6.89	-1.45	5.45	-4.17	6.89	1.45	4.17	2.72	3.19
AA1	-6.60	-1.14	5.46	-3.87	6.60	1.14	3.87	2.73	2.74
AA2	-5.64	-1.86	3.78	-3.75	5.64	1.86	3.75	1.89	3.72
Ag (111)	-4.50	-4.41	0.09	-4.46	4.50	4.41	4.46	0.04	228.15
Ag (111)-1FA	-4.75	-4.48	0.27	-4.62	4.75	4.48	4.62	0.13	79.20
Ag (111)-2FA	-4.74	-4.46	0.27	-4.60	4.74	4.46	4.60	0.14	76.99
Ag (111)-3FA	-4.71	-4.44	0.28	-4.57	4.71	4.44	4.57	0.14	75.39
Ag (111)-1AA1	-4.50	-4.42	0.08	-4.46	4.50	4.42	4.46	0.04	251.60
Ag (111)-2AA1	-4.46	-4.39	0.07	-4.43	4.46	4.39	4.43	0.04	277.05
Ag (111)-3AA1	-4.71	-4.43	0.28	-4.57	4.71	4.43	4.57	0.14	75.30
Ag (111)-1AA2	-4.44	-4.38	0.06	-4.41	4.44	4.38	4.41	0.03	311.07
Ag (111)-2AA2	-4.66	-4.37	0.29	-4.52	4.66	4.37	4.52	0.14	70.74
Ag (111)-3AA2	-4.69	-4.40	0.29	-4.54	4.69	4.40	4.54	0.14	72.23
Ag (111)-1AA1,1FA	-4.73	-4.46	0.27	-4.60	4.73	4.46	4.60	0.14	76.90
Ag (111)-1AA2,1FA	-4.70	-4.42	0.28	-4.56	4.70	4.42	4.56	0.14	74.25
Ag (111)-1AA1,1AA2	-4.70	-4.43	0.27	-4.56	4.70	4.43	4.56	0.14	76.53
Ag (111)-1FA,1AA1,1AA2	-4.67	-4.38	0.29	-4.52	4.67	4.38	4.52	0.14	71.63
Ag (111)-2FA,2AA1,2AA2	-4.71	-4.40	0.31	-4.55	4.71	4.40	4.55	0.16	66.81
Ag (111)-4FA,2AA1,2AA2	-4.80	-4.51	0.29	-4.65	4.80	4.51	4.65	0.14	75.82

Table 5.3.4.2: Calculated global reactivity descriptors (eV) in the gas phase.

System	EHOMO	ELUMO	Eg	μ	IP	EA	χ	η	ω
				DFT-D Gas phase					
FA	-6.74	-1.43	5.31	-4.08	6.74	1.43	4.08	2.65	3.14
AA1	-6.29	-1.00	5.29	-3.65	6.29	1.00	3.65	2.65	2.51
AA2	-5.57	-1.78	3.79	-3.68	5.57	1.78	3.68	1.90	3.56
Ag (111)	-4.50	-4.41	0.09	-4.45	4.5	4.41	4.45	0.04	227.88
Ag (111)-1FA	-4.74	-4.47	0.27	-4.61	4.74	4.47	4.61	0.13	78.83
Ag (111)-2FA	-4.71	-4.43	0.27	-4.57	4.71	4.43	4.57	0.14	76.00
Ag (111)-3FA	-4.67	-4.40	0.27	-4.53	4.67	4.40	4.53	0.14	74.82
Ag (111)-1AA1	-4.47	-4.39	0.08	-4.43	4.47	4.39	4.43	0.04	248.54
Ag (111)-2AA1	-4.40	-4.33	0.07	-4.37	4.4	4.33	4.37	0.04	269.60
Ag (111)-3AA1	-4.63	-4.36	0.28	-4.50	4.63	4.36	4.50	0.14	72.81
Ag (111)-1AA2	-4.41	-4.35	0.06	-4.38	4.41	4.35	4.38	0.03	306.10
Ag (111)-2AA2	-4.57	-4.28	0.29	-4.42	4.57	4.28	4.42	0.14	68.48
Ag (111)-3AA2	-4.63	-4.33	0.30	-4.48	4.63	4.33	4.48	0.15	67.60
Ag (111)-1AA1,1FA	-4.69	-4.41	0.28	-4.55	4.69	4.41	4.55	0.14	74.67
Ag (111)-1AA2,1FA	-4.63	-4.35	0.28	-4.49	4.63	4.35	4.49	0.14	71.97
Ag (111)-1AA1,1AA2	-4.62	-4.34	0.28	-4.48	4.62	4.34	4.48	0.14	72.37
Ag (111)-1FA,1AA1,1AA2	-4.55	-4.28	0.27	-4.41	4.55	4.28	4.41	0.14	71.59
Ag (111)-2FA,2AA1,2AA2	-4.52	-4.22	0.30	-4.37	4.52	4.22	4.37	0.15	63.19
Ag (111)-4FA,2AA1,2AA2	-4.53	-4.23	0.30	-4.38	4.53	4.23	4.38	0.15	64.67

Moreover, we observed that the energy gap (Eg) decreased after adsorption. Previous studies (Rad 2016b, Rad & Abedini 2016, Rad 2016a, Zhou et al. 2009) showed that lower Eg means higher electrical conductivity and in contrast higher Eg corresponds to the lower electrical conductivity. Relatively small changes after adsorption and co-adsorption (Table 5.3.4.1-5.3.4.2) in both gas phase and COSMO, Eg again indicate limited perturbation(s) on Ag (111) surface.

The calculated µ values in Table 5.3.4.1 for the Ag (111) surface indicate that after adsorption and co-adsorption with 1FA, 2FA and 3FA, the chemical potential increased from -4.46 to -4.62, -4.60 and -4.57 eV, respectively. Something different for the Ag (111) surface with 1AA1, 2AA1 and 3AA1, after adsorption and co-adsorption was observed, the µ values, remained the same, decreased and increased from -4.46 to -4.46, -4.43 and -4.57 eV, respectively. Similar observation was observed for the Ag (111) surface with 1AA2, 2AA2 and 3AA2, after adsorption and co-adsorption the µ values decreased and increased from -4.46 to -4.41, 4.52 and -4.54 eV. The adsorption of different NOM's on Ag (111) surface showed an increase in the values of µ from -4.46 for a pristine Ag (111) surface to -4.60, -4.56, -4.56, -4.52, -4.55 and -4.65 eV on Ag (111)-1AA1,1FA, Ag (111)-1AA2,1FA, Ag (111)-1AA1,1AA2, Ag (111)-1FA, 1AA1,1AA2, Ag (111)-2FA,2AA1,2AA2 and Ag (111)-4FA,2AA1,2AA2.

Moving from water to gas phase, it has been observed in Table 5.3.4.2, a similar trend after adsorption and co-adsorption was observed, the µ values increased from -4.47 eV for the Ag (111) surface pristine to -4.61, -4.57 and -4.53 eV for 1FA, 2FA and 3FA respectively. In the case of Ag (111) surface with 1AA1, 2AA1 and 3AA1, after adsorption and co-adsorption decreased and increased from -4.47 to -4.43, -4.37 and 4.50 eV, respectively. For the Ag (111) surface with 1AA2, 2AA2, 3AA2 after adsorption and co-adsorption the µ values decreased and increased from -4.47 to -4.29, -4.31 and -4.51 respectively. Unlike in water as in solvent, in the gas phase as shown in Table 5.3.4.2, the co-adsorption of different NOM's on Ag (111) surface showed an increase, decrease and increase again in the values of µ from -4.47 eV for the Ag (111) surface for the pristine before co-adsorption to -4.41, -4.59, -4.48, -4.49, -4.55 and -4.39 eV for Ag (111)-1FA,1AA1,1AA2, Ag (111) -2FA,2AA1,2AA2, Ag (111) -1AA1, 1AA2, Ag (111) -1AA2,1FA, Ag (111) -1AA1,1FA and Ag (111)-2AA2,4FA,2AA1 respectively.

A close look at Table 5.3.4.1 the values of μ are very similar the difference is very small even though the COSMO values are a bit higher than the μ values in gas phase expect in the case of Ag (111) -2FA, 2AA1, 2AA2 where a μ value of -4.55 and -4.59 eV in the water as a solvent and in the gas phase respectively were observed. Based on the μ values obtained in Table 5.3.4.1 and Table 5.3.4.2, it can be concluded that water as the solvent enhances the reactivity. Compared to μ values, ionization potential also followed the same trend before and after adsorption and co-adsorption, increased, decreased, increased and decreased. In the case of EA different results were observed, the EA values increase from 4.43 eV for the Ag (111) surface pristine to 4.48 eV and 4.46 eV for 1FA and 2FA respectively while remain unchanged for 3FA at 4.43 eV. For other adsorption and co-adsorption as shown in Table 5.3.4.2, IP decreased except for Ag (111) -1AA1, 1FA where we observed 4.45 eV, after co-adsorption.

Similar to u values, values for electronegativity (χ) after adsorption and co-adsorption with 1FA, 2FA and 3FA, the chemical potential increased respectively. Something dissimilar for the Ag (111) surface with 1AA1, 2AA1 and 3AA1, after adsorption and co-adsorption the chemical potential (μ) values decreased and increased respectively. Similar observation was observed for the Ag (111) surface with 1AA2, 2AA2 and 3AA2, after adsorption and co-adsorption the χ values decreased and increased. The adsorption of different NOM's on Ag (111) surface showed an increase in the values of χ as shown in Table 5.3.4.2.The higher the value of ω, the higher the electrophilic power of the investigated structure. Based on the above statement, from our calculated results we noticed that the electrophilicity index of Ag (111) surface was higher than that of adsorbates i.e. FA, AA1 and AA2, indicating a charge transfer from FA, AA1 and AA2 to Ag (111) surface.

5.3.5 Electronic structure properties

To better elucidate the interaction between Ag (111) and NOM's it is worthwhile to study the electronic properties. For these purposes, analysis of total density of states (TDOS) is predominantly valuable. The TDOS of all NOM's on Ag (111) surface species in Fig. 5.3.5.1 (a-d) are drawn in the -30 to 4 eV ranges, in order to show the electronic structures near the Fermi level. TDOS of NOM's only and NOM with Ag (111) surface have also been studied and the data are shown in Fig. 5.3.5.1 (a-d). Based on Figure 5.3.5.1 (a-d), upon interaction of Ag (111) surface with NOM's, no major changes in the energy states, the states kept the

shape of Ag (111) surface which means there is not much done by the NOM's on Ag (111) surface. Before adsorption in Figure C.2 (Appendix C), it has been observed that the TDOS of isolated Ag (111) surface, FA, AA1 and AA2 have distinct peaks corresponding to separate energy levels. For the Ag (111) surface, the dominant peaks were observed at -6.8 eV, -5.2 eV, -4.1 eV and -2.8 eV which are all below Fermi level. For FA and AA1 the dominant peaks were observed at -7.1 eV, -5.2 eV, -2.8 eV and 0 eV which are all below Fermi level. In the case of AA2 the dominant peaks were observed at -7.2 eV, -5.0 eV and -2.1 eV which are all below Fermi level and 0.4, and 1.2 eV above Fermi level.

After adsorption of FA, AA1, AA2 and a mixture of different NOM's on Ag (111) surface, their TDOS demonstrates an alteration and the peaks move to the low energy level near the Fermi level even though the prominent peaks remain those of Ag (111) surface. After adsorption the dominant peaks were observed at -5.1 eV,-4.8 eV,-4.4 eV and 0 eV all below the Fermi level as shown in Figure 5.3.5.1 (a-d). The small changes after adsorption in the TDOS of Ag (111) surface, FA, AA1 and AA2 show the interaction between the NOM's and Ag (111) surface. It can be concluded that the results of TDOS calculation show that after the interaction, the NOM's do not do much on the structure of silver, as confirmed by the results of after adsorption in Figure 5.3.5.1 (a-d). Results of TDOS in the gas phase are shown in Appendix C Figures C.3 (a-d) they are the same as the results of TDOS in water as a solvent.

In Figures 5.3.5.2-5.3.5.3 (a-i) PDOS plots for NOM's on Ag (111) surface calculated using DFT-D/GGA in water as a solvent, PDOS in gas phase are shown in Figures C.4 and C.5 in Appendix C. PDOS in Figures 5.3.5.2-5.3.5.3 (a-i) show intense peaks below and one above Fermi level, prominent shoulder peaks corresponding to separate energy levels between -7.8 and -0.3 eV below the Fermi level and 0.3 eV above the Fermi level.
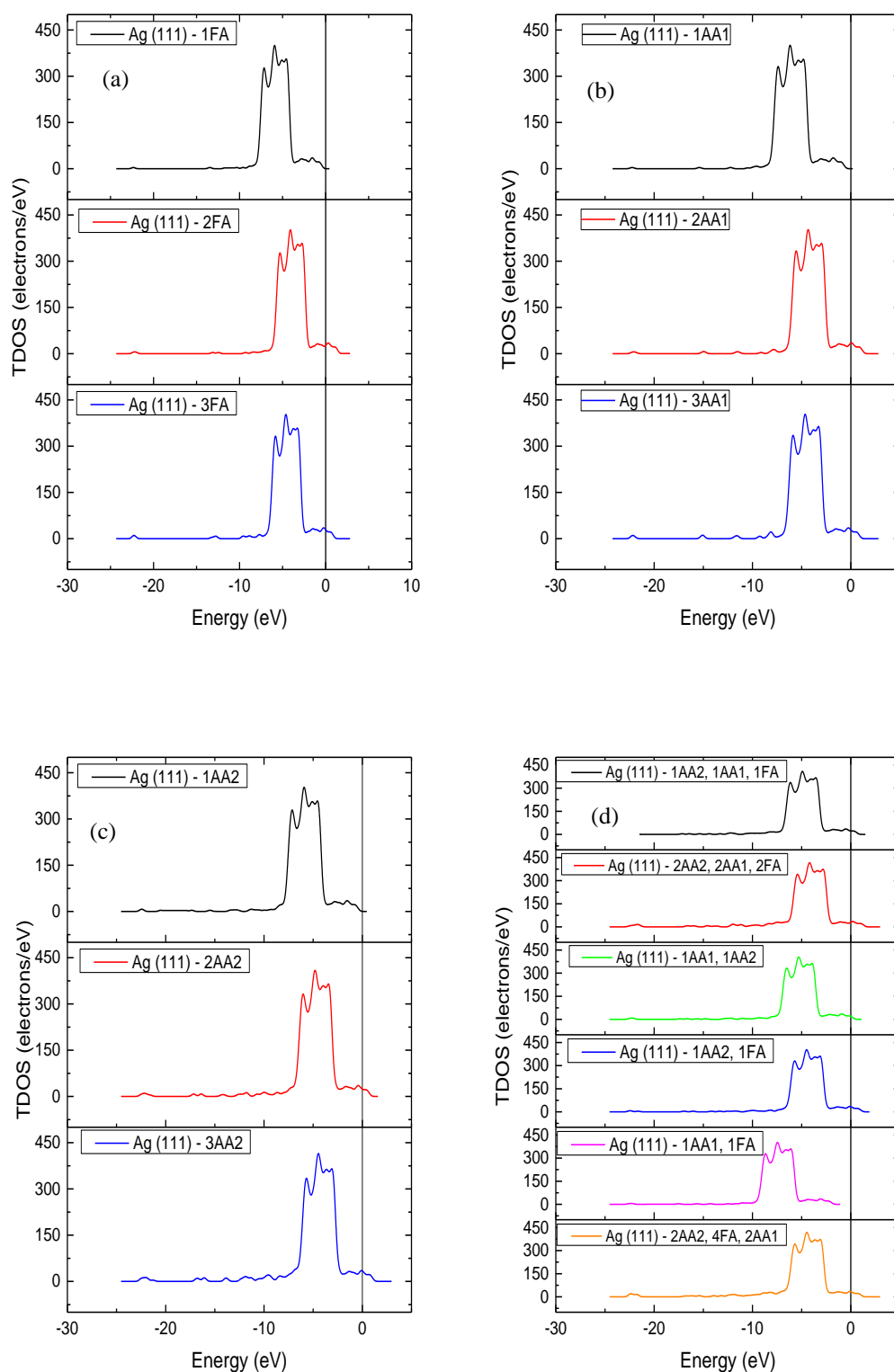
Figure 5.3.5.1: The total density of states (TDOS) in water as a solvent for (a) Ag (111) - 1FA, Ag (111) – 2FA and Ag (111) – 3FA (b) Ag (111) – 1AA1, Ag (111) – 2AA1 and Ag (111) – 3AA1 (c) Ag (111) – 1AA2, Ag (111) – 2AA2 and Ag (111) – 3AA2 and (d) Ag (111) surface with a mixture of NOM's. The Fermi level is indicated with a black vertical line.
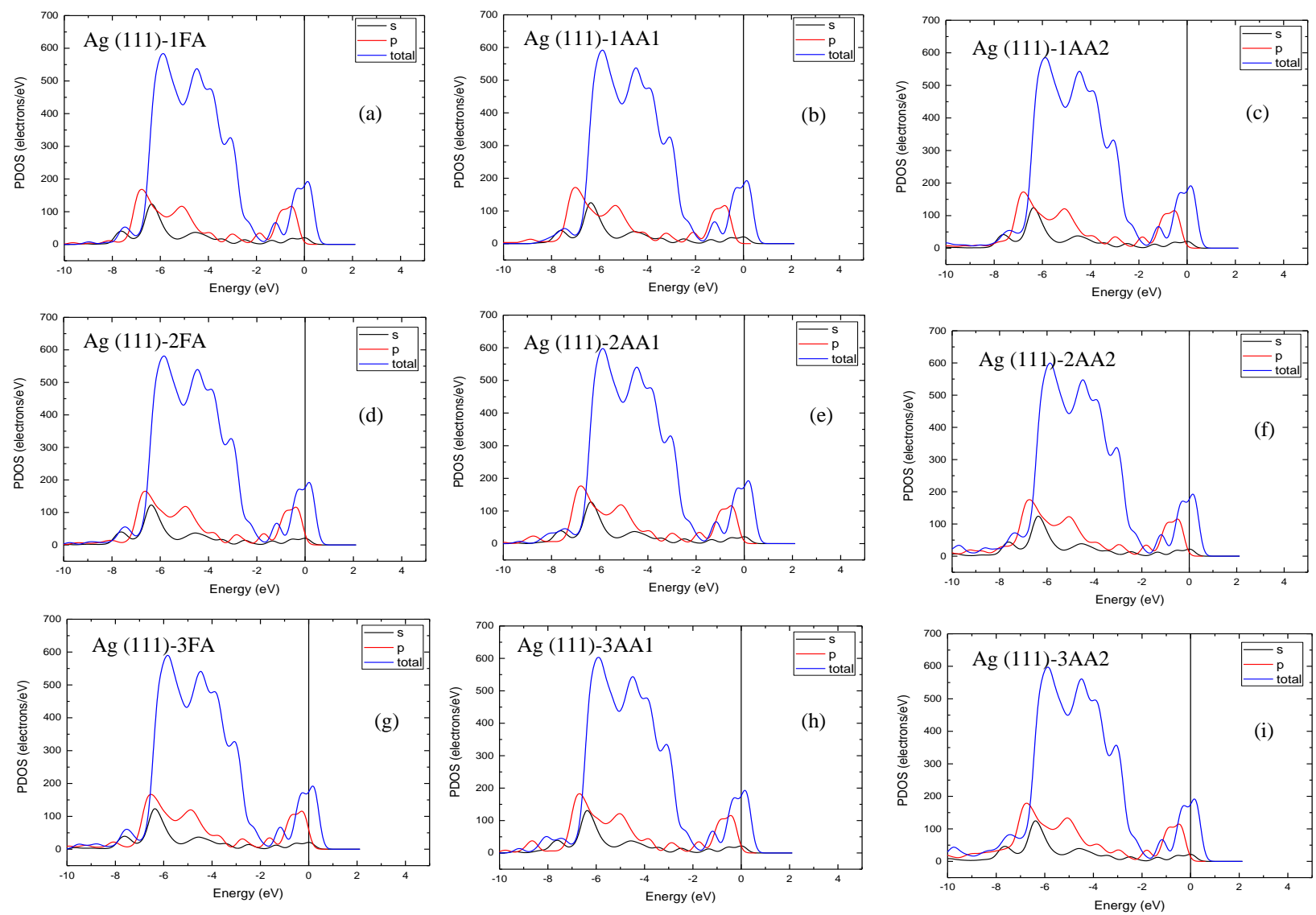
Figure 5.3.5.2: Projected density of states of NOM's on Ag (111) surface (a-f) in COSMO using DFT-D/GGA level of theory.
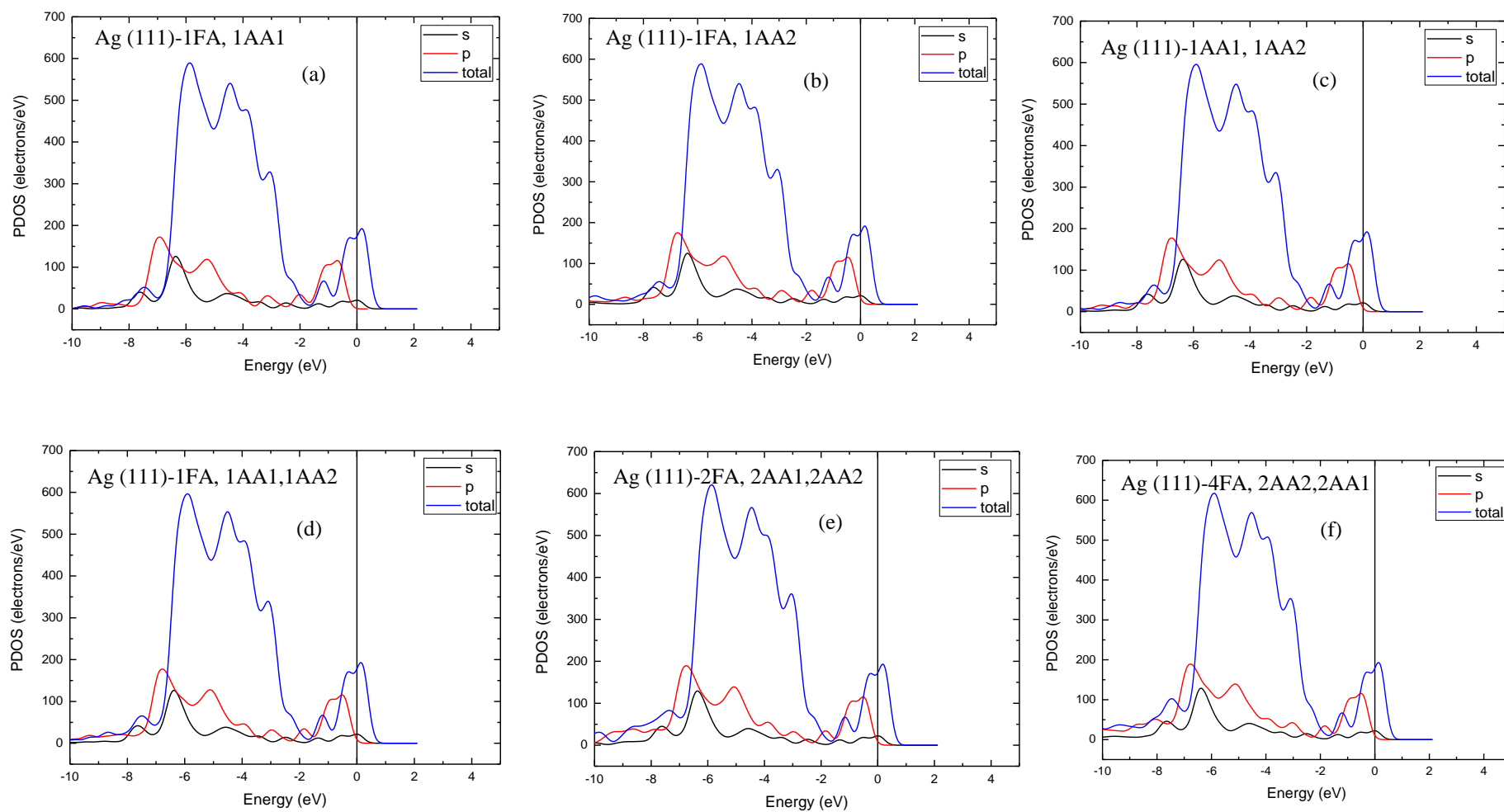
Figure 5.3.5.3: Projected density of states of NOM's on Ag (111) surface (a-f) in COSMO using DFT-D/GGA level of theory.

5.4 Summary findings of adsorption and co-adsorption of single and multi NOM's on Ag (111) surface: A DFT-D study

The main purpose of the work was to gain insight on the adsorption and co-adsorption of natural organic matter on Ag (111) surface. Thus the work aimed at answering the following questions: Can we adsorb more than one NOM on the Ag (111) surface? From this part of the work, it has been confirmed that well indeed, it is possible to co-adsorb a mixture of NOM's on Ag (111) surface. The adsorption and co-adsorption properties of one, more than one and a mixture of NOM's on Ag (111) surface using density functional theory dispersion-corrected (DFT-D) in the gas phase and water as a solvent have been investigated. The calculated adsorption energy results suggest that the interaction of 4FA, 2AA1 and 2AA2 molecules with Ag (111) surface is the strongest with most negative energy values (-6.54 and -3.84 eV) in both gas phase and COSMO, respectively, which reveals that is the most stable system. The reason for the co-adsorption of 4FA, 2AA1 and 2AA2 molecules with Ag (111) surface to absorb more on Ag (111) surface can be attributed to the fact that when they are combined they have the highest molecular weight. In this section, the question of the competition between FA, AA1 and AA2 for the adsorption sites has been addressed; it is well known that different adsorbates with different properties will compete for the active sites when adsorbed on one Ag (111) surface. From the Table 5.3.4.2, it has been observed that from individual adsorption energies of FA, AA1 and AA2, the adsorbate with the highest adsorption energy will adsorb first on the Ag (111) surface, in our case AA2 from Table 5.3.4.2 has the highest adsorption energies compared to FA and AA1.

It has been found that water as a solvent does not play a crucial in enhancing the adsorption because the calculated adsorption energies in water as a solvent are not higher compared to adsorption energies in the gas phase. The global reactivity descriptors such as HOMO, LUMO, LUMO-HOMO, e.g. IP, EA, η and ω in the gas phase and water as a solvent were calculated. To better elucidate the adsorption characteristics of Ag (111) surface, total density of states (TDOS) analyses were performed, TDOS results showed little changes after the adsorption of low molecular weight NOM's on Ag (111) surface. The calculations have given a better understanding of the interaction of Ag (111) surface toward FA, AA1, and AA2 organics in the gas phase and in water as a solvent. In summary, the present work shows that

it is possible to adsorb more than one NOM or a mixture of NOM's on one Ag (111) surface which one of the objectives of this thesis.

Chapter 6: General conclusion, future research and perspective

To pursue and achieve the overall objective of the study, *in silico* techniques have been be exploited based on *ab initio* modelling of nanoparticle properties using density functional theory (DFT) and dispersion density functional theory (DFT-D). The research focus has been on exploiting the capabilities of *in silico* techniques to develop descriptors to enhance our collective understanding and account at a fundamental level the exposure, fate and behavior of engineered nanoparticles in the aquatic systems. In particular, the density functional theory (DFT), classical lattice dynamics (CLD), and quantum mechanical calculations based on frontier molecular orbital (FMO) theory were applied to elucidate the interactions of ENPs and NOMs. For example, using computer simulations the effects of static properties such as size, shape, surface characteristics and properties as well as dynamic properties like aggregation state, dissolution among others of engineered nanoparticles have been investigated to elucidate their fate and behavior in aquatic systems. To study the fate and behavior of nanoparticles, one needs to consider that when nanoparticles are in solution, their surface establishes a dipole layer if charged which in turn stabilizes the particles and prevents aggregation. However, as the nanoparticles surface (s) interacts with abiotic factors such as natural organic matter (NOM), the properties of the nanoparticle's surface are likely to be modified. Arising from such interactions are two plausible scenarios, namely; nanoparticles stabilization where no aggregation occurs or aggregation occurs primarily depended on factors such as pH, NOM charge, and electrolytes present. Thus, in order to investigate the stability of nanoparticles (e.g. aggregation, dissolution, etc.) in this study different monovalent and divalent molecules and NOM have been adsorbed at different sites of the nanoparticle; and establish the stability effect on the nanoparticles.

The first objective of the study has been to properties of (LMW) NOM on Ag nanoparticles that can be used as global descriptors, to achieve that low molecular weight NOM's were adsorbed on different Ag nanoparticles (i.e. Ag (111) surface, tetrahedron Ag (111) surface, cylindrical Ag (111) surface and spherical Ag nanoparticles). From this part of the study, it has been observed that indeed these low molecular weight NOM's do attach on different Ag

nanoparticles that has been confirmed by negative adsorption energies. In the terms of adsorption stabilities, (LMW) NOM adsorbs differently on different Ag (111) surface, for example it has been on observed that the adsorption energy of formic acid on Ag (111) surface in not the same when the same adsorbate attached on tetrahedron Ag (111) surface.

The second objective has been to understand the adsorption properties of (HMW) NOM (humic acid, fulvic acid and cryptochrome) on Ag (111) surface in gas phase and water as a solvent. These (HMW) NOM's were considered because they are ambiguously found in the aquatic systems. From this objective, it has been observed that indeed the (HMW) NOM do attach on the Ag (111) surface and the adsorption energies increased with increasing molecular weight.

The third objective has been to address the question of competition for the adsorption sites when two or more different NOM's of different properties are placed on Ag (111) surface. The conclusion from this study is that , to know which NOM adsorbs first on the Ag (111) surface, the first thing to do is to calculate the adsorption energies of the individual NOM's the from the, the one with the highest adsorption energy is likely to adsorb first.

From all these objectives properties that can be used as global descriptors have been calculated, such properties include HOMO, LUMO, LUMO-HOMO (Eg), the chemical potential (μ), ionization potential (IP), electron affinity (EA), electronegativity (χ), hardness (η) and electrophilicity (ω) in the gas phase and water as a solvent were calculated. In future another plan is to adsorb the NOM;s that have been used to this study on other transition metals such as gold, copper, nickel, palladium and platinum.

Even though the three objectives of this thesis were achieved, the methods or the computational techniques used had their limitations and problems were experienced. For example, it was difficult to run simulations of constructed ENPs (>100 nm), they were computationally too demanding not feasible for using first principles calculations and that led to problems of convergence when absorbing more than one large molecule like Cry on the Ag (111) surface. Moving forward this issue can be solved by using molecular dynamics (MD), which deals with larger molecules. Also when dealing with mixtures on the surface, the mixtures first interact with each other because they have unique properties before they

interact with the surface. To allow the interaction to happen smoothly, the study suggest building a bigger surface unlike the 3x3 and 4x4 surfaces used in this study, maybe increasing the surface may improve the interaction that will lead to improvement of the results.

References

Abad-Álvaro, I, C Trujillo, E Bolea, F Laborda, M Fondevila, M A Latorre, and J R Castillo. 2019. "Silver Nanoparticles-Clays Nanocomposites as Feed Additives: Characterization of Silver Species Released during in Vitro Digestions. Effects on Silver Retention in Pigs." *Microchemical Journal* 149: 104040.

Afzal, Mohammad Atif Faiz, and Johannes Hachmann. 2019. "High-Throughput Computational Studies in Catalysis and Materials Research, and Their Impact on Rational Design." *ArXiv Preprint ArXiv:1902.03721*.

Ahamed, T K Shameera, Vijisha K Rajan, and K Muraleedharan. 2019. "QSAR Modeling of Benzoquinone Derivatives as 5-Lipoxygenase Inhibitors." *Food Science and Human Wellness*.

AIKEN, George R. 1985. "Isolation and Concentration Techniques for Aquatic Humic Substances." *Humic Substances in Soils Sediment, and Water. Geochemistry, Isolation, and Characterization*, 363–85.

Ajayan, P M, and L D Marks. 1988. "Quasimelting and Phases of Small Particles." *Physical Review Letters* 60 (7): 585.

Ali, Attarad, Muhammad Zia Hira Zafar, Ihsan ul Haq, Abdul Rehman Phull, Joham Sarfraz Ali, and Altaf Hussain. 2016. "Synthesis, Characterization, Applications, and Challenges of Iron Oxide Nanoparticles." *Nanotechnology, Science and Applications* 9: 49.

Alibakhshi, Eiman, Mohammad Ramezanzadeh, Ghasem Bahlakeh, Bahram Ramezanzadeh, Mohammad Mahdavian, and Milad Motamedi. 2018. "Glycyrrhiza Glabra Leaves Extract as a Green Corrosion Inhibitor for Mild Steel in 1 M Hydrochloric Acid Solution: Experimental, Molecular Dynamics, Monte Carlo and Quantum Mechanics Study." *Journal of Molecular Liquids* 255: 185–98.

Alizadeh, Sanaz, Subhasis Ghoshal, and Yves Comeau. 2019. "Fate and Inhibitory Effect of Silver Nanoparticles in High Rate Moving Bed Biofilm Reactors." *Science of The Total Environment* 647: 1199–1210.

Anafcheh, Maryam, and Reza Ghafouri. 2013. "Silicon Doping of Defect Sites in Stone--

Wales Defective Carbon Nanotubes: A Density Functional Theory Study." *Superlattices and Microstructures* 60: 1–9.

Andzelm, Jan, Christoph Kölmel, and Andreas Klamt. 1995. "Incorporation of Solvent Effects into Density Functional Calculations of Molecular Energies and Geometries." *The Journal of Chemical Physics* 103 (21): 9312–20.

Angel, Brad M, Graeme E Batley, Chad V Jarolimek, and Nicola J Rogers. 2013. "The Impact of Size on the Fate and Toxicity of Nanoparticulate Silver in Aquatic Systems." *Chemosphere* 93 (2): 359–65.

Armaković, Stevan, Sanja J Armaković, Jovan P Šetrajčić, Stevo K Jaćimovski, and Vladimir Holodkov. 2014. "Sumanene and Its Adsorption Properties towards CO, CO2 and NH3 Molecules." *Journal of Molecular Modeling* 20 (4): 2170.

Azcárate, Julio C, Gastón Corthey, Evangelina Pensa, Carolina Vericat, Mariano H Fonticelli, Roberto C Salvarezza, and Pilar Carro. 2013. "Understanding the Surface Chemistry of Thiolate-Protected Metallic Nanoparticles." *The Journal of Physical Chemistry Letters* 4 (18): 3127–38.

Barnard, Amanda S. 2009. "How Can Ab Initio Simulations Address Risks in Nanotech?" *Nature Nanotechnology* 4 (6): 332–35.

Barnard, Amanda S, and Peter Zapol. 2004. "A Model for the Phase Stability of Arbitrary Nanoparticles as a Function of Size and Shape." *The Journal of Chemical Physics* 121 (9): 4276–83.

Baun, Anders, Nanna B Hartmann, Khara D Grieger, and Steffen Foss Hansen. 2009. "Setting the Limits for Engineered Nanoparticles in European Surface Waters--Are Current Approaches Appropriate?" *Journal of Environmental Monitoring* 11 (10): 1774–81.

Becke, Axel D, and Kenneth E Edgecombe. 1990. "A Simple Measure of Electron Localization in Atomic and Molecular Systems." *The Journal of Chemical Physics* 92 (9): 5397–5403.

Beckett, Ronald, and Ngoc P Le. 1990. "The Role or Organic Matter and Ionic Composition in Determining the Surface Charge of Suspended Particles in Natural Waters." *Colloids and Surfaces* 44: 35–49.

Behravan, Mahmoodreza, Ayat Hossein Panahi, Ali Naghizadeh, Masood Ziaee, Roya

Mahdavi, and Aliyar Mirzapour. 2019. "Facile Green Synthesis of Silver Nanoparticles Using Berberis Vulgaris Leaf and Root Aqueous Extract and Its Antibacterial Activity." *International Journal of Biological Macromolecules* 124: 148–54.

Ben-Naim, Arieh. 2006. *Molecular Theory of Solutions*. Oxford University Press.

Benn, Troy M, and Paul Westerhoff. 2008. "Nanoparticle Silver Released into Water from Commercially Available Sock Fabrics." *Environmental Science & Technology* 42 (11): 4133–39.

Biovia, Dassault Systèmes. 2016. "Discovery Studio Modeling Environment, Release 2017." *Dassault Syst{è}mes, San Diego, CA*.

BIOVIA, Dassault Systèmes. 2016. "Discovery Studio Modeling Environment, Release 3.5." *Accelrys Software Inc., San Diego*.

Borck, Øyvind, and Elsebeth Schröder. 2005. "First-Principles Study of the Adsorption of Methanol at the α-Al2O3 (0001) Surface." *Journal of Physics: Condensed Matter* 18 (1): 1.

Born, Max, and Robert Oppenheimer. 1927. "Zur Quantentheorie Der Molekeln." *Annalen Der Physik* 389 (20): 457–84.

Brezonik, PatrickL. 2018. *Chemical Kinetics and Process Dynamics in Aquatic Systems*. Routledge.

Brivio, G P, and M I Trioni. 1999. "The Adiabatic Molecule--Metal Surface Interaction: Theoretical Approaches." *Reviews of Modern Physics* 71 (1): 231.

Carr, Jessica A, Hong Wang, Anuji Abraham, Terry Gullion, and James P Lewis. 2012. "L-Cysteine Interaction with Au55 Nanoparticle." *The Journal of Physical Chemistry C* 116 (49): 25816–23.

Chantaramolee, Bhume, Allan Abraham B Padama, Hideaki Kasai, and Yogi Wibisono Budhi. 2015. "First Principles Study of N and H Atoms Adsorption and NH Formation on Pd (111) and Pd3Ag (111) Surfaces." *Journal of Membrane Science* 474: 57–63.

Chen, Feiran, Zhenggao Xiao, Le Yue, Jing Wang, Yan Feng, Xiaoshan Zhu, Zhenyu Wang, and Baoshan Xing. 2019. "Algae Response to Engineered Nanoparticles: Current Understanding, Mechanisms and Implications." *Environmental Science: Nano*.

Chen, Kai Loon, Steven E Mylon, and Menachem Elimelech. 2007. "Enhanced Aggregation of Alginate-Coated Iron Oxide (Hematite) Nanoparticles in the Presence of Calcium,

Strontium, and Barium Cations." *Langmuir* 23 (11): 5920–28.

Chermahini, Alireza Najafi, Abbas Teimouri, and Hossein Farrokhpour. 2015. "A DFT-D Study on the Interaction between Lactic Acid and Single-Wall Carbon Nanotubes." *RSC Advances* 5 (118): 97724–33.

Cho, Kyung-Hwan, Jong-Eun Park, Tetsuya Osaka, and Soo-Gil Park. 2005. "The Study of Antimicrobial Activity and Preservative Effects of Nanosilver Ingredient." *Electrochimica Acta* 51 (5): 956–60.

Contado, Catia. 2015. "Nanomaterials in Consumer Products: A Challenging Analytical Problem." *Frontiers in Chemistry* 3: 48.

Cornelis, Geert. 2015. "Fate Descriptors for Engineered Nanoparticles: The Good, the Bad, and the Ugly." *Environmental Science: Nano* 2 (1): 19–26.

Cramer, Christopher J, and Donald G Truhlar. 1999. "Implicit Solvation Models: Equilibria, Structure, Spectra, and Dynamics." *Chemical Reviews* 99 (8): 2161–2200.

Davey, Wheeler P. 1925. "Precision Measurements of the Lattice Constants of Twelve Common Metals." *Physical Review* 25 (6): 753.

Delley, B. 2002. "Hardness Conserving Semilocal Pseudopotentials." *Physical Review B* 66 (15): 155125.

Delley, Bernard. 2000. "From Molecules to Solids with the DMol3 Approach." *The Journal of Chemical Physics* 113 (18): 7756–64.

Dewar, Michael J S, and Walter Thiel. 1977. "Ground States of Molecules. 38. The MNDO Method. Approximations and Parameters." *Journal of the American Chemical Society* 99 (15): 4899–4907.

Domenicano, Aldo, and Istvan Hargittai. 1992. *Accurate Molecular Structures: Their Determination and Importance*. Vol. 1. Oxford University Press.

Domingos, Rute F, Mohamed A Baalousha, Yon Ju-Nam, M Marcia Reid, Nathalie Tufenkji, Jamie R Lead, Gary G Leppard, and Kevin J Wilkinson. 2009. "Characterizing Manufactured Nanoparticles in the Environment: Multimethod Determination of Particle Sizes." *Environmental Science & Technology* 43 (19): 7277–84.

Donia, D T, and M Carbone. 2019. "Fate of the Nanoparticles in Environmental Cycles." *International Journal of Environmental Science and Technology* 16 (1): 583–600.

Dreizler, Reiner M, and Eberhard K U Gross. 1990. "Density Functional Theory: An

Approach to the Quantum Many-Body Problem Springer." Berlin.

Duncan, Timothy V, and Karthik Pillai. 2014. "Release of Engineered Nanomaterials from Polymer Nanocomposites: Diffusion, Dissolution, and Desorption." *ACS Applied Materials & Interfaces* 7 (1): 2–19.

Erbs, Jasmine J, Thelma S Berquó, Brian C Reinsch, Gregory V Lowry, Subir K Banerjee, and R Lee Penn. 2010. "Reductive Dissolution of Arsenic-Bearing Ferrihydrite." *Geochimica et Cosmochimica Acta* 74 (12): 3382–95.

Espinasse, Benjamin P, Nicholas K Geitner, Ariette Schierz, Mathieu Therezien, Curtis J Richardson, Gregory V Lowry, Lee Ferguson, and Mark R Wiesner. 2018. "Comparative Persistence of Engineered Nanoparticles in a Complex Aquatic Ecosystem." *Environmental Science & Technology* 52 (7): 4072–78.

Feliu, Neus, Dominic Docter, Markus Heine, Pablo del Pino, Sumaira Ashraf, Jelena Kolosnjaj-Tabi, Paolo Macchiarini, et al. 2016. "In Vivo Degeneration and the Fate of Inorganic Nanoparticles." *Chemical Society Reviews* 45 (9): 2440–57.

Fock, Vladimir. 1930. "N{ä}herungsmethode Zur L{ö}sung Des Quantenmechanischen Mehrk{ö}rperproblems." *Zeitschrift F{ü}r Physik A Hadrons and Nuclei* 61 (1): 126–48.

Francioso, Ornella, Eduardo Lopez-Tobar, Armida Torreggiani, Mercedes Iriarte, and Santiago Sanchez-Cortes. 2019. "Stimulated Adsorption of Humic Acids on Capped Plasmonic Ag Nanoparticles Investigated by Surface-Enhanced Optical Techniques." *Langmuir*.

Franklin, Natasha M, Nicola J Rogers, Simon C Apte, Graeme E Batley, Gerald E Gadd, and Philip S Casey. 2007. "Comparative Toxicity of Nanoparticulate ZnO, Bulk ZnO, and ZnCl2 to a Freshwater Microalga (Pseudokirchneriella Subcapitata): The Importance of Particle Solubility." *Environmental Science & Technology* 41 (24): 8484–90.

Fukui, Kenichi. 1992. "The Role of Frontier Orbitals in Chemical Reactions." *Physiology or Medicine Literature Peace Economic Sciences*, 9.

Fulde, Peter. 2012. *Electron Correlations in Molecules and Solids*. Vol. 100. Springer Science & Business Media.

Gajewicz, Agnieszka, Bakhtiyor Rasulev, Tandabany C Dinadayalane, Piotr Urbaszek, Tomasz Puzyn, Danuta Leszczynska, and Jerzy Leszczynski. 2012. "Advancing Risk

Assessment of Engineered Nanomaterials: Application of Computational Approaches." *Advanced Drug Delivery Reviews* 64 (15): 1663–93.

Gao, Xiaoyu, and Gregory V Lowry. 2018. "Progress towards Standardized and Validated Characterizations for Measuring Physicochemical Properties of Manufactured Nanomaterials Relevant to Nano Health and Safety Risks." *NanoImpact* 9: 14–30.

Gatoo, Manzoor Ahmad, Sufia Naseem, Mir Yasir Arfat, Ayaz Mahmood Dar, Khusro Qasim, and Swaleha Zubair. 2014. "Physicochemical Properties of Nanomaterials: Implication in Associated Toxic Manifestations." *BioMed Research International* 2014.

Gece, Gökhan. 2008. "The Use of Quantum Chemical Methods in Corrosion Inhibitor Studies." *Corrosion Science* 50 (11): 2981–92.

Gece, Gökhan, and Semra Bilgiç. 2009. "Quantum Chemical Study of Some Cyclic Nitrogen Compounds as Corrosion Inhibitors of Steel in NaCl Media." *Corrosion Science* 51 (8): 1876–78.

Geerlings, Paul, and Frank De Proft. 2002. "Chemical Reactivity as Described by Quantum Chemical Methods." *International Journal of Molecular Sciences* 3 (4): 276–309.

Ghosh Chaudhuri, Rajib, and Santanu Paria. 2011. "Core/Shell Nanoparticles: Classes, Properties, Synthesis Mechanisms, Characterization, and Applications." *Chemical Reviews* 112 (4): 2373–2433.

Gilbert, Benjamin, Guoping Lu, and Christopher S Kim. 2007. "Stable Cluster Formation in Aqueous Suspensions of Iron Oxyhydroxide Nanoparticles." *Journal of Colloid and Interface Science* 313 (1): 152–59.

Gobre, Vivekanand V, and Alexandre Tkatchenko. 2013. "Scaling Laws for van Der Waals Interactions in Nanostructured Materials." *Nature Communications* 4: 2341.

Goerigk, Lars, and Stefan Grimme. 2010. "Assessment of TD-DFT Methods and of Various Spin Scaled CIS (D) and CC2 Versions for the Treatment of Low-Lying Valence Excitations of Large Organic Dyes." *The Journal of Chemical Physics* 132 (18): 184103.

Gondikas, Andreas P, Frank von der Kammer, Robert B Reed, Stephan Wagner, James F Ranville, and Thilo Hofmann. 2014. "Release of TiO2 Nanoparticles from Sunscreens into Surface Waters: A One-Year Survey at the Old Danube Recreational Lake." *Environmental Science & Technology* 48 (10): 5415–22.

Gong, Yulong, Zhenqiang Wang, Fang Gao, Shengtao Zhang, and Hongru Li. 2015.

"Synthesis of New Benzotriazole Derivatives Containing Carbon Chains as the Corrosion Inhibitors for Copper in Sodium Chloride Solution." *Industrial & Engineering Chemistry Research* 54 (49): 12242–53.

Gramatica, Paola. 2007. "Principles of QSAR Models Validation: Internal and External." *QSAR & Combinatorial Science* 26 (5): 694–701.

Grimme, Stefan. 2006. "Semiempirical GGA-Type Density Functional Constructed with a Long-Range Dispersion Correction." *Journal of Computational Chemistry* 27 (15): 1787–99.

Grimme, Stefan, Jens Antony, Stephan Ehrlich, and Helge Krieg. 2010. "A Consistent and Accurate Ab Initio Parametrization of Density Functional Dispersion Correction (DFT-D) for the 94 Elements H-Pu." *The Journal of Chemical Physics* 132 (15): 154104.

Gruiz, K. 2019. "In Situ Soil Remediation: The Reactor Approach." *Engineering Tools for Environmental Risk Management: 4. Risk Reduction Technologies and Case Studies*, 39.

Guo, Lei, Chengwei Qi, Xingwen Zheng, Renhui Zhang, Xun Shen, and Sava\cs Kaya. 2017. "Toward Understanding the Adsorption Mechanism of Large Size Organic Corrosion Inhibitors on an Fe (110) Surface Using the DFTB Method." *RSC Advances* 7 (46): 29042–50.

Haas, Philipp, Fabien Tran, and Peter Blaha. 2009. "Calculation of the Lattice Constant of Solids with Semilocal Functionals." *Physical Review B* 79 (8): 85104.

Hahn, Jae Ryang, and Hong Seok Kang. 2010. "Role of Molecular Orientation in Vibration, Hopping, and Electronic Properties of Single Pyridine Molecules Adsorbed on Ag (1 1 0) Surface: A Combined STM and DFT Study." *Surface Science* 604 (3–4): 258–64.

Hammer, Bjørk, and Jens Kehlet Nørskov. 2000. "Theoretical Surface Science and Catalysis—Calculations and Concepts." In *Advances in Catalysis*, 45:71–129. Elsevier.

Hansen, Steffen Foss, Laura Roverskov Heggelund, Pau Revilla Besora, Aiga Mackevica, Alessio Boldrin, and Anders Baun. 2016. "Nanoproducts--What Is Actually Available to European Consumers?" *Environmental Science: Nano*.

Hartmann, Nanna Isabella Bloch, Lars Michael Skjolding, Steffen Foss Hansen, Anders Baun, Jesper Kjølholt, and Fadri Gottschalk. 2014. "Environmental Fate and Behaviour of Nanomaterials: New Knowledge on Important Transfomation Processes."

Hartree, Douglas R. 1928. "The Wave Mechanics of an Atom with a Non-Coulomb Central

Field. Part I. Theory and Methods." In *Mathematical Proceedings of the Cambridge Philosophical Society*, 24:89–110.

Hatchett, David W, and Henry S White. 1996. "Electrochemistry of Sulfur Adlayers on the Low-Index Faces of Silver." *The Journal of Physical Chemistry* 100 (23): 9854–59.

Heyd, Jochen, Gustavo E Scuseria, and Matthias Ernzerhof. 2003. "Hybrid Functionals Based on a Screened Coulomb Potential." *The Journal of Chemical Physics* 118 (18): 8207–15.

Hill, Charles G. 1977. *An Introduction to Chemical Engineering Kinetics & Reactor Design*. Рипол Классик.

Hohenberg, Pierre, and Walter Kohn. 1964. "Inhomogeneous Electron Gas." *Physical Review* 136 (3B): B864.

Ji, Wenchao, Zhemin Shen, Maohong Fan, Pingru Su, Qingli Tang, and Congyang Zou. 2016. "Adsorption Mechanism of Elemental Mercury (Hg0) on the Surface of MnCl2 (1 1 0) Studied by Density Functional Theory." *Chemical Engineering Journal* 283: 58–64.

Johnson, Richard L, Graham O'Brien Johnson, James T Nurmi, and Paul G Tratnyek. 2009. "Natural Organic Matter Enhanced Mobility of Nano Zerovalent Iron." *Environmental Science & Technology* 43 (14): 5455–60.

Kaegi, Ralf, Brian Sinnet, Steffen Zuleeg, Harald Hagendorfer, Elisabeth Mueller, Roger Vonbank, Markus Boller, and Michael Burkhardt. 2010. "Release of Silver Nanoparticles from Outdoor Facades." *Environmental Pollution* 158 (9): 2900–2905.

Karelson, Mati, Victor S Lobanov, and Alan R Katritzky. 1996. "Quantum-Chemical Descriptors in QSAR/QSPR Studies." *Chemical Reviews* 96 (3): 1027–44.

Khaled Abdella Ahmed, Ahmed, Cuizhen Sun, Likun Hua, Zhibin Zhang, Yanhao Zhang, Taha Marhaba, and Wen Zhang. 2018. "Colloidal Properties of Air, Oxygen, and Nitrogen Nanobubbles in Water: Effects of Ionic Strength, Natural Organic Matters, and Surfactants." *Environmental Engineering Science* 35 (7): 720–27.

Khaled, K F. 2008. "Molecular Simulation, Quantum Chemical Calculations and Electrochemical Studies for Inhibition of Mild Steel by Triazoles." *Electrochimica Acta* 53 (9): 3484–92.

Khan, Rizwan, Muhammad Ali Inam, Saba Zam Zam, Du Ri Park, and Ick Tae Yeom. 2018. "Assessment of Key Environmental Factors Influencing the Sedimentation and Aggregation Behavior of Zinc Oxide Nanoparticles in Aquatic Environment." *Water* 10

(5): 660.

Khan, Rizwan, Muhammad Inam, Muhammad Iqbal, Muhammad Shoaib, Du Park, Kang Lee, Sookyo Shin, Sarfaraz Khan, and Ick Yeom. 2019. "Removal of ZnO Nanoparticles from Natural Waters by Coagulation-Flocculation Process: Influence of Surfactant Type on Aggregation, Dissolution and Colloidal Stability." *Sustainability* 11 (1): 17.

Klamt, Andreas. 1995. "Conductor-like Screening Model for Real Solvents: A New Approach to the Quantitative Calculation of Solvation Phenomena." *The Journal of Physical Chemistry* 99 (7): 2224–35.

Klamt, Andreas, and GJGJ Schüürmann. 1993. "COSMO: A New Approach to Dielectric Screening in Solvents with Explicit Expressions for the Screening Energy and Its Gradient." *Journal of the Chemical Society, Perkin Transactions 2*, no. 5: 799–805.

Kohn, Walter, and Lu Jeu Sham. 1965. "Self-Consistent Equations Including Exchange and Correlation Effects." *Physical Review* 140 (4A): A1133.

Kovačević, Nataša, and Anton Kokalj. 2011. "DFT Study of Interaction of Azoles with Cu (111) and Al (111) Surfaces: Role of Azole Nitrogen Atoms and Dipole--Dipole Interactions." *The Journal of Physical Chemistry C* 115 (49): 24189–97.

Krasner, Stuart W, Michael J McGuire, Joseph G Jacangelo, Nancy L Patania, Kevin M Reagan, and E Marco Aieta. 1989. "The Occurrence of Disinfection By-Products in US Drinking Water." *Journal-American Water Works Association* 81 (8): 41–53.

Kunhikrishnan, Anitha, Ho Kyong Shon, Nanthi S Bolan, Ibrahim El Saliby, and Saravanamuthu Vigneswaran. 2015. "Sources, Distribution, Environmental Fate, and Ecological Effects of Nanomaterials in Wastewater Streams." *Critical Reviews in Environmental Science and Technology* 45 (4): 277–318.

Lakshmanan, G, A Sathiyaseelan, P T Kalaichelvan, and K Murugesan. 2018. "Plant-Mediated Synthesis of Silver Nanoparticles Using Fruit Extract of Cleome Viscosa L.: Assessment of Their Antibacterial and Anticancer Activity." *Karbala International Journal of Modern Science* 4 (1): 61–68.

Lavanya, C, R Geetha Balakrishna, Khantong Soontarapa, and Mahesh S Padaki. 2019. "Fouling Resistant Functional Blend Membrane for Removal of Organic Matter and Heavy Metal Ions." *Journal of Environmental Management* 232: 372–81.

Lead, Jamie R, Graeme E Batley, Pedro J J Alvarez, Marie-Noële Croteau, Richard D Handy,

Michael J McLaughlin, Jonathan D Judy, and Kristin Schirmer. 2018. "Nanomaterials in the Environment: Behavior, Fate, Bioavailability, and Effects—An Updated Review." *Environmental Toxicology and Chemistry*.

Levard, Clement, E Matt Hotze, Gregory V Lowry, and Gordon E Brown Jr. 2012. "Environmental Transformations of Silver Nanoparticles: Impact on Stability and Toxicity." *Environmental Science & Technology* 46 (13): 6900–6914.

Levard, Clément, Sumit Mitra, Tiffany Yang, Adam D Jew, Appala Raju Badireddy, Gregory V Lowry, and Gordon E Brown Jr. 2013. "Effect of Chloride on the Dissolution Rate of Silver Nanoparticles and Toxicity to E. Coli." *Environmental Science & Technology* 47 (11): 5738–45.

Li, Xianghong, Shuduan Deng, Hui Fu, and Taohong Li. 2009. "Adsorption and Inhibition Effect of 6-Benzylaminopurine on Cold Rolled Steel in 1.0 M HCl." *Electrochimica Acta* 54 (16): 4089–98.

Liang, Ting, Wei-Xue Li, and Hong Zhang. 2009. "A First-Principles Study on the Behavior of HCl inside SWCNT." *Journal of Molecular Structure: THEOCHEM* 905 (1): 44–47.

Liu, Anmin, Xuefeng Ren, Maozhong An, Jinqiu Zhang, Peixia Yang, Bo Wang, Yongming Zhu, and Chong Wang. 2014. "A Combined Theoretical and Experimental Study for Silver Electroplating." *Scientific Reports* 4: 3837.

Liu, Jingyu, and Robert H Hurt. 2010. "Ion Release Kinetics and Particle Persistence in Aqueous Nano-Silver Colloids." *Environmental Science & Technology* 44 (6): 2169–75.

Liu, Li, Xian Zhao, Honggang Sun, Chuanyi Jia, and Weiliu Fan. 2013. "Theoretical Study of H2O Adsorption on Zn2GeO4 Surfaces: Effects of Surface State and Structure--Activity Relationships." *ACS Applied Materials & Interfaces* 5 (15): 6893–6901.

Liu, Xuyang, Mahmoud Wazne, Yun Han, Christos Christodoulatos, and Kristin L Jasinkiewicz. 2010. "Effects of Natural Organic Matter on Aggregation Kinetics of Boron Nanoparticles in Monovalent and Divalent Electrolytes." *Journal of Colloid and Interface Science* 348 (1): 101–7.

Lojk, Jasna, Jernej Repas, Peter Veranič, Vladimir B Bregar, and Mojca Pavlin. 2020. "Toxicity Mechanisms of Selected Engineered Nanoparticles on Human Neural Cells in Vitro." *Toxicology*, 152364.

Lok, Chun-Nam, Chi-Ming Ho, Rong Chen, Qing-Yu He, Wing-Yiu Yu, Hongzhe Sun, Paul

Kwong-Hang Tam, Jen-Fu Chiu, and Chi-Ming Che. 2006. "Proteomic Analysis of the Mode of Antibacterial Action of Silver Nanoparticles." *Journal of Proteome Research* 5 (4): 916–24.

Loosli, Frédéric, Philippe Le Coustumer, and Serge Stoll. 2015. "Impact of Alginate Concentration on the Stability of Agglomerates Made of TiO2 Engineered Nanoparticles: Water Hardness and PH Effects." *Journal of Nanoparticle Research* 17 (1): 1–9.

Lopez, Christian Vianey Paz, Salomón Ramiro Vásquez Garc\'\ia, Nelly Flores Ramirez, Leandro Garc\'\ia González, and José Luis Rico Cerda. 2018. "Reactive Sites Influence in PMMA Oligomers Reactivity: A DFT Study." *Materials Research Express*.

Louie, Stacey M, Rui Ma, and Gregory V Lowry. 2014. "Transformations of Nanomaterials in the Environment." In *Frontiers of Nanoscience*, 7:55–87. Elsevier.

Louie, Stacey M, Eleanor R Spielman-Sun, Mitchell J Small, Robert D Tilton, and Gregory V Lowry. 2015. "Correlation of the Physicochemical Properties of Natural Organic Matter Samples from Different Sources to Their Effects on Gold Nanoparticle Aggregation in Monovalent Electrolyte." *Environmental Science & Technology* 49 (4): 2188–98.

Louie, Stacey M, Robert D Tilton, and Gregory V Lowry. 2013. "Effects of Molecular Weight Distribution and Chemical Properties of Natural Organic Matter on Gold Nanoparticle Aggregation." *Environmental Science & Technology* 47 (9): 4245–54.

Lowry, Gregory V, Kelvin B Gregory, Simon C Apte, and Jamie R Lead. 2012. "Transformations of Nanomaterials in the Environment." ACS Publications.

Lowry, Gregory V, Ernest M Hotze, Emily S Bernhardt, Dionysios D Dionysiou, Joel A Pedersen, Mark R Wiesner, and Baoshan Xing. 2010. "Environmental Occurrences, Behavior, Fate, and Ecological Effects of Nanomaterials: An Introduction to the Special Series." *Journal of Environmental Quality* 39 (6): 1867–74.

Lu, Xiaoqing, Zhigang Deng, Chen Guo, Weili Wang, Shuxian Wei, Siu-Pang Ng, Xiangfeng Chen, Ning Ding, Wenyue Guo, and Chi-Man Lawrence Wu. 2016. "Methanol Oxidation on Pt3Sn (111) for Direct Methanol Fuel Cells: Methanol Decomposition." *ACS Applied Materials & Interfaces* 8 (19): 12194–204.

MacCarthy, P, and J A Rice. 1985. "Spectroscopic Methods (Other than NMR) for Determining Functions in Humic Substances. p. 527--560. GR Aiken et Al.(Ed.) Humic

Substances in Soil, Sediment, and Water: Geochemistry, Isolation, and Characterization. Wiley Interscience, New York." *Spectroscopic Methods (Other than NMR) for Determining Functions in Humic Substances. p. 527--560. In GR Aiken et Al.(Ed.) Humic Substances in Soil, Sediment, and Water: Geochemistry, Isolation, and Characterization. Wiley Interscience, New York.*

Maneerung, Thawatchai, Seiichi Tokura, and Ratana Rujiravanit. 2008. "Impregnation of Silver Nanoparticles into Bacterial Cellulose for Antimicrobial Wound Dressing." *Carbohydrate Polymers* 72 (1): 43–51.

Mannix, Andrew J, Xiang-Feng Zhou, Brian Kiraly, Joshua D Wood, Diego Alducin, Benjamin D Myers, Xiaolong Liu, et al. 2015. "Synthesis of Borophenes: Anisotropic, Two-Dimensional Boron Polymorphs." *Science* 350 (6267): 1513–16.

Markiewicz, Marta, Jolanta Kumirska, Iseult Lynch, Marianne Matzke, Jan Köser, Steve Bemowsky, Dominic Docter, Roland Stauber, Dana Westmeier, and Stefan Stolte. 2018. "Changing Environments and Biomolecule Coronas: Consequences and Challenges for the Design of Environmentally Acceptable Engineered Nanoparticles." *Green Chemistry* 20 (18): 4133–68.

Marzbanrad, Ehsan, Geoffrey Rivers, Peng Peng, Boxin Zhao, and Norman Y Zhou. 2015. "How Morphology and Surface Crystal Texture Affect Thermal Stability of a Metallic Nanoparticle: The Case of Silver Nanobelts and Pentagonal Silver Nanowires." *Physical Chemistry Chemical Physics* 17 (1): 315–24.

Mattsson, Karin, Simonne Jocic, Isa Doverbratt, and Lars-Anders Hansson. 2018. "Nanoplastics in the Aquatic Environment." In *Microplastic Contamination in Aquatic Environments*, 379–99. Elsevier.

Mitrano, Denise M, Anna Beltzung, Stefan Frehland, Michael Schmiedgruber, Alberto Cingolani, and Felix Schmidt. 2019. "Synthesis of Metal-Doped Nanoplastics and Their Utility to Investigate Fate and Behaviour in Complex Environmental Systems." *Nature Nanotechnology* 14 (4): 362–68.

Mohammed, Leena, Hassan G Gomaa, Doaa Ragab, and Jesse Zhu. 2017. "Magnetic Nanoparticles for Environmental and Biomedical Applications: A Review." *Particuology* 30: 1–14.

Molleman, Bastiaan, and Tjisse Hiemstra. 2015. "Surface Structure of Silver Nanoparticles as

a Model for Understanding the Oxidative Dissolution of Silver Ions." *Langmuir* 31 (49): 13361–72.

Monkhorst, Hendrik J., and James D. Pack. 1976. "Special Points for Brillouin-Zone Integrations." *Physical Review B* 13 (12): 5188–92. https://doi.org/10.1103/PhysRevB.13.5188.

Morones, Jose Ruben, Jose Luis Elechiguerra, Alejandra Camacho, Katherine Holt, Juan B Kouri, Jose Tapia Ramírez, and Miguel Jose Yacaman. 2005. "The Bactericidal Effect of Silver Nanoparticles." *Nanotechnology* 16 (10): 2346.

Mostofa, Khan M G, Cong-qiang Liu, M Abdul Mottaleb, Guojiang Wan, Hiroshi Ogawa, Davide Vione, Takahito Yoshioka, and Fengchang Wu. 2013. "Dissolved Organic Matter in Natural Waters." In *Photobiogeochemistry of Organic Matter*, 1–137. Springer.

Mudunkotuwa, Imali A, Thilini Rupasinghe, Chia-Ming Wu, and Vicki H Grassian. 2011. "Dissolution of ZnO Nanoparticles at Circumneutral PH: A Study of Size Effects in the Presence and Absence of Citric Acid." *Langmuir* 28 (1): 396–403.

Musa, Ahmed Y, Abdul Amir H Kadhum, Abu Bakar Mohamad, Abdalhamid Ahmad B Rahoma, and Hussein Mesmari. 2010. "Electrochemical and Quantum Chemical Calculations on 4, 4-Dimethyloxazolidine-2-Thione as Inhibitor for Mild Steel Corrosion in Hydrochloric Acid." *Journal of Molecular Structure* 969 (1): 233–37.

Nalaparaju, A, X S Zhao, and J W Jiang. 2010. "Molecular Understanding for the Adsorption of Water and Alcohols in Hydrophilic and Hydrophobic Zeolitic Metal- Organic Frameworks." *The Journal of Physical Chemistry C* 114 (26): 11542–50.

Nel, Andre E, Lutz Mädler, Darrell Velegol, Tian Xia, Eric M V Hoek, Ponisseril Somasundaran, Fred Klaessig, Vince Castranova, and Mike Thompson. 2009. "Understanding Biophysicochemical Interactions at the Nano--Bio Interface." *Nature Materials* 8 (7): 543–57.

Nowack, Bernd, James F Ranville, Stephen Diamond, Julian A Gallego-Urrea, Chris Metcalfe, Jerome Rose, Nina Horne, Albert A Koelmans, and Stephen J Klaine. 2012. "Potential Scenarios for Nanomaterial Release and Subsequent Alteration in the Environment." *Environmental Toxicology and Chemistry* 31 (1): 50–59.

Odzak, Niksa, David Kistler, Renata Behra, and Laura Sigg. 2014. "Dissolution of Metal and

Metal Oxide Nanoparticles in Aqueous Media." *Environmental Pollution* 191: 132–38.

Ollikainen, Elisa, Dongfei Liu, Arttu Kallio, Ermei Mäkilä, Hongbo Zhang, Jarno Salonen, Hélder A Santos, and Tiina M Sikanen. 2017. "The Impact of Porous Silicon Nanoparticles on Human Cytochrome P450 Metabolism in Human Liver Microsomes in Vitro." *European Journal of Pharmaceutical Sciences* 104: 124–32.

Ordejón, Pablo, Emilio Artacho, and José M Soler. 1996. "Self-Consistent Order-N Density-Functional Calculations for Very Large Systems." *Physical Review B* 53 (16): R10441.

Ortmann, F, F Bechstedt, and W G Schmidt. 2006. "Semiempirical van Der Waals Correction to the Density Functional Description of Solids and Molecular Structures." *Physical Review B* 73 (20): 205101.

Paier, Joachim, Martijn Marsman, K Hummer, Georg Kresse, Iann C Gerber, and János G Ángyán. 2006. "Screened Hybrid Density Functionals Applied to Solids." *The Journal of Chemical Physics* 124 (15): 154709.

Pal, Sukdeb, Yu Kyung Tak, and Joon Myong Song. 2007. "Does the Antibacterial Activity of Silver Nanoparticles Depend on the Shape of the Nanoparticle? A Study of the Gram-Negative Bacterium Escherichia Coli." *Applied and Environmental Microbiology* 73 (6): 1712–20.

Pasricha, Aneesh, Sant Lal Jangra, Nahar Singh, Neeraj Dilbaghi, K N Sood, Kanupriya Arora, and Renu Pasricha. 2012. "Comparative Study of Leaching of Silver Nanoparticles from Fabric and Effective Effluent Treatment." *Journal of Environmental Sciences* 24 (5): 852–59.

Pauli, Wolfgang. 1940. "The Connection between Spin and Statistics." *Physical Review* 58 (8): 716.

Perdew, John P, Kieron Burke, and Matthias Ernzerhof. 1996. "Generalized Gradient Approximation Made Simple." *Physical Review Letters* 77 (18): 3865.

Perdew, John P, Adrienn Ruzsinszky, Gábor I Csonka, Oleg A Vydrov, Gustavo E Scuseria, Lucian A Constantin, Xiaolan Zhou, and Kieron Burke. 2008. "Restoring the Density-Gradient Expansion for Exchange in Solids and Surfaces." *Physical Review Letters* 100 (13): 136406.

Perdew, John P, and Yue Wang. 1992. "Accurate and Simple Analytic Representation of the Electron-Gas Correlation Energy." *Physical Review B* 45 (23): 13244.

Peters, Ruud J B, Greet van Bemmel, Nino B L Milani, Gerco C T den Hertog, Anna K Undas, Martijn van der Lee, and Hans Bouwmeester. 2018. "Detection of Nanoparticles in Dutch Surface Waters." *Science of the Total Environment* 621: 210–18.

Petschenka, Georg, and Anurag A Agrawal. 2016. "How Herbivores Coopt Plant Defenses: Natural Selection, Specialization, and Sequestration." *Current Opinion in Insect Science* 14: 17–24.

Philippe, Allan, and Gabriele E Schaumann. 2014. "Interactions of Dissolved Organic Matter with Natural and Engineered Inorganic Colloids: A Review." *Environmental Science & Technology* 48 (16): 8946–62.

Puchana-Rosero, M J, Matthew A Adebayo, Eder C Lima, Fernando M Machado, Pascal S Thue, Julio C P Vaghetti, Cibele S Umpierres, and Mariliz Gutterres. 2016. "Microwave-Assisted Activated Carbon Obtained from the Sludge of Tannery-Treatment Effluent Plant for Removal of Leather Dyes." *Colloids and Surfaces A: Physicochemical and Engineering Aspects* 504: 105–15.

Puzyn, Tomasz, Bakhtiyor Rasulev, Agnieszka Gajewicz, Xiaoke Hu, Thabitha P Dasari, Andrea Michalkova, Huey-Min Hwang, Andrey Toropov, Danuta Leszczynska, and Jerzy Leszczynski. 2011. "Using Nano-QSAR to Predict the Cytotoxicity of Metal Oxide Nanoparticles." *Nature Nanotechnology* 6 (3): 175–78.

Rad, Ali Shokuhi. 2016a. "Adsorption of C 2 H 2 and C 2 H 4 on Pt-Decorated Graphene Nanostructure: Ab-Initio Study." *Synthetic Metals* 211: 115–20.

———. 2016b. "Al-Doped Graphene as a New Nanostructure Adsorbent for Some Halomethane Compounds: DFT Calculations." *Surface Science* 645: 6–12.

Rad, Ali Shokuhi, and Ehsan Abedini. 2016. "Chemisorption of NO on Pt-Decorated Graphene as Modified Nanostructure Media: A First Principles Study." *Applied Surface Science* 360: 1041–46.

Ramos, K, Lourdes Ramos, and M Milagros Gómez-Gómez. 2017. "Simultaneous Characterisation of Silver Nanoparticles and Determination of Dissolved Silver in Chicken Meat Subjected to in Vitro Human Gastrointestinal Digestion Using Single Particle Inductively Coupled Plasma Mass Spectrometry." *Food Chemistry* 221: 822–28.

Ratkova, Ekaterina L, David S Palmer, and Maxim V Fedorov. 2015. "Solvation Thermodynamics of Organic Molecules by the Molecular Integral Equation Theory:

Approaching Chemical Accuracy." *Chemical Reviews* 115 (13): 6312–56.

Roothaan, C C J, Lester M Sachs, and A W Weiss. 1960. "Analytical Self-Consistent Field Functions for the Atomic Configurations 1 s 2, 1 s 2 2 s, and 1 s 2 2 s 2." *Reviews of Modern Physics* 32 (2): 186.

Saikia, Nabanita, and Ramesh C Deka. 2013. "A Comparison of the Effect of Nanotube Chirality and Electronic Properties on the π--π Interaction of Single-Wall Carbon Nanotubes with Pyrazinamide Antitubercular Drug." *International Journal of Quantum Chemistry* 113 (9): 1272–84.

Saleh, Navid B, Lisa D Pfefferle, and Menachem Elimelech. 2008. "Aggregation Kinetics of Multiwalled Carbon Nanotubes in Aquatic Systems: Measurements and Environmental Implications." *Environmental Science & Technology* 42 (21): 7963–69.

———. 2010. "Influence of Biomacromolecules and Humic Acid on the Aggregation Kinetics of Single-Walled Carbon Nanotubes." *Environmental Science & Technology* 44 (7): 2412–18.

Salehzadeh, Sadegh, Mehdi Bayat, and Yasin Gholiee. 2013. "A Theoretical Study on the Importance of Steric Effects, Electronic Properties, Interaction and Solvation Energies in the 'Host--Guest'Chemistry of Protonated Azacryptands and Halide Anions." *Tetrahedron* 69 (44): 9183–91.

Sangani, Mahmood Fazeli, Gary Owens, Bijan Nazari, Alireza Astaraei, Amir Fotovat, and Hojat Emami. 2019. "Different Modelling Approaches for Predicting Titanium Dioxide Nanoparticles Mobility in Intact Soil Media." *Science of The Total Environment*.

Sani-Kast, Nicole, Jérôme Labille, Patrick Ollivier, Danielle Slomberg, Konrad Hungerbühler, and Martin Scheringer. 2017. "A Network Perspective Reveals Decreasing Material Diversity in Studies on Nanoparticle Interactions with Dissolved Organic Matter." *Proceedings of the National Academy of Sciences*, 201608106.

Sargent Jr, John F. 2013. "The National Nanotechnology Initiative: Overview, Reauthorization, and Appropriations Issues." In .

Sastri, V S, and J R Perumareddi. 1997. "Molecular Orbital Theoretical Studies of Some Organic Corrosion Inhibitors." *Corrosion* 53 (8): 617–22.

Schrödinger, Erwin. 1926. "Quantisierung Als Eigenwertproblem." *Annalen Der Physik* 385 (13): 437–90.

Shakiba, Sheyda, Alireza Hakimian, Luis R Barco, and Stacey M Louie. 2018. "Dynamic Intermolecular Interactions Control Adsorption from Mixtures of Natural Organic Matter and Protein onto Titanium Dioxide Nanoparticles." *Environmental Science & Technology* 52 (24): 14158–68.

Shang, Honghui, Zhenyu Li, and Jinlong Yang. 2011. "Implementation of Screened Hybrid Density Functional for Periodic Systems with Numerical Atomic Orbitals: Basis Function Fitting and Integral Screening." *The Journal of Chemical Physics* 135 (3): 34110.

Sharma, Virender K, Karolina M Siskova, Radek Zboril, and Jorge L Gardea-Torresdey. 2014. "Organic-Coated Silver Nanoparticles in Biological and Environmental Conditions: Fate, Stability and Toxicity." *Advances in Colloid and Interface Science* 204: 15–34.

Shevlin, David, Niall O'Brien, and Enda Cummins. 2018. "Silver Engineered Nanoparticles in Freshwater Systems--Likely Fate and Behaviour through Natural Attenuation Processes." *Science of the Total Environment* 621: 1033–46.

Silva Ribeiro, Tamires C da, Roner F da Costa, Eveline M Bezerra, Valder N Freire, Marcelo L Lyra, and Vin\'\icius Manzoni. 2014. "The Quantum Biophysics of the Isoniazid Adduct NADH Binding to Its InhA Reductase Target." *New Journal of Chemistry* 38 (7): 2946–57.

Singla, Preeti, Mohd Riyaz, Sonal Singhal, and Neetu Goel. 2016. "Theoretical Study of Adsorption of Amino Acids on Graphene and BN Sheet in Gas and Aqueous Phase with Empirical DFT Dispersion Correction." *Physical Chemistry Chemical Physics* 18 (7): 5597–5604.

Slater, John C. 1929. "The Theory of Complex Spectra." *Physical Review* 34 (10): 1293.

———. 1951. "A Simplification of the Hartree-Fock Method." *Physical Review* 81 (3): 385.

Sotomatsu, Tomoko, Yoshiyuki Murata, and Toshio Fujita. 1989. "Correlation Analysis of Substituent Effects on the Acidity of Benzoic Acids by the AM1 Method." *Journal of Computational Chemistry* 10 (1): 94–98.

Stevenson, Frank J. 1994. *Humus Chemistry: Genesis, Composition, Reactions*. John Wiley & Sons.

Suh, In-Kook, H Ohta, and Y Waseda. 1988. "High-Temperature Thermal Expansion of Six

Metallic Elements Measured by Dilatation Method and X-Ray Diffraction." *Journal of Materials Science* 23 (2): 757–60.

Supiandi, Nurul Izyan, Gaëlle Charron, Mickael Xavier Tharaud, Laure Cordier, Jean-Michel Guigner, Marc F Benedetti, and Yann Sivry. 2019. "Isotopically Labelled Nanoparticles at Relevant Concentrations: How Low Can We Go?-The Case of CdSe/ZnS QDs in Surface Waters." *Environmental Science & Technology*.

Sutton, Rebecca, and Garrison Sposito. 2005. "Molecular Structure in Soil Humic Substances: The New View." *Environmental Science & Technology* 39 (23): 9009–15.

Tangaa, Stine Rosendal, Henriette Selck, Margrethe Winther-Nielsen, and Farhan R Khan. 2016. "Trophic Transfer of Metal-Based Nanoparticles in Aquatic Environments: A Review and Recommendations for Future Research Focus." *Environmental Science: Nano* 3 (5): 966–81.

Thio, Beng Joo Reginald, Dongxu Zhou, and Arturo A Keller. 2011. "Influence of Natural Organic Matter on the Aggregation and Deposition of Titanium Dioxide Nanoparticles." *Journal of Hazardous Materials* 189 (1): 556–63.

Timón, Vicente, Mar\'\ia Luisa Senent, and M Hochlaf. 2015. "Structural Single and Multiple Molecular Adsorption of CO2 and H2O in Zeolitic Imidazolate Framework (ZIF) Crystals." *Microporous and Mesoporous Materials* 218: 33–41.

Tkatchenko, Alexandre, and Matthias Scheffler. 2009. "Accurate Molecular van Der Waals Interactions from Ground-State Electron Density and Free-Atom Reference Data." *Physical Review Letters* 102 (7): 73005.

Tomasi, Jacopo, and Maurizio Persico. 1994. "Molecular Interactions in Solution: An Overview of Methods Based on Continuous Distributions of the Solvent." *Chemical Reviews* 94 (7): 2027–94.

Troeye, Benoit Van, Marc Torrent, and Xavier Gonze. 2016. "Interatomic Force Constants Including the DFT-D Dispersion Contribution." *Physical Review B* 93 (14): 144304.

Tsyusko, Olga V, Jason M Unrine, David Spurgeon, Eric Blalock, Daniel Starnes, Michael Tseng, Greg Joice, and Paul M Bertsch. 2012. "Toxicogenomic Responses of the Model Organism Caenorhabditis Elegans to Gold Nanoparticles." *Environmental Science & Technology* 46 (7): 4115–24.

Valdiglesias, Vanessa, Gözde Kiliç, Carla Costa, Natalia Fernández-Bertólez, Eduardo

Pásaro, João Paulo Teixeira, and Blanca Laffon. 2015. "Effects of Iron Oxide Nanoparticles: Cytotoxicity, Genotoxicity, Developmental Toxicity, and Neurotoxicity." *Environmental and Molecular Mutagenesis* 56 (2): 125–48.

Vance, Marina E, Todd Kuiken, Eric P Vejerano, Sean P McGinnis, Michael F Hochella Jr, David Rejeski, and Matthew S Hull. 2015. "Nanotechnology in the Real World: Redeveloping the Nanomaterial Consumer Products Inventory." *Beilstein Journal of Nanotechnology* 6 (1): 1769–80.

Vincent, Mark A, and Ian H Hillier. 2014. "Accurate Prediction of Adsorption Energies on Graphene, Using a Dispersion-Corrected Semiempirical Method Including Solvation." *Journal of Chemical Information and Modeling* 54 (8): 2255–60.

Wagner, Stephan, Andreas Gondikas, Elisabeth Neubauer, Thilo Hofmann, and Frank von der Kammer. 2014. "Spot the Difference: Engineered and Natural Nanoparticles in the Environment—Release, Behavior, and Fate." *Angewandte Chemie International Edition* 53 (46): 12398–419.

Wang, Hengliang, Xueye Wang, Hanlu Wang, Ling Wang, and Aihong Liu. 2007. "DFT Study of New Bipyrazole Derivatives and Their Potential Activity as Corrosion Inhibitors." *Journal of Molecular Modeling* 13 (1): 147–53.

Wang, Xiaonan, Xiangliang Pan, and Geoffrey Michael Gadd. 2019. "Soil Dissolved Organic Matter Affects Mercury Immobilization by Biogenic Selenium Nanoparticles." *Science of The Total Environment* 658: 8–15.

Wang, Zhenyu, Lei Zhang, Jian Zhao, and Baoshan Xing. 2016. "Environmental Processes and Toxicity of Metallic Nanoparticles in Aquatic Systems as Affected by Natural Organic Matter." *Environmental Science: Nano* 3 (2): 240–55.

Wei, Liuya, Jingran Lu, Huizhong Xu, Atish Patel, Zhe-Sheng Chen, and Guofang Chen. 2015. "Silver Nanoparticles: Synthesis, Properties, and Therapeutic Applications." *Drug Discovery Today* 20 (5): 595–601.

Westerhoff, Paul, and Bernd Nowack. 2012. "Searching for Global Descriptors of Engineered Nanomaterial Fate and Transport in the Environment." *Accounts of Chemical Research* 46 (3): 844–53.

Wiley, Benjamin, Yugang Sun, Brian Mayers, and Younan Xia. 2005. "Shape-Controlled Synthesis of Metal Nanostructures: The Case of Silver." *Chemistry-A European Journal*
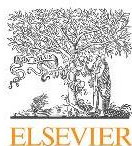
11 (2): 454–63.

Wu, Shubiao, Haiming Wu, Mark Button, Dennis Konnerup, and Hans Brix. 2019. "Impact of Engineered Nanoparticles on Microbial Transformations of Carbon, Nitrogen, and Phosphorus in Wastewater Treatment Processes--A Review." *Science of The Total Environment*.

Xiu, Zong-Ming, Jie Ma, and Pedro J J Alvarez. 2011. "Differential Effect of Common Ligands and Molecular Oxygen on Antimicrobial Activity of Silver Nanoparticles versus Silver Ions." *Environmental Science & Technology* 45 (20): 9003–8.

Yang, Xuezhi, Qi Wang, Xiaolei Qu, and Wei Jiang. 2017. "Bound and Unbound Humic Acids Perform Different Roles in the Aggregation and Deposition of Multi-Walled Carbon Nanotubes." *Science of the Total Environment* 586: 738–45.

Yang, Yu, Qian Chen, Judy D Wall, and Zhiqiang Hu. 2012. "Potential Nanosilver Impact on Anaerobic Digestion at Moderate Silver Concentrations." *Water Research* 46 (4): 1176–84.

Yin, Yongguang, Mohai Shen, Zhiqiang Tan, Sujuan Yu, Jingfu Liu, and Guibin Jiang. 2015. "Particle Coating-Dependent Interaction of Molecular Weight Fractionated Natural Organic Matter: Impacts on the Aggregation of Silver Nanoparticles." *Environmental Science & Technology* 49 (11): 6581–89.

Yu, Su-juan, Yong-guang Yin, and Jing-fu Liu. 2013. "Silver Nanoparticles in the Environment." *Environmental Science: Processes & Impacts* 15 (1): 78–92.

Yu, Sujuan, Jingfu Liu, Yongguang Yin, and Mohai Shen. 2017. "Interactions between Engineered Nanoparticles and Dissolved Organic Matter: A Review on Mechanisms and Environmental Effects." *Journal of Environmental Sciences*.

Zarrouk, A, H Zarrok, R Salghi, B Hammouti, S S Al-Deyab, R Touzani, M Bouachrine, I Warad, and T B Hadda. 2012. "A Theoretical Investigation on the Corrosion Inhibition of Copper by Quinoxaline Derivatives in Nitric Acid Solution." *Int. J. Electrochem. Sci* 7: 6353–64.

Zhang, Fan, Yongming Tang, Ziyi Cao, Wenheng Jing, Zhenglei Wu, and Yizhong Chen. 2012. "Performance and Theoretical Study on Corrosion Inhibition of 2-(4-Pyridyl)-Benzimidazole for Mild Steel in Hydrochloric Acid." *Corrosion Science* 61: 1–9.

Zhang, Jie, Wenli Guo, Qingqing Li, Zhe Wang, and Sijin Liu. 2018. "The Effects and the

Potential Mechanism of Environmental Transformation of Metal Nanoparticles on Their Toxicity in Organisms." *Environmental Science: Nano* 5 (11): 2482–99.

Zhang, Minhua, Rui Yao, Haoxi Jiang, Guiming Li, and Yifei Chen. 2017. "Catalytic Activity of Transition Metal Doped Cu (111) Surfaces for Ethanol Synthesis from Acetic Acid Hydrogenation: A DFT Study." *RSC Advances* 7 (3): 1443–52.

Zhang, Xiaoxing, Qinchuan Chen, Weihua Hu, and Jinbin Zhang. 2013. "A DFT Study of SF 6 Decomposed Gas Adsorption on an Anatase (101) Surface." *Applied Surface Science* 286: 47–53.

Zhang, Zipei, Ruojie Zhang, Hang Xiao, Kunal Bhattacharya, Dimitrios Bitounis, Philip Demokritou, and David Julian McClements. 2019. "Development of a Standardized Food Model for Studying the Impact of Food Matrix Effects on the Gastrointestinal Fate and Toxicity of Ingested Nanomaterials." *NanoImpact* 13: 13–25.

Zhao, Jian, Zhenyu Wang, Yanhui Dai, and Baoshan Xing. 2013. "Mitigation of CuO Nanoparticle-Induced Bacterial Membrane Damage by Dissolved Organic Matter." *Water Research* 47 (12): 4169–78.

Zhao, Jian, Zhenyu Wang, Xiaoyun Liu, Xiaoyan Xie, Kai Zhang, and Baoshan Xing. 2011. "Distribution of CuO Nanoparticles in Juvenile Carp (Cyprinus Carpio) and Their Potential Toxicity." *Journal of Hazardous Materials* 197: 304–10.

Zhou, Wei, Yen-Ling Liu, Audrey M Stallworth, Chunsong Ye, and John J Lenhart. 2016. "Effects of PH, Electrolyte, Humic Acid, and Light Exposure on the Long-Term Fate of Silver Nanoparticles." *Environmental Science & Technology* 50 (22): 12214–24.

Zhou, Y G, Xiaotao T Zu, Fei Gao, J L Nie, and H Y Xiao. 2009. "Adsorption of Hydrogen on Boron-Doped Graphene: A First-Principles Prediction." *Journal of Applied Physics* 105 (1): 14309.

Zhu, Motao, Guangjun Nie, Huan Meng, Tian Xia, Andre Nel, and Yuliang Zhao. 2013. "Physicochemical Properties Determine Nanomaterial Cellular Uptake, Transport, and Fate." *Accounts of Chemical Research* 46 (3): 622–31.
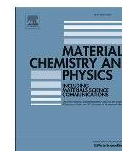
Appendix B: Publications

Publication 1

Contents lists available at ScienceDirect

Materials Chemistry and Physics

Study on the interactions of Ag nanoparticles with low molecular weight organic matter using first principles calculations
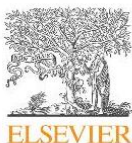
N.N. Nyangiwe [a, b], C.N. Ouma [a], N. Musee [b, *]

[a] Natural Resources and the Environment, Council for Scientific and Industrial Research (CSIR), P O BOX 395, Pretoria, 0001, South Africa
[b] University of Pretoria, Department of Chemical Engineering, Private Bag X 20, Hatfield, 0028, South Africa

Publication 2

Contents lists available at ScienceDirect

Journal of Molecular Graphics and Modelling

Modelling the adsorption of natural organic matter on Ag (111) surface: Insights from dispersion corrected density functional theory calculations

N.N. Nyangiwe [a, b, *], C.N.M. Ouma [a, c]

[a] Natural Resources and the Environment, Council for Scientific and Industrial Research (CSIR), P O BOX 395, Pretoria, 0001, South Africa
[b] University of Pretoria, Department of Chemical Engineering, Private Bag X 20, Hatfield, 0028, South Africa
[c] HySA-Infrastructure, North-West University, Faculty of Engineering, Private Bag X6001, Potchefstroom, 2520, South Africa

Publication 3

Contents lists available at ScienceDirect

Applied Surface Science

Full Length Article

Adsorption and coadsorption of single and multiple natural organic matter on Ag (1 1 1) surface: A DFT-D study

Nangamso Nathaniel Nyangiwe[a,b,*], Cecil Naphtaly Moro Ouma[a,c]

[a] Natural Resources and the Environment, Council for Scientific and Industrial Research (CSIR), P O BOX 395, Pretoria 0001, South Africa
[b] University of Pretoria, Department of Chemical Engineering, Private Bag X 20, Hatfield 0028, South Africa
[c] HySA-Infrastructure, North-West University, Faculty of Engineering, Private Bag X6001, Potchefstroom 2520, South Africa